Solubility, particle formation and immune display of trimers of major capsid protein 7 of African horsesickness virus fused with enhanced green fluorescent protein

by

Eshchar Mizrachi

Submitted in partial fulfilment of the requirements for the degree

Magister Scientiae

In the Faculty of Natural and Agricultural Sciences
Department of Genetics
University of Pretoria
Pretoria
May 2008
Under the supervision of Prof. Henk Huismans

Declaration

I declare that the dissertation that I hereby submit for the degree M.Sc. in Genetics at the University of Pretoria has not previously been submitted by me for degree purposes at any other university.

Eshchar Mizrachi

October 2008

Acknowledgements

I would like to thank the following people and organizations:

- My family and Jo, for their never-ending belief in my abilities.
- Prof. Henk Huismans, for introducing me to molecular biology, stubborn arguments, stimulating conversations, insight and teaching me to think.
- Dr. Vida van Staden and Dr. Wilma Fick, for their patience and support.
- Tracy Leonora Meiring, for being a teacher and friend from start to finish.
- All other members, past and present, of team VIRO, for their friendship, technical assistance and insight.
- My present colleagues in FMG, for their encouragement and assistance.
- BioPAD and the NRF for financial support during the first two years of my M.Sc.

Summary

Modified Viral Protein 7 (VP7) of African horsesickness virus (AHSV) is being investigated as a peptide display protein. The protein represents a good candidate for recombinant peptide display due to its tertiary structure, which contains flexible hydrophilic loops on the top domain of the protein where small peptides can potentially be inserted. In addition, wild type (WT) AHSV VP7 tends to form hexagonal crystals of predictable shape and size when expressed in a recombinant expression system. Previous research has resulted in a number of AHSV VP7 genes containing modified cloning sites where DNA representing immunologically relevant peptides can be inserted. When these chimeric proteins are expressed the peptides should be displayed on the surface of the VP7 platform. Several studies have tested the ability to insert peptides of varying lengths into these sites and successfully express the chimeric protein. In these past cases, successful expression of a recombinant chimeric protein was gauged by the observation of particles formed by multimers of VP7 proteins that resemble the one formed by WT-VP7.

However, little is known about the ability of these chimeric proteins to act as successful peptide presentations vectors. Specifically, it is not known whether the fusion peptides would retain their correct tertiary structure, or indeed be displayed to the surrounding environment in order to generate a specific immune response. Furthermore, there has been no investigation to track these chimeric proteins' expression in a heterologous expression system. This dissertation attempts to answer several of these questions through the use of a fluorescent protein, enhanced green fluorescent protein (eGFP), as a model peptide. The use of eGFP as a model peptide can prove correct tertiary structure of the fusion peptide via function of the protein (fluorescence), as well as act as a means of monitoring expression of chimeric VP7-eGFP proteins.

Chapter 1 of this dissertation reviews literature that is relevant to AHSV VP7 and the use of fluorescent proteins as fluorescent markers. In addition, the recombinant expression of proteins is discussed, with a focus on solubility and expression levels of expressed proteins. Next, a brief overview is given with regards to vaccination strategies that can be undertaken, with a focus on subunit vaccines and their viability as successful alternatives to live-attenuated vaccines. Finally, the progress with regards to using modified AHSV VP7 as a peptide presentation vector is discussed.

Chapter 2 investigates the chimeric protein VP7-177-eGFP, including its construction via a recombinant DNA cloning strategy, its expression in Insect cells using a recombinant Baculovirus expression system, and the ability of eGFP to act as a model fusion peptide on the top domain of a modified VP7 protein. Several experiments investigate whether the chimeric protein maintains its tertiary structure under a series of purification steps, and investigate the solubility of the chimeric protein throughout the expression cycle. Finally, purified forms of the chimeric protein are examined for their ability to generate an immune response specific to the fusion protein, eGFP.

This dissertation has adequately demonstrated that eGFP was indeed displayed on the top domain of the VP7 protein. In addition fluorescence data, combined with testing of sera from immunized guinea pigs, has shown that the display of the peptide is improved when soluble trimers formed by chimeric proteins are used, rather than the insoluble form of the protein. Data and conclusions from this dissertation have contributed to the following oral presentations.

Huismans, H. and Mizrachi, E. The development of a general purpose vaccine display system based on the use of trimers of major capsid protein VP7 of African horsesickness virus".
Virology Africa 2005 conference, Cape Town, South Africa, December 2005.

Mizrachi, E.; Fick, W. and Huismans, H. The solubility, particle formation and immune display of a modified capsid protein 7 of African horsesickness virus fused with green fluorescent protein. *19th South African Genetics Society (SAGS) Congress*, Bloemfontein, South Africa. April 2006.

Huismans, H.; Mizrachi, E.; Meyer, Q.; Rutkowska, D.; Vosloo, W.; Fick, W.C. Soluble trimers of AHSV VP7, displaying foreign peptides inserted into its top domain, as a general purpose vaccine delivery system. *9th International Symposium on Double-Stranded RNA Viruses*, Cape town, South Africa, October 2006

Fick, W.; Ratkawska, D.; Mizrachi, E.; Vosloo, W.; Huismans, H. Soluble trimers of AHSV VP7 as a display system for foreign antigens. Oral presentation, *From Genomes to Protective Antigens – Designing Vaccines Congress*, Prague, Czech Republic, November 2006.

Table of Contents

Chapter 1: Literature Review

1. Introduction

This study focuses on the recombinant expression of chimeric proteins derived from viruses and their application in vaccinology. As a result, the introductory review will discuss in detail topics that are relevant to this investigation. Specifically, the topics of discussion can fall under four main aspects relevant to this study. The first topic of discussion contains an overview of orbiviruses in general and African Horsesickness Virus in particular. This will serve to put in context the structure of Orbivirus viral protein 7 (VP7), and the implications regarding inter-protein interactions of this protein in the formation of higher order structures. Second, the prototypal peptide selected for display in this study – enhanced green fluorescent protein (eGFP)– will be discussed, as well as the advantage of using fluorescence as a tool to qualitatively and quantitatively track expression of proteins. Third, heterologous expression of proteins and the implications regarding recombinant protein expression and purification will be discussed. Fourth, the topic of vaccination will be discussed, with a focus on the role of subunit vaccines in this diversifying field. Finally, the potential of using VP7 of African horsesickness virus as a peptide display vector will be reviewed, in the context of previous research on this protein.

1.1. Orbiviruses

African horsesickness virus (AHSV) is a member of the genus *Orbivirus*. This genus is part of the family *Reoviridae*, a family of non-enveloped viruses that have icosahedral capsids, and contain 10-12 genome segments in the form of double-stranded RNA (dsRNA). For recent reviews see Gould and Hyatt, 1994; Mertens and Diprose, 2004; Roy, 2008; Stuart and Grimes, 2006. The 11 genera within the *Reoviridae* family affect a range of different hosts, and include major viruses of medical (e.g. viruses from the *Rotavirus* genus) and veterinary (e.g. viruses from the *Orbivirus* genus) significance (Mertens and Diprose 2004).

Orbivirus members are about 70nm in diameter, consisting of an inner and outer protein capsid (Hewat et al., 1992b). The outer capsid is composed of two proteins, viral protein (VP) 5 and VP2, and the inner capsid (core) is composed of two major proteins, viral protein (VP) 3 and VP7 (Grimes et al., 1997; Nason et al., 2004). The core encases the dsRNA genome, which comprises 10 segments, and is packed close to the inner core proteins (Diprose et al., 2001; Diprose et al., 2002; Gouet et al., 1999; Prasad et al., 1992).

Orbiviruses enter mammalian cells by means of the hydrophobic outer capsid, which is taken up by phagocytotic molecules upon entry into a cell, leading to the release of the inner capsid into

the cytoplasm (Bhattacharya et al., 2007; Forzan et al., 2007). When the outer capsid is removed, the cores become transcriptionally active (Huismans et al., 1987c; Van Dijk and Huismans, 1980). The segmented double-stranded RNA genome distinguishes orbiviruses from DNA viruses in several aspects. Primarily, the inherent nature of the genetic material means that upon entry into the cell the virus cannot use the cytoplasmic cellular machinery for the purpose of replication. Rather, the virus itself must contain the necessary apparatus to autonomously replicate (Bamford, 2000). Thus, the 10 dsRNA segments contained in the core of orbiviruses encode all the necessary functional proteins (helicase, polymerase, etc.) for the virus to replicate and transcribe.

AHSV is a relative of Bluetongue virus (BTV), which is considered to be the prototypal *Orbivirus* in its structure and behaviour, and since it has been more extensively researched than AHSV, much of AHSV's characteristics are inferred from it. This review will thus consider many BTV properties as *Orbivirus* properties to illustrate AHSV traits, unless otherwise specified.

1.1.1. Structural proteins

The orbivirus double capsid is composed of seven structural proteins (VP1-VP7), organized into two layers (Burroughs et al., 1994; Huismans et al., 1987c; Mertens et al., 1987; Van Dijk and Huismans 1988). The outer capsid is composed of two viral proteins, VP2 and VP5 (Huismans and Erasmus 1981; Mecham et al., 1986). The inner capsid (core) houses 10 double stranded RNA segments (L1-L3, M4-M6 and S7-S10) and is composed of the major components VP3 and VP7, as well as the minor components VP1, VP4 and VP6 (Mertens and Diprose 2004; Prasad et al., 1992; Roy 1996; Stuart and Grimes 2006). Heterologous co-expression in insect cells of the major core proteins VP3 and VP7 of BTV (French and Roy 1990) or AHSV (Maree et al., 1998b) results in spontaneous assembly of core-like particles (CLPs). Expression of all four main core proteins of BTV (VP2, VP3, VP5 and VP7) results in the spontaneous assembly of virus like particles (VLPs) (French et al., 1990).

1.1.1.1. Outer capsid proteins

VP2, the major outer capsid protein, is the most variable protein in Orbivirus with about 80% amino acid variation observed between VP2 sequences of AHSV, BTV and epizootic hemorrhagic disease virus (EHDV) (Iwata et al., 1992). VP2 contains the neutralizing epitopes of orbiviruses, and is the serotype-specific antigenic determinant (Burrage et al., 1993; Huismans and Erasmus 1981; Huismans et al., 1985; Kahlon et al., 1983). It is arranged in a triskelion motif (Fig. 1.1) on the surface of the outer capsid, where 60 VP2 trimers are arranged atop a globular region composed of 120 VP5 trimers (Hewat et al., 1992b; Nason et al., 2004). Studies comparing purified VP2 dimers/trimers and complete virion particles have shown that

both bind to the same molecules on the cell surface, and mediate attachment before internalization of the virion into cells (Hassan and Roy 1999). The molecule with which VP2 interacts is glycophorin A, a surface molecule of erythrocytes, and this could mark the interacting target when the virus must enter its vertebrate host (Hassan and Roy 1999). VP2 is has also been shown to be involved in virus egress from cells via interactions with the cytoskeletal element vimentin (Bhattacharya et al., 2007).

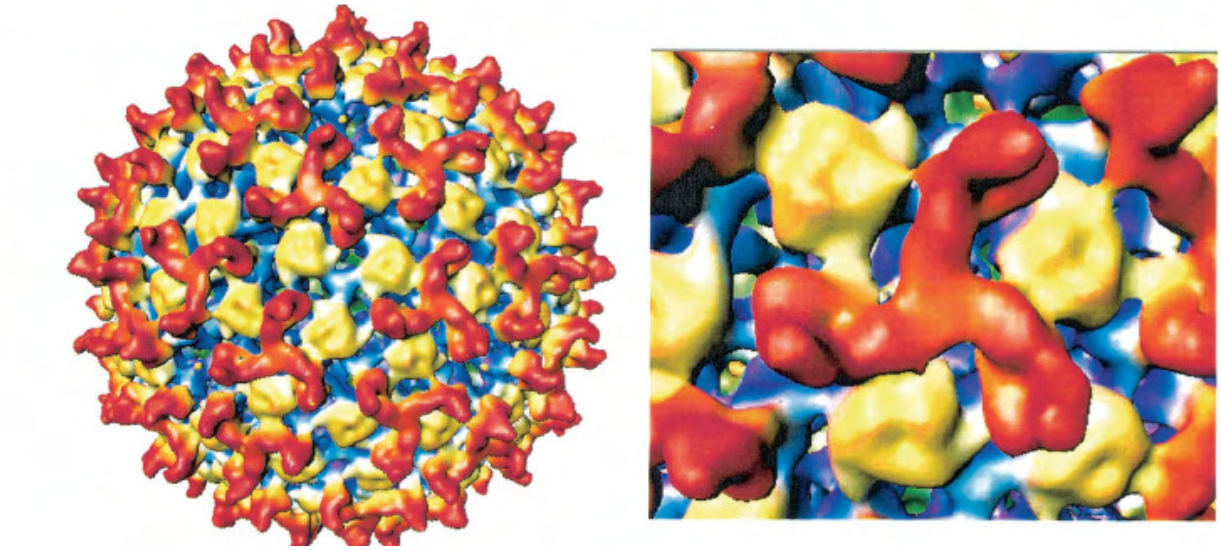

Figure 1.1. Left: Electron cryomicroscopy reconstruction of complete BTV virion. The VP2 trimers (red) are positioned between globular VP5 trimers (yellow). The VP5 proteins interact with the core, specifically with VP7 trimers (blue). Right: close up of the triskelion structure of VP2. The tightly associated core proteins VP7 (blue) and VP3 (green) can be seen underneath the more porous arrangement of the outer capsid. Figure taken from Nason et al., 2004).

VP5, the other outer capsid protein, is more conserved among AHSV serotypes, showing approximately 19% amino acid variation (du Plessis and Nel, 1997). The protein is approximately 526 amino acids (aa) in length (59kDa) in BTV (Purdy et al., 1986) and 505 aa (57kDa) in AHSV (du Plessis and Nel, 1997). VP2 proteins VP5 trimers were observed by electron cryomicroscopy as globular proteins underlying the VP2 triskelion motif (Fig. 1.1 and Nason et al., 2004). VP5 contains two amphipathic helices at the N-terminus and a globular region at the C-terminus, and plays a role in membrane permeabilization (Hassan et al., 2001). The N-terminal region plays a role in fusing membranes and can form a syncytium between neighbouring cells when directed to the cell membrane (Forzan et al., 2004). This function is completely dependent on an acidic pH environment, and is inhibited by the presence of VP2 on capsids (Forzan et al., 2004). The role of VP5 is thought to be in entry of virions into cells, via clathrin-mediated endocytocis (Forzan et al., 2007). The current hypothesis is that virions identify target cells by VP2 mediated interactions (Hassan and Roy, 1999), after which the virus enters the cell by clathrin-mediated endocytosis and passed on to endosomes. Here, the acidic

environment degrades VP2, and VP5 accommodates the release of transcriptionally active cores into the cytoplasm by interacting with the endosomal membrane (Forzan et al., 2007).

1.1.1.2. Major core proteins

The two major core proteins are VP3 and VP7. VP3 proteins (901 aa, 100kDa) form the base of the core - a thin, flat subcore onto which VP7 trimers attach via level, hydrophobic surfaces (Grimes et al., 1998; Grimes et al., 1997). The subcore structure has been observed in BTV infected cells, after an initial uncoating event (stripping of outer capsid), followed by a second uncoating, or the removal of VP7 proteins (Huismans et al., 1987c). The structure of the subcore is icosahedral, and is composed of 120 VP3 proteins, which can be distinguished into two conformations of the protein, A and B (Fig. 1.2 D). Each VP3 protein forms a "plate" of the icosahedron surface, and the morphology of each "plate" can be subdivided into the apical domain (close to the 5-fold axis), carapace domain (which forms the flat surfaces of approximately 50Å-70Å) and the dimerisation domain (Fig. 1.2 C). The two protein conformations, A and B, are thought to form decamers (centred around the 5-fold axis – Fig. 1.2 D), which interact with one another through the formation of a β-sandwich between the dimerisation domains of two A and B VP3 proteins at the 2-fold axes (Grimes et al., 1998).

The VP7 protein is approximately 353 aa (38,107Da) in AHSV (Roy et al., 1991) and 349 aa (38,619Da) in BTV (Kowalik and Li 1989). Orbivirus VP7 is fairly conserved among serotypes and serogroups (Zientara et al., 1998), and has been shown to be the group-specific antigen in *Orbivirus* (Chuma et al., 1992; Huismans and Erasmus 1981). The highest conservation is observed in the N- and C-terminal regions (Roy et al., 1991), which, are involved in the protein's association with VP3 in the core (Grimes et al., 1998; Grimes et al., 1997). VP7 monomers interact with one another to form trimers (Fig. 1.2 A), described originally as having "tripod like shapes and each consists of an upper (innermost) and lower (outermost) domain" (Hewat et al., 1992a). The shape of the monomer is made up of nine α-helices in the bottom domain, with a top domain made up of β-sheets in a "jellyroll" arrangement (Grimes et al., 1995; Grimes et al., 1997). In bluetongue the VP7 trimers, as well as the trimers' interactions with one another and with VP3 in the core, have been characterized to great detail (Basak et al., 1996; Basak et al., 1997; Basak et al., 1992; Grimes et al., 1998; Grimes et al., 1997).

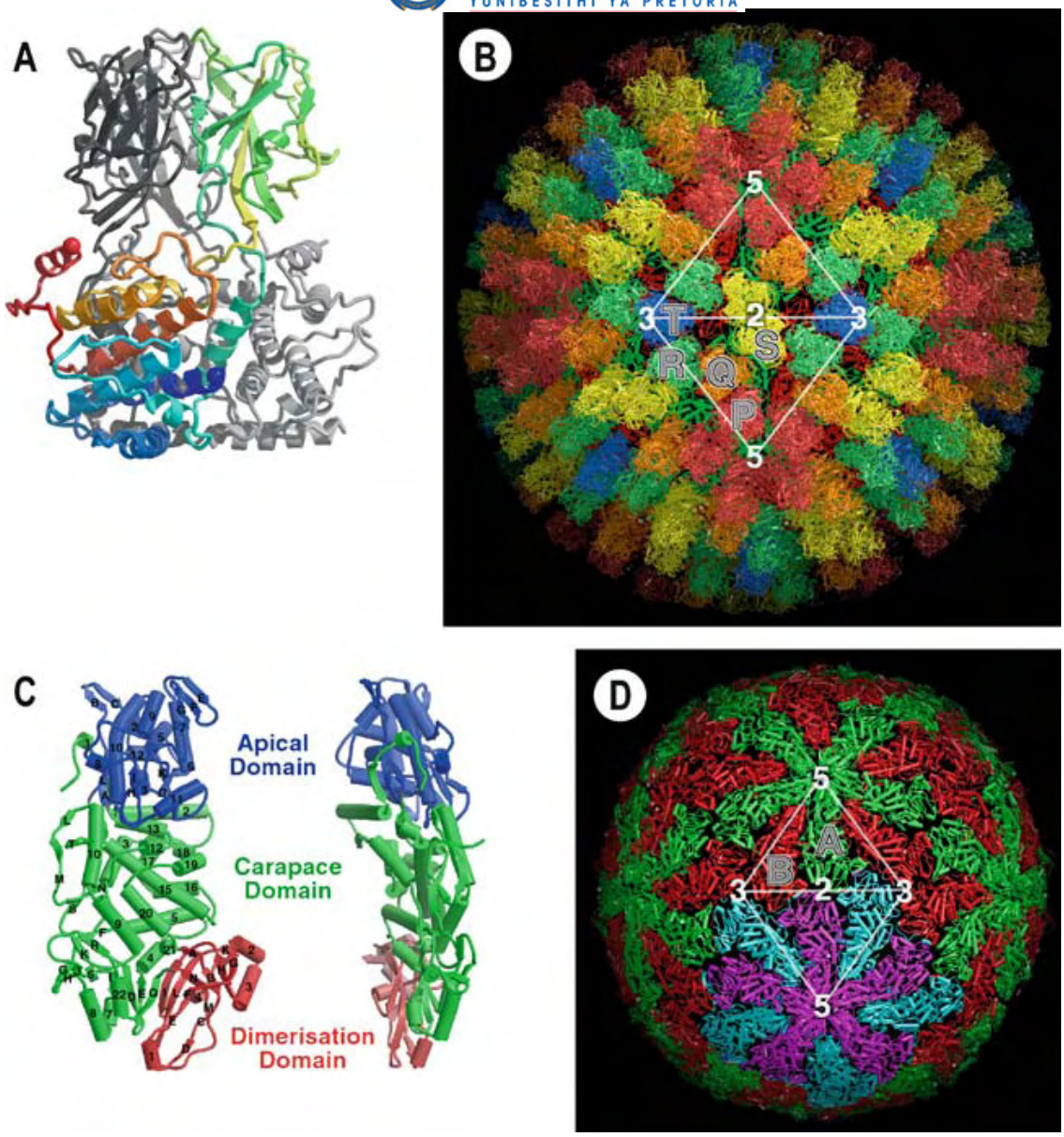

Fig. 1.2. A–D "BTV-1 core architecture. **A** Diagram showing the structure of the VP7 (T13) trimer. A single subunit has been coloured from the N-terminus to the C-terminus *blue to red*, whilst the other subunits are in *grey*. The trimer sits on the exterior surface of the VP3 (T2) subcore, making contact through the bottom surface (in this view), whilst inter-VP7 (T13) contacts are mediated through the sides of the lower domain of the molecule. **B** Diagram showing the core structure. The icosahedral asymmetric unit (which is a triangular area delineated by the symmetry axes marked on the icosahedron) contains 13 copies of VP7(T13) arranged as five trimers, P, Q, R, S and T, coloured *red*, *orange*, *green*, *yellow* and *blue*, respectively. Trimer T sits on the icosahedral three-fold axis and thus contributes a monomer to the unique portion. **C** Diagram showing the domain structure of VP3 (T2), colouring is by domain: apical is *blue* (residues 297–588), carapace is *green* (residues 7–297, 588–698 and 855–901) and dimerization is *red* (residues 698–855). The *left image* shows the molecule as if it were in the subcore when viewed from outside the particle looking towards the centre, with secondary structural elements labelled as defined in Grimes et al., (1998). The *right* image is an orthogonal view. **D** The BTV subcore, made up of 120 copies of VP3 (T2). The icosahedrally unique molecules A and B are coloured *green* and *red*, respectively. Note the different structural environment of the A and B molecules. The icosahedral five-fold, three-fold and two-fold symmetry axes have been marked. One decamer, a putative assembly intermediate, has been highlighted. Figure adapted from Grimes et al., (1998)". (Stuart and Grimes, 2006).

In the core, 260 VP7 trimers are arranged in a T=13 *Laevo* icosahedral lattice, with a T=2 scaffold of 120 VP3 protein dimers (Grimes et al., 1997; Prasad et al., 1992). This configuration, implies a flexible interaction between VP7 trimers, and is discussed in detail in Grimes et al. (1997). It has been shown that AHSV VP7 trimers aggregate to form hexagonal crystals (Burroughs et al., 1994) through the initial interaction of two VP7 trimers to form pseudo dimers (as can be observed in the two-fold interaction in the T=13 lattice). Furthermore, VP3 self-assembles to form single shelled particles independently (Huismans et al., 1987c). While it has not yet been established how the configuration switches from that of a hexameric configuration to a pentameric one, it is thought that the configuration of the T=13 lattice is driven by the interaction of the VP3 core and the relatively flexible C-terminal region of VP7 (Limn and Roy, 2003; Limn et al., 2000).

Furthermore, Limn et al. (2000) and Limn and Roy (2003) investigated several key residues in the VP7 polypeptide that are involved in the interaction of trimers with one-another, as well as with the VP3 scaffold. Residues were selected by using an initial comparison of the amino acid sequence of VP7 between three Orbiviruses, BTV-10, EHDV-1 and AHSV-4, which show conserved motifs related to the structure of the protein (Fig. 1.3), as well as previously obtained structures of BTV cores and VP7 proteins (Fig. 1.4) (Burroughs et al., 1995; Grimes et al., 1995; Grimes et al., 1998; Grimes et al., 1997). Some residues investigated include aspartate (318) and arginine (321), where loss of charge distorted trimer stability, and a change of arginine to phenylalanine (111) that resulted in distortion of two salt links, implying weaker contacts between the VP7 monomer subunits of the trimer. In addition the effect of the loss of residues tryptophan (119) and phenylalanine (268) was observed which, while not necessarily influencing trimer formation had a severe impact on core formation due to a distortion of trimer-trimer interactions, as well as a compromised interaction with the VP3 sub-core. Other residues affecting interactions of trimers with the subcore include methionine (30), arginine (22) and asparginine (38), the latter of which totally abrogated trimer-subcore interactions (Limn and Roy, 2003). These findings concluded that while the interaction between VP7 monomers to form trimers is highly specific – the interaction between trimers to form pseudo multimers is more flexible (Limn and Roy, 2003; Limn et al., 2000); this serves to support the variety of interaction of trimers in the inner core (two, three or five) to result in a T=13 lattice, observed by (Grimes et al., 1997).

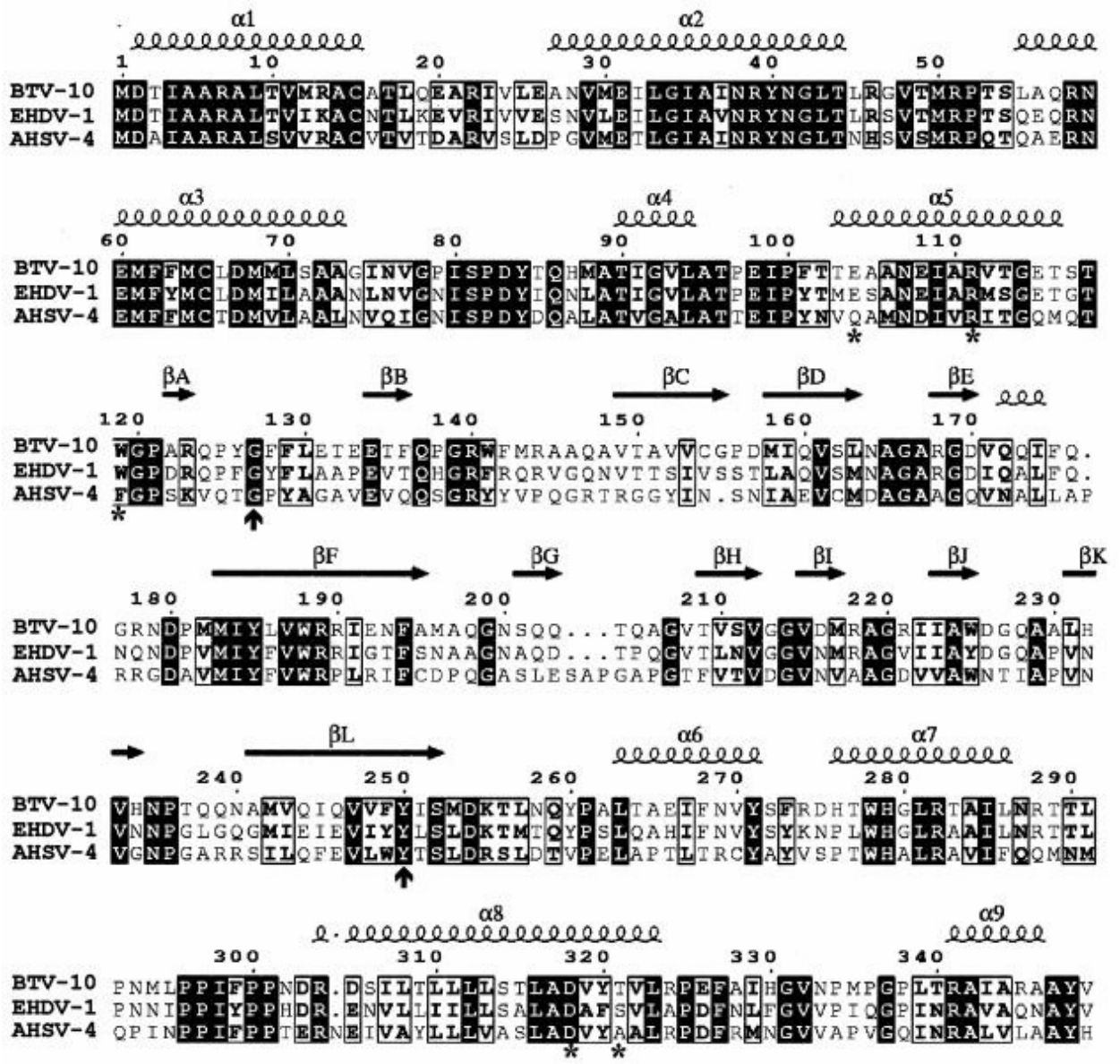

Figure 1.3. Amino acid sequence comparison of VP7 between three Orbiviruses – BTV-10, EHDV-1 and AHSV-4. Conserved residues are indicated in black. Vertical arrows flank the region that comprises the top domain of the protein. β-strands (βA-L) and α-helices (α1-9) are indicated by horizontal arrows and spirals, respectively. (Limn et al., 2000).

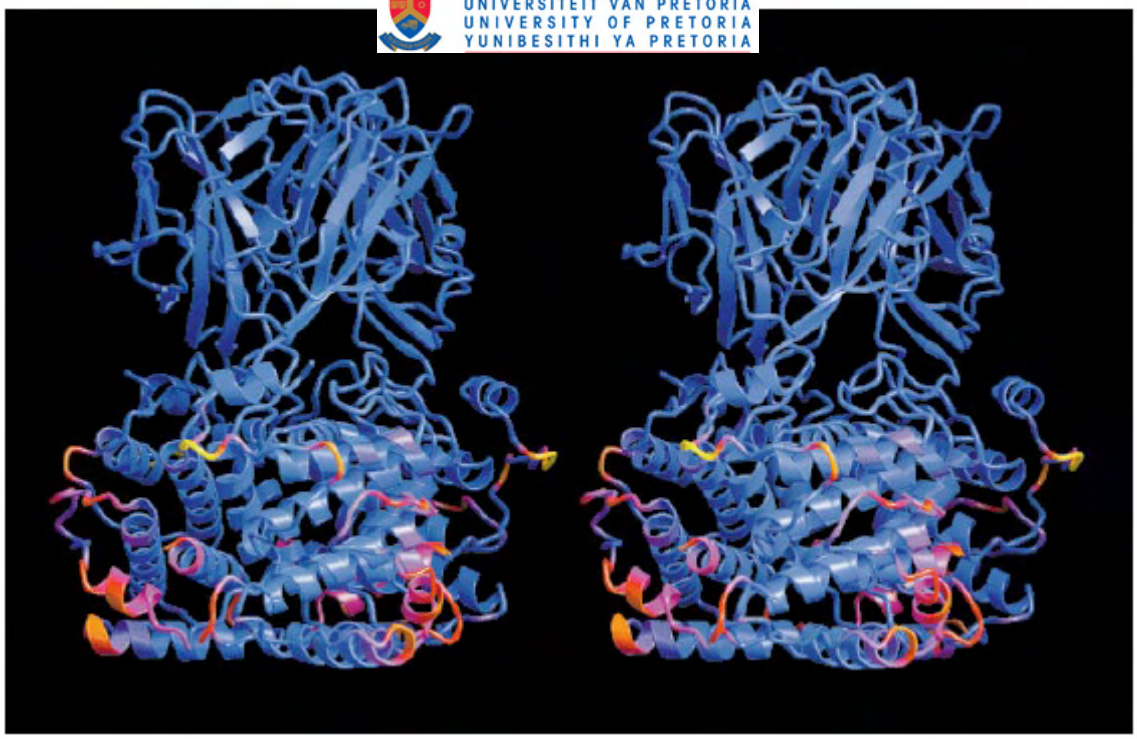

Figure 1.4. "Fold of the trimer of VP7 colour-coded to highlight the areas of VP7 involved in trimer–trimer interactions. There are 3 different sets of interactions between the trimers on the core surface, P–Q, Q–P, Q–R, R–Q, R–S, S–R, R–T, T–R plus P–P′, P′–P, S–Q′, Q′–S and S–S′, where the primes refer to icosahedral symmetry-related trimers. Each trimer was examined in turn and those residues in any one subunit of the trimer within 8Å of a residue in a contacting dimer were marked as being in the contact region. The sum was taken, over all the trimers, of the number of occasions each residue was contacted. This was then mapped onto the fold of the trimer, coloured from blue (0–1 contacts) through to yellow (greater than 11 contacts)." (Grimes et al., 1997)

1.1.1.3. Minor core proteins

VP1, encoded by L1, is the largest viral protein (1032 aa, 149.5kDa), and is an RNA-dependent RNA polymerase (Urakawa et al., 1989). This function was proved for the first time when cell lysates of insect cells heterologously expressing VP1 showed polymerase activity *in vitro* (Urakawa et al., 1989). In BTV, it was shown that VP1 forms part of the inner core through specific interactions with VP3 (Loudon and Roy 1991). The VP1 protein was also demonstrated *in vitro* to possess replicase activity, where double stranded RNA was formed from a plus-strand RNA template (Boyce et al., 2004). Although the structure of the protein has not been resolved, a recent study (Wehrfritz et al., 2007) modelled the N- and C-terminal regions on Reovirus RNA-dependent RNA polymerase, λ3, whose VP1 structure has been determined (Tao et al., 2002). The N-terminal domain (aa 1-373), along with a pore-forming bracelet structure of the C-terminal domain (aa 874-1295), forms a cage around a central polymerase domain (PD, aa 581-880) (Wehrfritz et al., 2007). The central PD domain can, when expressed as a truncated peptide, bind NTP like the full length protein, but cannot by itself display polymerase activity. However, when all three peptides representing the N-terminal, C-terminal

and central polymerase domains are mixed together the RNA-dependent RNA polymerase activity can be reconstituted (Wehrfritz et al., 2007).

VP4, a 76.4kDa has multiple enzymatic functions and is ultimately responsible for capping of ssRNA (plus strand). Studies on BTV VP4 have shown that the protein has guanylyl transferase function (Le Blois et al., 1992; Martinez-Costas et al., 1998), a methylation and capping function (Ramadevi et al., 1998a). Inside the core, the protein is present as a dimer (Ramadevi et al., 1998b), and forms part of the viral transcription complex along with VP6 and VP1 (Diprose et al., 2001; Gouet et al., 1999; Grimes et al., 1998). Recently, the protein's structure has been resolved to a 2.5Å resolution, revealing the multi-domain architecture (Sutton et al., 2007).

VP6, a member of the transcription complex inside the core, has nucleoside triphosphatase, RNA binding and helicase functions, and is responsible for ATP-mediated unwinding of double-stranded RNA (Stauber et al., 1997). The binding of VP6 to single-stranded or double stranded RNA has been shown in BTV (Stauber et al., 1997) and AHSV (De Waal and Huismans, 2005). In solution the protein forms a hexameric structure in the presence of nucleic acids, similar to that formed by other helicase proteins (Kar and Roy, 2003).

1.1.2. Non-structural proteins

The non-structural (NS) 1 protein is the most abundantly expressed viral protein and forms tubular structure in BTV infected cells (Huismans, 1979). The AHSV protein has been shown to be highly conserved between serotypes, forming tubules that are approximately 23nm in diameter and up to 4µm when heterologously expressed in insect cells (Maree and Huismans, 1997). In BTV, dimers of NS1 form helically coiled ribbons that can be observed in the cells during infection (Eaton et al., 1988). The tubular structures formed by BTV NS1 multimers is broader (52nm diameter) and shorter on average (100-1000nm) than AHSV NS1 tubules (Hewat et al., 1992c; Roy 2008). Although the structure of BTV NS1 has been characterized (Roy et al., 1994), its function in orbiviruses is as yet not well understood, though it is suspected that it is involved in the transport of virions through the cytoplasm (Owens et al., 2004).

The NS2 protein is somewhat conserved among serogroups, with the primary functional region at the N-terminal being the most conserved (Van Staden et al., 1991). BTV NS2 can bind single-stranded RNA (ssRNA) (Huismans et al., 1987b). In BTV and AHSV infected cells, it was observed that aggregations of NS2 form centres in the cytoplasm called viral inclusion bodies (VIBs) to which ssRNA is attracted (Devaney et al., 1988). During viral replication the NS2 aggregations protect the free ssRNAs from cytoplasmic degradation and act as the packaging

centres for viral genomic material (Theron et al., 1996; Thomas et al., 1990). While ssRNA binding ability of NS2 is generally non-specific, some preference was shown for virus-specific genomic segments using BTV NS2, with the protein showing preference for the 3' end of the segments (Theron and Nel, 1997). The N-terminal half of the protein was initially shown to be important for ssRNA-binding (Zhao et al., 1994), while (Fillmore et al., 2002) attributed this property to three specific amino acid regions (2-11, 153-156 and 274-286) by a series of truncations and specific peptide synthesis, followed by electrophoretic mobility shift assays with ssRNA. Subsequently, the structure of the N-terminal region of BTV NS2 was determined, where it was shown that interactions of β-sandwich regions of monomers interacted to expose surfaces that bind the ssRNA (Butan et al., 2004). Recently, Mumtsidu et al. (2007) resolved the structure of the C-terminal half (177 amino acids) of BTV NS2 to a 2.4Å resolution, and assembled a composite model of the decamer formed by NS2 dimers, using the obtained data and combining it with previously obtained structure of the N-terminal half (Butan et al., 2004). This model represents the closest structure known today of the multimeric components formed by NS2.

NS3 and NS3A are both coded for by the S10 segment, from two in-frame start codons (Van Staden and Huismans, 1991); the difference between them being a region of about 11 amino acids where the alternate start codons are positioned (Van Staden et al., 1998). NS3 is approximately 91% conserved among BTV serotypes and shows much less conservation (around 64%) between AHSV serotypes (Van Niekerk et al., 2001). All NS3 proteins contain two cytoplasmic domains (the N- and C-terminal regions), which are separated by two transmembrane domains in the last third of the polypeptide chain that anchor the protein in cell membranes (Bansal et al., 1998; Beaton et al., 2002; Van Staden and Huismans 1991). NS3 is often implicated for its involvement (directly or indirectly) in the release of mature virions from cells. It has been associated with the final stages of the viral life cycle, specifically as a mechanism of increasing the permeability of the host cell membrane, to allow the release of virions (Stoltz et al., 1996). In addition, studies on BTV NS3 have shown that the C-terminal region (cytoplasmic) interacts with VP2 (Beaton et al., 2002), as well as association of the protein with intra-cellular vesicles (Hyatt et al., 1993). NS3 is an obligate component of viral release from cells, and mediates release of complete VLPs, but not immature CLPs from cells (Hyatt et al., 1993). The N-terminal cytoplasmic region was shown to interact with p11, a component of the Annexin II complex involved in exocytosis (Beaton et al., 2002). Based on these results, the current model poses that the cytoplasmic N- and C-terminal regions, anchored in the cell membrane by the two trans-membrane domains, link up mature virions (via VP2-mediated interactions) and the cellular exocytosis machinery to mediate viral release (Beaton et al., 2002).

1.2. Enhanced Green Fluorescent Protein (eGFP)

Fluorescent proteins (FPs) have revolutionized the possibilities of visualizing biological processes at a microscopic level. Since the initial illustration of a recombinantly expressing stable green fluorescent protein (GFP)-fusion protein was reported in *Escherichia coli* and *Caenorhabditis elegans* (Chalfie et al., 1994), commercial variants of FPs have flourished. The variants are customized for expression (codon use, folding, colour, etc.) and cellular environments, particularly those of mammalian (Ward and Brandizzi 2004; Yu et al., 2003) and plant cells (Berg and Beachy, 2008; Chapman et al., 2005), but suited for expression in cells representing all kingdoms of life (Stewart Jr., 2006). Tagging by FP markers can facilitate in situ visualization of biological processes, from tracking single or multiple proteins in a cellular environment, to visualizing entire cells, to marking multiple cells in a tissue type by mosaic expression of colour variants (Feng et al., 2000; Livet et al., 2007; Zhang et al., 2002; Zimmer 2002). Analysis of cells expressing FPs is significantly less obtrusive than other visualization methods e.g. fluorescent or radioactive labelling of proteins and subsequent screening. This is due to the fact that the recombinant fusion of an FP and the protein to be studied allows one step of in situ expression, instead of conjugating purified proteins to dyes (Chalfie et al., 1994; Stearns 1995; Zhang et al., 1996).

Originally green fluorescent protein (GFP) was discovered as a naturally produced bioluminescent in the jellyfish *Aequorea victoria* (Shimomura et al., 1962). Since then the protein has been characterized in great detail, and many colour variants are today commercially available that are, for all intents and purposes, the same tertiary structure, (Chudakov et al., 2005; Dixit et al., 2006; Miyawaki, 2003). In *Aequorea victoria*, the wild type GFP protein receives its excitation energy from aequorin, a bioluminescent molecule (Shimomura et al., 1962), and emits its own fluorescence around 509nm (Morise et al., 1974). The structure of the chromophore was initially hypothesized by (Shimomura, 1979), but was more accurately described later on (Cody et al., 1993). Ultimately, the crystal structure of the entire protein was resolved to a resolution of 1.9Å (Ormo et al., 1996). The basic structure of the protein consists of a chromophore (Fig. 1.5 A) attached to an alpha helix, which is buried in the centre of a β-barrel – an arrangement of 11β-sheets (Fig. 1.5 B). The mechanism of fluorescence is the cyclic oxidation of serine (65), tyrosine (66) and glycine (67) (Fig. 1.6), and a single substitution in the chromophore from tyrosine (66) to histidine alters the fluorescence emission from green to blue (Heim et al., 1994). The structure of the protein is such that the N- and C-termini of the protein are proximal to one another at the base of the “barrel”, so that the barrel can be attached as a whole via either or both termini of the protein. This means that GFP can be used

as a reliable tag fused to the N-terminus or C-terminus of the target protein (Kratz et al., 1999; Miyawaki et al., 2003).

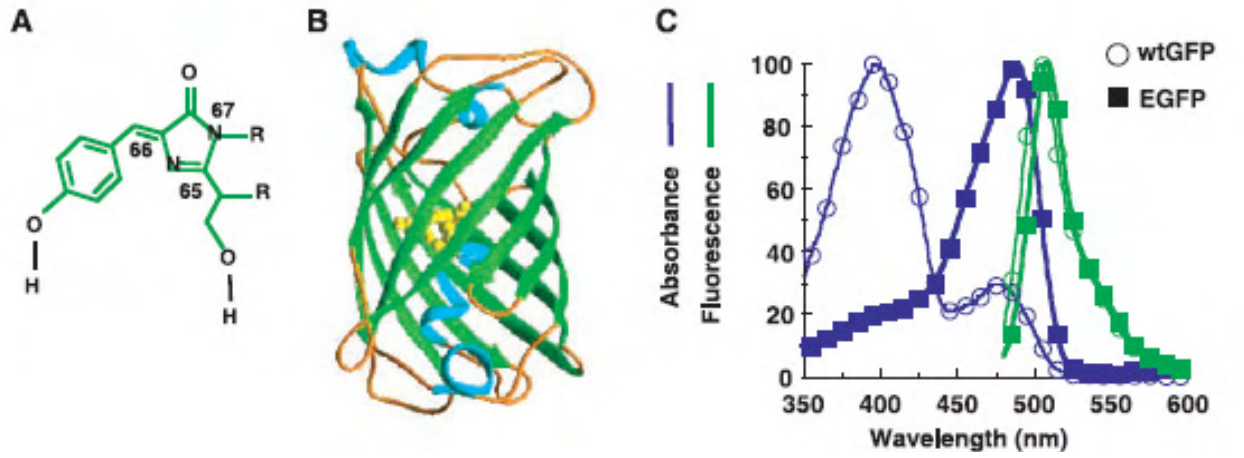

Figure 1.5. A. A cyclized tripeptide (serine 65, tyrosine 66 and glycine 67) makes up the WTGFP chromophore. (Cody et al., 1993). B. The chromophore (yellow), attached to an α-helix, is surrounded by a β barrel, first resolved by (Ormo et al., 1996). C. The major and minor absorbance peaks of WTGFP (blue circles) and single fluorescence emission peak (green circles) were converted to single absorbance (blue squares) and fluorescence emission (blue circles) peaks in eGFP. (Heim et al., 1994).

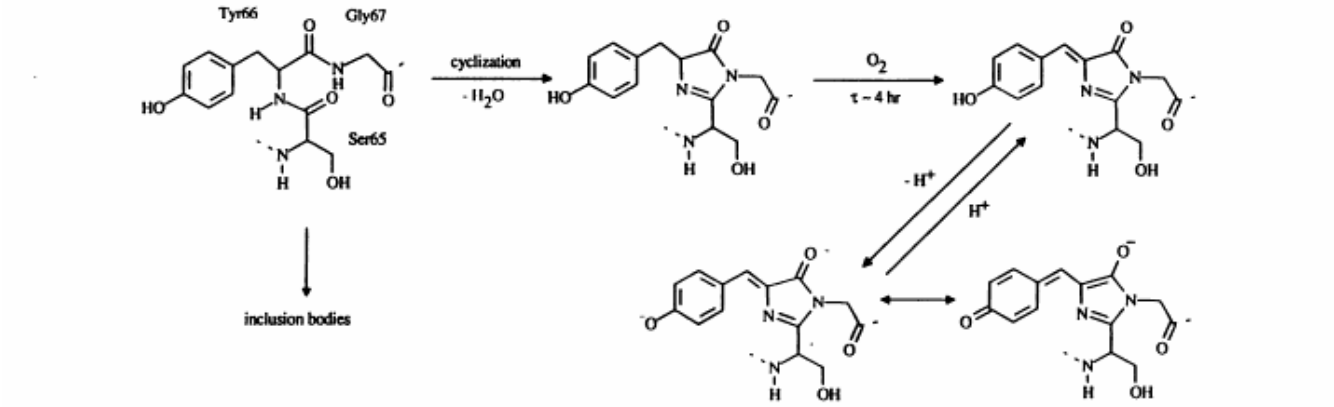

Figure 1.6. "Proposed biosynthetic scheme for the chromophore of GFP. The freshly translated protein (upper left) could be trapped by inclusion bodies or remain soluble and nonfluorescent (upper center) until oxidation by 0_2, which would dehydrogenate Tyr-66 to form the fluorophore (upper right). The protonated and deprotonated species (upper and lower right) may be responsible for the 395- and 470- to 475-nm excitation peaks, respectively. The excited states of phenols are much more acidic than their ground states, so that emission would come only from the deprotonated species." (Heim et al., 1994).

One of the variants of WTGFP is enhanced green fluorescent protein (eGFP) (Cormack et al., 1996; Kain et al., 1996; Zhang et al., 1996), which is approximately thirty five times brighter than WTGFP. The enhanced GFP was optimized by a screen of variant GFPs that were randomly mutated in residues proximal to the chromophore, as well as optimization of codon usage (Cormack et al., 1996; Zhang et al., 1996). Some of the main differences include the following

alterations: first, the substitution of Serine (65) with threonine, alanine, glycine, cysteine or leucine to convert the major and minor absorbance peak to a single absorbance peak (Fig. 4 C) (Heim et al., 1994). Second, acceleration of fluorophore formation and folding of the protein at 37℃ (Cormack et al., 1996; Heim et al., 1995; Tsien, 1998). Third, dimerisation of GFP in high concentrations was abrogated by changing alanine to lysine (206), leucine to lysine (221) or phenylalanine to argenine (223) (Campbell et al., 2002). The modified and commercially produced eGFP protein is 239aa (27kDa) in size, has an excitation maximum of 480nm and an emission maximum of 505nm (UV or blue light is sufficient), and requires no substrate or coenzyme to fluoresce under excitation.

While the majority of cases include attaching a FP as an N- or C-terminal fusion to the target protein, there have been cases where the FP is inserted as a fusion within the amino acid sequence of the target protein (Hughes et al., 2001; Kratz et al., 1999; Siegel and Isacoff, 1997). This is usually not recommended as the FP can affect the correct folding of the target protein, but can usually be tolerated in hydrophilic loops that fold separately from the rest of the protein. However finding these sites within a target protein sequence can be difficult, and as a result several methods of high-throughput random transposition of FP sequences into a target sequence are available. The resulting proteins can be screened, and this allows the selection of appropriate sites of insertion (Biondi et al., 1998; Giraldez et al., 2005; Sheridan et al., 2002; Sheridan and Hughes, 2004). One way to make the attachment of an FP less invasive is the recombinant addition of linker amino acids to the N- and/or C-terminal ends of the FP or the target protein. These linkers usually consist of simple, non-polar amino acids such as glycine or alanine, with the possible inclusion of serines to increase solubility of the linker (Nagai and Miyawaki, 2004).

The use of FPs as single molecule tags allows for complex spatio-temporal visualizations such as protein localization/translocation, small molecule detection and transcriptional activity of promoters (March et al., 2003). In addition, effects such as protein-protein interactions can be studied, as long as the parameters that would affect saturation of fluorescence data is taken into account (Lalonde et al., 2008). In addition to these qualitative assays, it is the *quantitative* nature of fluorescence that adds another dimension to the data, whether in terms of tracking enzymatic activity (Li et al., 2007) or serving as a non-invasive marker of protein expression levels (Cha et al., 2005; Hyung et al., 2005; Shin et al., 2003). In general terms, using FPs as quantitative tools will give a relative value that can be correlated to protein quantity, although variations of fluorescence values per unit of protein can occur when considering different cellular environments (Zou et al., 2005). Differences in levels of fluorescence between soluble

or insoluble aggregates of FPs can be due to incorrect folding of the FP as in the case of inclusion bodies (Tsumoto et al., 2003; Vera et al., 2007).

1.3. Recombinant expression of proteins

Recombinant expression of proteins allows the synthesis of a single protein, or often multiple proteins simultaneously, in an expression system of choice. Today, many options are available for recombinantly expressing any potential gene product *in vivo*, and the most commonly used systems are based on bacteria (Baneyx 1999; Hockney, 1994; Sørensen and Mortensen, 2005; Wong, 1995), yeast (Romanos, 1995; Romanos et al., 1992), insect cells (Beljelarskaya, 2002) or larvae (Cha et al., 1999; Medin et al., 1990), or mammalian cells (Kost et al., 2005; Moss et al., 1990).

The recombinant expression of proteins *in vivo*, as opposed to *in vitro*, is a far more cost-effective and efficient method of producing large scale (milligram-gram) quantities of a desired protein product, and allows for a conducive environment for the protein to fold correctly. The factors that should be considered when selecting an appropriate system are numerous and range from simple considerations such as overall protein yield and ease of mass culture, to more particular factors. These usually include traits of proteins that are associated with eukaryotes, such as glycosylation or chaperone-mediated folding. While these factors will not be discussed in detail in this review, each has been reviewed extensively and is unique to the protein in consideration. A comparison of different expression systems has been summarized thoroughly in (Hyung et al., 2005) and references therein, and is replicated below in Table 1.1.).

Table 1.1. Factors that should considered when selecting a recombinant expression system. The table is taken directly from (Hyung et al., 2005), and references 1-12 (bottom row in the table) can be found in the manuscript.

Comparison of recombinant expression systems

	E. coli	Yeast	Insect	Mammalian
Growth rate	Very fast	Fast	Slow	Slow
Expression yield (based on dry weight)	High (1–5%)	High (>1%)	Very high (30%)	Very low (<1%)
Productivity	Very high	High	High	Low
Media cost	Very low	Low	High	Very high
Culture techniques	Very easy	Easy	Difficult	Very difficult
Production cost	Very low	Low	High	Very high
Protein folding	Fair	Good	Very good	Very good
Simple glycosylation	No	Yes	Yes	Yes
Complex glycosylation	No	No	Yes[a]	Yes
Secretion	Poor	Very good	Very good	Very good
Functionality of expressed eukaryotic protein	Poor	Good	Very good	Very good
Availability of genetic systems	Very good	Good	Fair	Fair
Pyrogen problem	Possible	No	No	No
References	[1–3]	[4–6]	[7–9]	[10–12]

[a] Glycosylation patterns differ from mammalian cells.

Baculovirus-mediated expression in cell culture has proven to be a highly effective method of over-expressing a protein of choice, in insect cells as well as in mammalian cells (Beljelarskaya, 2002; Hu 2005; Kost et al., 2005). In this method, a gene of interest is transposed into the genome of a baculovirus (e.g. the *Autographa californica* nuclear polyhedrosis virus – AcNPV), which is then used to infect cells in culture. Transposition replaces an existing gene that does not interfere with viral replication and infectivity of virions such as polyhedrin (Doerfler, 1986), and places the gene of choice under the control of the extremely powerful polyhedrin promoter. This results in expression yields of the target protein of approximately 30% compared to other expressed proteins, and represents a significantly higher percentage yield than other expression systems (table 1.1). The other main advantage is that recombinant baculoviruses can be replicated and used to infect any scale of culture that is required. Thus, when considering the use of Baculoviruses as a means of expression in cell culture, the benefits of high reproducibility and expression levels should be weighed up against the technical requirements and production costs.

One of the most common problems encountered when recombinantly expressing a protein is aggregation of misfolded proteins. This could be an effect of salts, detergents used during cell lysis, or pH variations during purification (Cherish Babu et al., 2008; Natalello et al., 2008). Improper folding of proteins can also occur due to expression in an inappropriate cellular environment (e.g. expressing a mammalian protein in a bacterial system) or simply the proteins' tendency to interact with one another when expressed at levels higher than in their natural environment (the reader is referred to Jahn and Radford (2008); Silva et al. (2006) and Stefani and Dobson (2003) for recent reviews on protein folding and aggregation). The problem of aggregation can often be overcome by adding certain compounds such as guanidine hydrochloride at low molarity (Tsumoto et al., 2003) or amino acids such as L-arginine. The latter has proved the most successful approach to circumventing hydrophobic interactions between proteins, and this has been shown by either the addition of L-arginine to the environment in which the protein is being expressed, or indeed post-purification of the aggregated protein. (Arakawa et al., 2007a; Arakawa et al., 2007b; Buchner and Rudolph, 1991; Tsumoto et al., 2007; Tsumoto et al., 2003; Tsumoto et al., 2004).

1.4. Vaccination

The administration of vaccines has proven to be the most effective protection against specific pathogens, and today vaccinations against once deadly diseases are common. Vaccination takes advantage of the adaptive immune response in the form of specificity and memory. Thus, the recognition and clonal multiplication of B-cells specific to an antigen allow the immune system to recognize a specific pathogen, and be able to mount a far more rapid immune

response the next time it encounters the same antigen (Roitt et al., 2001). In order to administer a successful vaccine the immunogenic agent should induce the correct type of immunity, ideally eliciting an effective B-cell and T-cell response (Mattion et al., 1994). In addition, vaccines should be safe i.e. in the case of live attenuated vaccines the attenuated virus should not revert to the virulent type (Roitt et al., 2001). Vaccines should also be realistically economic to produce.

The complexity and variation with which different pathogens interact with the immune system is reflected in the varied approaches to elicit an effective immune response. A vaccine can thus be live-attenuated or inactivated; based on nucleic acids or the actual pathogenic agent, or in the form of subunit vaccines (Purcell et al., 2007; Roitt et al., 2001). Live vaccines, the most commonly used form, are generated by repeated passaging of pathogens in cell culture until an attenuated form is obtained. They are generally difficult to produce, maintain and store. Furthermore attenuation by passaging is unpredictable and often inconsistent, and thus reversion of a vaccine is often a concern (Roitt et al., 2001). One of the ways in which this is combated is recombinant modification/deletion of genes that may cause reversion of the virus to its pathogenic form (MacLachlan et al., 2007).

In terms of vaccination against AHSV, the only current vaccines are live-attenuated cocktails representing groups of serotypes (MacLachlan et al., 2007), however there are several recent documented cases of reversions to pathogenic forms (Coetzer and Guthrie, 2004). A unique aspect of viruses with segmented genomes is that segments can easily become re-assorted with pathogenic forms of the virus inside a host, making reversion a more likely scenario (Sanchez-Vizcaino, 2004). The merits and disadvantages of alternate forms to traditional vaccines can be debated at length, and have been reviewed extensively in (Hilleman 2000; Moylett and Hanson, 2003; Purcell et al., 2007). For the purpose of this review, the focus will be on subunit vaccines.

1.4.1. Subunit vaccines

In the case of subunit vaccines, immunologically important proteins or epitopes can be produced in vitro or be heterologously expressed in a prokaryotic/eukaryotic host. Presentation of epitopes to the immune system can take the form of a virus like particle (VLP), a core like particle, attached to a carrier protein or as soluble peptides.

Immunogenicity stimulated by subunit vaccines is usually aided by co-administration of an adjuvant, generally requiring multiple booster doses (Roitt et al., 2001). The reason for this is that subunit antigens do not efficiently activate lymphocytes, thus the immune system does not

effectively progress from an innate immune response to an adaptive one (Medzhitov and Janeway, 1997). An adjuvant in this case is any substance assisting in the co-stimulatory signal necessary for an adaptive immune response, and can be represented by a number of biological and non-biological molecules (Medzhitov and Janeway, 1997). Unfortunately, the progression in understanding active components of adjuvants, as well as preventing unwanted side effects, has been slow (Purcell et al., 2007; Roitt et al., 2001). Some examples of biological adjuvants include heat shock proteins (Blachere et al., 1997; Castellino et al., 2000; Noessner et al., 2002; Suto and Srivastava, 1995; Tamura et al., 1997), immunostimulatory complexes (Morein et al., 1984; Sanders et al., 2005), liposomes (Kersten and Crommelin, 2003) or exosomes (Taïeb et al., 2005). Other adjuvants include polysaccharides (Petrovsky, 2006) and oil-emulsion such as Freund's adjuvant or montanide (Chianese-Bullock et al., 2005). The choice of adjuvant is related to its side effect and the target organism, for instance many oil-emultion based adjuvants are toxic to humans (Purcell et al., 2007).

Furthermore, and significantly, most subunit vaccines, even while stimulating adequate B-cell activation, are lacking in eliciting an effective T-cell response (Roitt et al., 2001). This inefficiency of T-cell activation in subunit vaccine attempts has been suggested to be due to a lack of organization of an antigen in the host, resulting in irregular presentation and load (Bachmann et al., 1998; Jegerlehner et al., 2002). Thus, to trigger effective response, a localized antigen load must be high and sustained, in an ordered pattern, as in the case of the subunit Hepatitis B capsid presentation system (Bachmann et al., 1998; Medzhitov and Janeway, 1997). In this way the presentation of the antigen can mimic most closely the live pathogen, which will stimulate an effective B- and T-cell response (Bachmann et al., 1998; Szomolanyi-Tsuda and Welsh, 1998).

Findings such as those of (Bachmann et al., 1998) had contributed to the development of Hepatitis B virus capsids as antigen presentation vectors. Indeed, the only licensed subunit vaccine based on VLP/CLP display in the United States of America is one based on this system (Hilleman, 2000). Another consequence is that researchers attempting to develop subunit antigen presentation systems focus on the principle of generating a repetitive and stable structure. This manifests in a few common mechanisms for epitope display, where peptides representing the proteins are expressed as fusions of proteins that act as carriers. The carrier molecule can be a single protein such as *Schistosoma japonicum* glutathione-s-transferase (GST – D'Apice et al., 2007), or it can form part of a larger complex. There are many examples where proteins or epitopes are expressed as fusions of coat proteins of viruses such as Baculovirus (Mäkelä and Oker-Blom, 2006; Mäkelä and Oker-Blom, 2008) or phage (Benguric et al., 2001; De Berardinis et al., 1999; De Berardinis et al., 2000; Nagesha et al., 2001). Fusion

proteins can also be co-expressed with other proteins to form only the outer core or coat of a virus/bacterium/spore, and extensive research has been carried out in papillomavirus VLPs (Chackerian, 2007; Chackerian et al., 2002), Bacillus subtillis spore coat proteins (D'Apice et al., 2007; Domingo et al., 2001), and Hepatitis B virus CLPs (Clarke et al., 1987; Jegerlehner et al., 2002).

Orbivirus proteins have also been tested as subunit vaccines, and several investigations have tested the potential use of VLPS/CLPs of BTV (French et al., 1990; Van Dijk, 1993) or AHSV (Maree et al., 1998a; Maree et al., 1998b). Single proteins from AHSV and BTV that are purified from virus infected cells or heterologously expressed and partially purified have also been used. This was initially done in the form of purified outer capsid proteins VP2 or VP5 from bluetongue (Huismans et al., 1987a; Roy et al., 1990) or AHSV (Martinez-Torrecuadrada et al., 1996; Roy et al., 1996; Stone-Marschat et al., 1996). However, these avenues of immunization have not progressed to a commercially available vaccine due to several reasons, including sub-optimal formation of CLPs or VLPs, inability to stimulate adequate T-cell response, and effects on economic viability due to complexity of production and efficacy of inducing a neutralizing response. In AHSV proteins in particular, one of the main problems is aggregation of proteins, such as AHSV VP2 when it is heterologously expressed prior to purification (Du Plessis et al., 1998), or aggregation of AHSV VP7, which hinders the formation of CLPs (Maree et al., 1998a). This has resulted in attempts to express epitopes as fusions of single proteins that form predictable structures when heterologously expressed. An example of this is AHSV VP7 (Discussed in 1.8.), BTV NS1 (Ghosh et al., 2002a; Ghosh et al., 2002b; Mikhailov et al., 1996) or AHSV NS1 (Lacheiner, 2006), where epitopes are expressed as C-terminal fusions of NS1 and are present on the surfaces of tubules that are formed.

The production of subunit vaccines is carried out in many different types of heterologous expression systems, in cells derived from bacteria, yeast, insects or mammals. This is because several factors have to be taken into account, such as the origin of the proteins to be expressed (viral, bacterial, eukaryotic), the level of expression obtained, expertise and mass-culture options, as well as implications with regards to legalization of the product (Schmidt, 2004; Soler and Houdebine, 2007). The Baculovirus expression system has been used extensively for large scale protein production or the production of fusion-proteins, CLPs or VLPs for vaccination purposes (Antonis et al., 2006; Aucoin et al., 2007; Condreay and Kost, 2007; Kost et al., 2005; Maranga et al., 2002).

1.4.1.1. Hepatitis B

The investigation of Hepatitis B components as alternatives to conventional vaccination has been progressing for some time. This system utilises the hepatitis B core antigen (HBcAg), which was initially purified directly from Hepatitis B carriers with high hepatitis B surface antigen (HbsAg) loads (Spence et al., 1975). The protein was later synthesized and purified, using eukariotic (Michel et al., 1984), but primarily bacterial expression systems (Kratz et al., 1999; Lechner et al., 2002). The HBcAg protein (183 aa) forms dimers when expressed (Kratz et al., 1999; Zhou and Standring, 1992), which spontaneously assemble into icosahedral core like particles by the interactions of 120 and 90 dimeric subunits in T=4 and T=3 arrangements, respectively (Crowther et al., 1994; Mancini et al., 1997). Each dimer forms a spike made up of "radial bundles of four long alpha helices" that is presented to the core's surrounding environment, the tip of which contains the immunodominant region (Bottcher et al., 1997). This region is represented by a short loop connecting 2 alpha helices of a monomer in a helix-turn helix motif (Fig. 1.7), containing the core antigen (HBcAg) and the sentinel e-antigen (HBeAg) (Conway et al., 1998; Kratz et al., 1999).

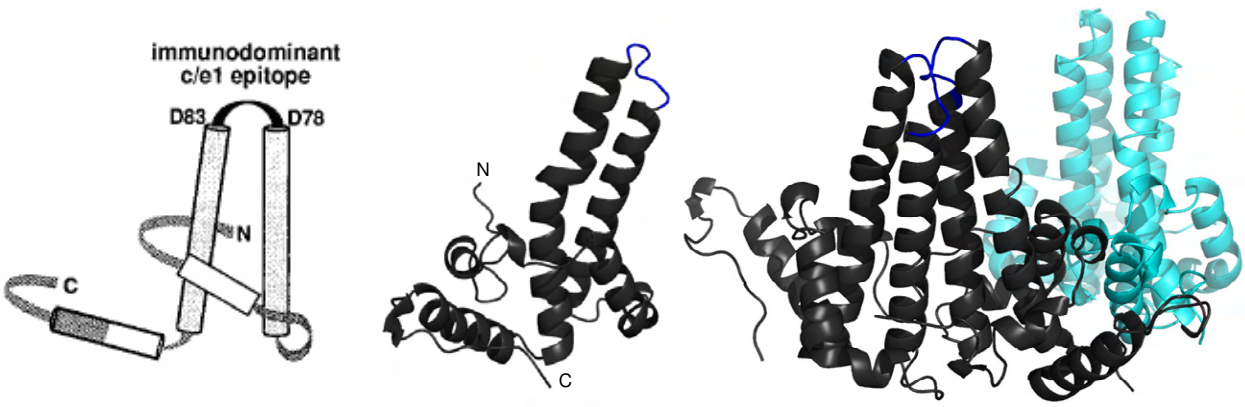

Figure 1.7. The core protein of Hepatitis B virus. Left: Diagram of secondary structure of the protein (Kratz et al., 1999). Middle and right: Crystal structure of the core protein. The epitope loop (dark blue) lies at the top of two α-helices. Dimers of the protein present in the core form 4-helix bundles (right). Images were generated using PyMOL v0.99 (Delano 2002) using the crystal structure (PDB code: 1QGT). The structure was resolved by (Wynne et al., 1999).

Thus, peptide presentation using this system takes advantage of this loop with insertions of immunologically relevant peptides. The stability of the formation of these cores despite peptide insertions in this region was most notably demonstrated by (Kratz et al., 1999), where proline (79) and alanine (80) were replaced with a complete protein – GFP, flanked by glycine rich linkers. The resulting core particles ("GFPcore") maintained their structural integrity, and the GFP insert retained its fluorescent properties. In addition, rabbits immunized with partially purified GFPcores produced antibodies that recognized purified GFP protein in an immune-precipitation reaction, indicating conformationally correct antibodies against the inserted peptide.

Despite its advantages, certain aspects of the Hepatitis B core presentation system have impaired its development. One of the problems is that of a pre-existing immunity in the human to human derived Hepatitis B virus cores, which confounds anti-HBc assays (i.e. diagnosing current or recent HBV infections), and is counteractive to the prolonged and structured display of the epitope presented on the core. The other is that of assembly of cores depending on the properties of the insert – "parameters such as length, high hydrophobicity, high β-strand index, or large volume may impede the proper assembly-folding of chimeric core particles" (Traore et al., 2000).

Nevertheless, it has been demonstrated that Hepatitis B core display systems raise neutralizing antibodies, and cases of note are those confirming protection against *Plasmodium beghei* (Schodel et al., 1994), *P.yoleii* (Schodel et al., 1997) and Foot and Mouth Disease virus (FMDV) (Clarke et al., 1987). Additionally, recently (Traore et al., 2000) have resolved to a degree the problems of pre-existing immunity and structure by using a woodchuck hepatitis core antigen (WhcAg), and investigated aspects that allow more flexible formation of CLPs. A system of antigen presentation based on HBcAg therefore still has potential and has displayed some of the more promising advances in subunit vaccines.

1.5. AHSV VP7 as an antigen display vector

The use of AHSV VP7 as a subunit vaccine first showed promise by expression of AHSV 9 VP7 in BHK cells and immunization of mice with purified VP7 crystals (Wade-Evans et al., 1997). This immunization of mice with VP7 particles, combined with Freund's adjuvant, provided complete protection compared to 80-100% mortality in the control groups. These results, combined with those of another similar trial in mice (Wade-Evans et al., 1998) concluded that VP7 crystals provide partial serogroup-specific protection. Furthermore, it was the conclusion of the latter study that the response was more likely mediated by a cellular, and not a humoral immune response (Wade-Evans et al., 1998).

Research in the University of Pretoria over the last ten years has focused on the utilization of AHSV VP7 as a peptide display vector. Initially a CLP strategy was attempted for by co-expression of AHSV VP3 and VP7 using recombinant bacmids in Sf9 cells (Maree et al., 1998a). However the extremely hydrophobic nature of AHSV VP7 limited the efficiency of CLP formation as VP7 trimers aggregated to form particles (Maree et al., 1998a; Maree et al., 1998b), resembling those described previously (Burroughs et al., 1994; Chuma et al., 1992). While a CLP strategy was not viable, the spontaneous and regular assembly of VP7 trimers into insoluble ordered hexagonal particles – as well as the stability and high expression levels of

these particles and the ease of their partial purification – prompted an investigation of using AHSV VP7 particles as a particulate peptide presentation system.

Since the crystal structure of BTV VP7 was well characterized (Grimes et al., 1995), and the crystal structure of the top domain of an AHSV VP7 trimer was described (Basak et al., 1996), regions on the top domain of the monomer could be identified that represented small hydrophilic loops (Fig. 1.8). The aim was to recombinantly express small peptides in these areas and present them on the VP7 top domain, which would be displayed to the immune system through the ordered structure of a hexagonal particle (Maree, 2000). To achieve this, modifications were made by inserting 18 nucleotides within AHSV-9 VP7 cDNA cloned into a plasmid, at regions coding for these predicted loops on the top domain of VP7. The inserted nucleotides contain unique endonuclease recognition sites, and code for six additional amino acids which extend the hydrophilic loops. Several of these modified VP7 mutant proteins have been developed as peptide display vectors, with different display sites (Fig. 1.9).

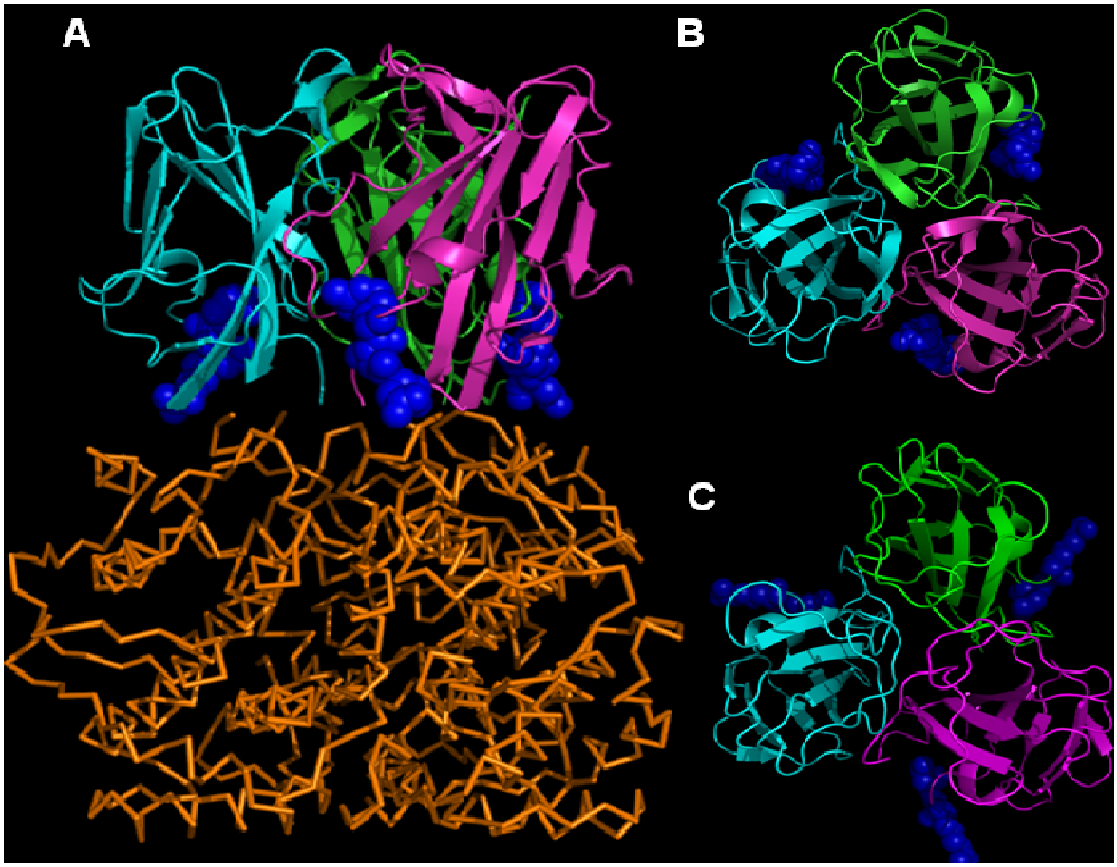

Figure 1.8. Structures of BTV (A, B) and AHSV (C) VP7 trimers. Images were modified with PyMol v0.99 (Delano, 2002) using X-Ray diffraction studies of a BTV VP7 trimer (PDB code: 1BVP, Grimes et al., 1995) and the top domain of an AHSV VP7 trimer (PDB code: 1AHS, Basak et al., 1996). The complete BTV VP7 trimer is shown in A, with the bottom domain containing complex alpha-helix interactions between the three subunits represented as orange ribbons. The top domain is coloured green, cyan and magenta, with each colour representing one subunit. The RGD motif is displayed as blue spheres on all subunits. B and C show the top domain of VP7 trimers of BTV and AHSV, respectively.

This was followed by several studies investigating the tolerance of the VP7 protein to the insertion of a variety of small peptides in these loops, while still maintaining its stability, as well as its tendency to aggregate into ordered structures. It was found that VP7 tolerated inserts of up to 200aa in its top domain (Van Rensburg, 2005) while still forming particles that resemble those formed by WT-VP7.

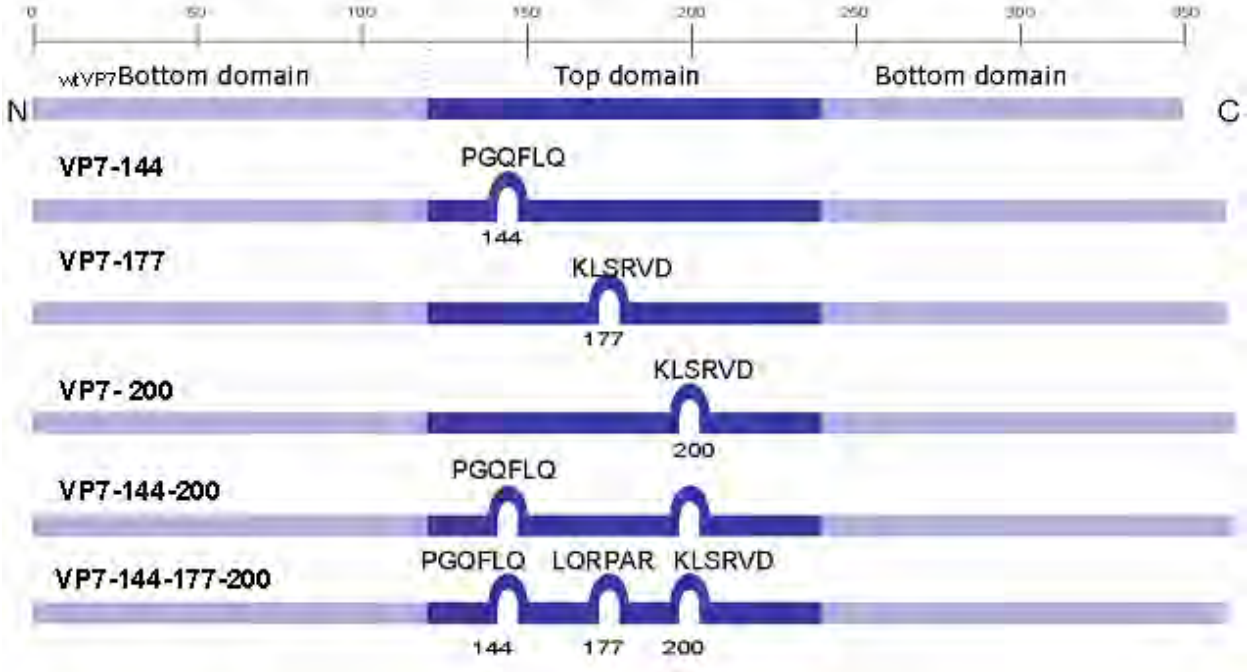

Figure 1.9. Modifications of the top domain of WT-VP7 included the insertion of six amino acids to extend small hydrophilic loops at amino acid positions 144 (Meyer, 2002; Riley, 2003), 177 (Maree, 2000), 200 (Maree, 2000) and combinations of these (Van Rensburg, 2005) as indicated. On a nucleotide level, these sites represent specific endonuclease recognition sites to allow directional subcloning of DNA inserts.

However the insertion of peptides and the influence of hydrophilic insertions resulted in an altered overall hydrophobicity of the chimeric proteins, and either decreased (Maree, 2000; Van Rensburg, 2005) or increased (Meyer, 2002; Riley, 2003) the solubility of higher order structures they formed. In addition, the particle structure was affected by the size and hydrophobicity of the insert, and the ordered formation of particles by chimeras into particles was less predictable, forming distorted shapes that only distantly resemble the particles formed by WT-VP7. This variation in the ratio of soluble to insoluble higher order structures formed by chimeric VP7 proteins is as yet not entirely predictable, but had opened up the avenue of using soluble VP7 trimers as display vectors as well. However, one such case was attempted and proved unsuccessful (Riley, 2003).

1.6. Aims of this study:

An aspect that has been lacking in AHSV VP7 vector research is a detailed investigation describing the expression of these proteins in vivo using the Baculovirus expression system. Specifically, the rates at which these chimeric proteins are expressed, the optimal time of harvesting the maximum amount of chimeric protein from cells, and the trends of assembly of the trimeric form into the particulate form are all details that are lacking. Perhaps most significantly, while structural stability of these chimeric proteins as insoluble particles has been discussed at length, relatively little progress has been made in terms of generating immune response to the epitopes displayed on the top domain of modified AHSV VP7 proteins.

Several key aspects were identified that should be considered for a successful subunit peptide display strategy utilizing modified AHSV VP7 proteins as epitope display vectors: First, the conformation of inserted peptides must be predictable, i.e. all chimeric VP7 proteins must be homologous in their conformation. Second, these peptides must be presented to the surrounding environment in an efficient manner and generate an immune response specific to the peptide. Finally, VP7 chimeric proteins should be relatively simple to produce and purify.

With the above requirements in mind, this project aimed to evaluate the efficacy of a modified AHSV VP7 protein, VP7mt177, as a peptide presentation vector. The chimeric VP7 tested in this case contains a modified extended loop possessing the RGD motif at the flexible amino acid loop 175-180 (Maree, 2000), where immunologically relevant peptides could be cloned and expressed as chimeric displayed epitopes. EGFP was selected as a prototypal peptide to be displayed on the surface of this chimeric protein, VP7-177-eGFP. Previous work by Burger (2005) included an AHSV 9 WT-VP7 protein that was expressed using the baculovirus expression system, where an eGFP protein was attached to the C-terminal of WT-VP7. This protein, VP7-C-eGFP did indeed display fluorescence and demonstrated AHSV VP7's characteristic ability to form aggregates (Burger, 2005).

The expression of eGFP on the top domain of AHSV VP7mt177 (Fig. 2.2 and 2.3) presents several advantages that would generate more accurate information regarding the nature of epitopes displayed on chimeric VP7 proteins: 1. Fluorescence of chimeric VP7-eGFP proteins can demonstrate the ability to insert an entire protein that can fold correctly with VP7 and be exposed to its surrounding environment. 2. Fluorescence is a relatively simple, non-invasive method of quantifying expression levels of chimeric VP7 proteins. 3. EGFP provides a means of tracking the assembly of chimeric VP7 proteins when expressed in the Baculovirus expression

system. 4. Since eGFP is a soluble protein, separation of components by centrifugation can show whether the insertion of soluble peptides affect the overall solubility of chimeric AHSV VP7 proteins.

Therefore the short term aims of this study were:

1. To investigate if a large peptide such as eGFP can be inserted in the top domain of VP7mt177 and retain its structural integrity.
2. To investigate the kinetics of expression of this fusion protein i.e. when and in what form the protein is expressed.
3. To investigate the efficacy of presentation of a peptide in the different forms of the fusion protein by testing for an immune response specific to eGFP.

Chapter 2

2.1. Introduction

The AHSV protein VP7 is being investigated as a peptide display vector, where peptides are recombinantly expressed on the top domain of modified AHSV VP7 proteins. In order for the VP7 protein to be an effective display vector, the peptide must be expressed on the surface of an ordered protein structure. One of the primary reasons for AHSV VP7 being selected as a candidate peptide presentation vector is the tendency of the wild type (WT) protein to form ordered, hexagonal crystalline particles when expressed in Sf9 cells via a recombinant baculovirus (Burroughs et al., 1994). Several VP7 peptide display vectors have been created that allow the recombinant insertion of peptides (Maree, 2000; Van Rensburg, 2005; Meyer, 2002; Riley 2002). A number of dissertations have described in detail the effects on the particles formed after inserting different peptides of varying lengths into these vectors (Van Rensburg, 2005; Meyer, 2002; Rutkowska, 2003; Riley, 2002; Kretzmann, 2005). In all these investigations, the resulting chimeric proteins were evaluated in terms of their ability to form particles which resemble those of WT-VP7. The tendency of chimeric VP7 vectors to form particles represents, to some extent, stability of the interactions of trimers of these proteins and therefore stability in VP7 protein folding when these peptides are expressed on the top domain of VP7 monomers. However, the formation of hexagonal-like particles does not necessarily imply that the inserted peptides/epitopes are optimally displayed to the immune system. Indeed, humoral immune response specific to the displayed epitope generated from injections of particles of these chimeric proteins has been relatively poor (Huismans, unpublished).

In a recent study, Burger (2005) constructed a recombinant baculovirus expressing a WT-AHSV VP7 protein with an eGFP protein attached at the C-terminus. The recombinant protein could be detected in cells by epifluorescent microscopy and retained fluorescence after partial purification by a sucrose sedimentation gradient. Scanning electron microscopy showed that particles formed by this protein were larger (approximately 11µm in diameter) and more densely compacted than WT-VP7 (approximately 6µm in diameter). In addition, the aggregates did not resemble the flat hexagonal crystals formed by WT-VP7. Further analysis of the VP7-C-eGFP protein on sucrose gradients indicated that 100% of the protein that was harvested from lysed Sf9 cells recombinantly expressing the protein was in the particulate form. Fractions containing soluble forms of the protein were not observed.

Thus, there is evidence that particles are formed by chimeric VP7 proteins with large peptide inserts (up to 220 amino acids) in the top domain of the protein (Van Rensburg, 2005). Particles are also observed when a full length protein (240 amino acids) such as eGFP is attached to the

C-terminus of VP7 (Burger, 2005). What is lacking is information on whether a full length protein could be displayed on the top domain of VP7 and retain its tertiary structure. Furthermore, it would be interesting to see how the insertion of a soluble protein that is largely hydrophilic in the top domain of an AHSV VP7 vector would affect the overall chimeric protein. Reducing the overall hydrophobicity of the chimeric protein may result in a shift in the particles:trimers ratio that is observed. The expression of eGFP as part of the top domain of VP7 can be analysed by the functional aspect of the displayed protein – fluorescence – which is indicative of correct structural conformation.

The following chapter describes the first investigation into the effect of the insertion of a complete, functional protein into the top domain of an AHSV VP7 peptide display vector. The prototypal protein, eGFP is expressed as a fusion protein in site 177 of VP7mt177 protein (Maree, 2000). The resulting chimeric protein, VP7-177-eGFP, is investigated with regards to its fluorescence, the formation of particles/aggregates and any evidence of soluble trimers, as well as the kinetics of the assembly of the protein when recombinantly expressed in Sf9 cells. In addition, partially purified fractions containing the protein are tested for their ability to stimulate an immune response and generate antibodies specific to the displayed protein, eGFP.

2.2. Materials and Methods

2.2.1. *In silico* analysis of VP7-177-eGFP

The amino acid sequence of VP7-177-eGFP was analysed *in silico* to predict certain properties of the protein. The overall hydrophobicity of WT-VP7, VP7mt177 and VP7-177-eGFP proteins was calculated using the Protscale tool (Gasteiger et al., 2005), which is available on the Expasy server (http://ca.expasy.org/tools/protscale.html). The hydrophobicity scale used was that of (Kyte and Doolittle, 1982). This involved a sliding window analysis (window size 9) of amino acid sequences, with hydrophobicity scores of individual amino acids range from -4.5 (highly hydrophilic) to 4.5 (highly hydrophobic). Averages of windows are then plotted against the amino acid sequence. In addition, the protein VP7-177-eGFP was modelled using Modeller 8 (Fiser and Šali, 2003) on a Linux system. The structures that were used to model on were those of BTV VP7 trimers (PDB code: 1BVP) and a variant of eGFP (PDB code: 1CV7).

2.2.2. Plasmid construction – pFB-VP7-177-eGFP

The eGFP gene was amplified from a pGEM-Teasy-eGFP plasmid, kindly provided by Prof. J. Theron (University of Pretoria, Department of Microbiology). The plasmid pFB-VP7mt177 was previously constructed (Maree, 2000). The plasmid is pFastbac1 plasmid containing a modified AHSV9 VP7 gene. The modification consists of an 18 nucleotide insertion starting at position

548-549, containing the endonuclease recognition sites for 5' *Hin*dIII, *Xba*I and *Sal*I 3', respectively. At the peptide level this represents a six-amino acid insertion (KLSRVD) between the two arginine residues in positions 177 and 178 of the native AHSV serotype 9 VP7 protein. The primers used to amplify eGFP were thus designed to insert the eGFP gene into this site. The forward primer 5'd(GCAAGCTTATGGTGAGCAAGGGCGAG) contained a *Hin*dIII site and the reverse primer 5'd(GCGTCGACCTTGTACAGCTCGTC) contained a *Sal*I site, to allow directional cloning into the VP7 mt177 cloning site. For the purpose of a positive eGFP control a recombinant pFastBac1 containing the eGFP gene (henceforth referred to as pFB-eGFP) was obtained from a colleague (M. Victor, University of Pretoria).

2.2.3. Agarose gel electrophoresis

Agarose gel electrophoresis was used to analyse PCR amplification and restriction enzyme digestions. All DNA analysis was performed by separation on a 1% agarose gel, prepared in 1xTAE buffer (40mM Tris-HCl, 20mM Na-Acetate, 1mM EDTA) along with 1% Ethidium Bromide. All samples were analysed alongside appropriate DNA molecular weight markers (Fermentas). In the case of DNA fragments to be purified, samples were loaded onto a 0.8% agarose gel prior to excision.

2.2.4. Plasmid isolation

Plasmids were grown in *E.coli* cells (XLIBlue – Tet^R) on agar plates containing the appropriate selective antibiotics (pFastbac – Amp^R, Tet^R, $Gent^R$; VP7 mt177 – Amp^R, Tet^R, $Gent^R$; DH10Bac – Kan^R). Colonies containing potentially recombinant plasmids were picked and cultured overnight in LB-broth (1% Bacto-Tryptone, 0.5% Bacto-Yeast extract, 1% NaCl pH 7.4) containing the appropriate antibiotics. Plasmid DNA was extracted by the alkaline- lysis method as described by Sambrook and Russel (2001). Briefly, bacterial cells containing the recombinant plasmid were harvested at 5000rpm for 5 minutes. The pellet containing the cells was resuspended in 200 µl Solution I (50mM glucose, 10mM EDTA, 25mM Tris) and incubated on ice for 10 minutes. This was followed by the addition of 400 µl Solution II (0.2M NaOH, 1% vol/vol SDS), gentle mixing and incubation on ice for 5 minutes. 300 µl ice-cold Solution III (3M NaAc pH 4.8) was then added, gently mixed and incubated on ice for 15 minutes, to precipitate genomic DNA and proteins. This mixture was centrifuged at high speed (16 200 xg) for 10 minutes and the supernatant collected. Plasmid DNA was precipitated and collected by mixing this supernatant with 500 µl Propan-2-ol, incubating at -20°C for 60 minutes, followed by centrifugation at 16 200 xg for 10 minutes. The pellet containing plasmid DNA was washed once with 500 µl 70% EtOH, dried and resuspended in ddH_2O. To minimize the presence of DNAses and RNA in the plasmid solution, plasmid DNA was standardly purified (discussed below) using the GFX PCR Purification kit (Amersham Biosciences, Little Chalfont, Buckinghamshire UK), and re-eluted in ddH_2O.

2.2.5. DNA Purification

In the case of preparation of the eGFP PCR amplicon, as well as the pFastBac1-VP7mt177 plasmid for ligation, DNA was purified using the GFX Gel Purification Kit (Amersham Bioscience). The DNA was loaded onto a 0.8% agarose gel, and later excised using a razor blade. Purification was as per the manufacturer's specifications - the gel slice containing the band was dissolved in equal volume of capture buffer and the agarose denatured at 60°C for 60 minutes. The solution of dissolved agarose and DNA is then passed through a column by centrifugation, after which it is washed using a buffer containing 70% ethanol. The DNA is then eluted in ddH_2O.

2.2.6. Polymerase chain reaction (PCR)

PCRs were performed in a Perkin Elmer 9600 GeneAmp PCR system under the following conditions: an initial denaturation step at 95ºC for 5 minutes prior to adding Taq DNA Polymerase (Promega Corp., Madison, WI) followed by 35 cycles of denaturation (95ºC for 30s), primer annealing (53ºC for 30s) and elongation (72ºC for 45s), and a final elongation step (72ºC for 5 minutes). The 50 µl PCR reactions contained approximately 100ng template DNA, 100pmol of each primer, 1.25mmol each of dATP, dTTP, dGTP and dCTP, $MgCl_2$ (Promega) and 10X reaction buffer and 1U Taq DNA Polymerase (Promega).

2.2.7. Sequencing

DNA sequencing was performed in a Perkin Elmer 9600 GeneAmp PCR system using the ABI Prim Big Dye Terminator Cycle Sequencing Ready Reaction Kit™, V. 3.0. (Perkin Elmer Applied Biosciences), and an ABI Prism™ 310 genetic analyser. To confirm the insertion of the eGFP gene in the VP7mt177 gene a PCR product was generated from recombinant bacmids using the internal VP7 primers (forward primer 5'd(TTACGTACCGCAAGGTCG), which binds at position 423 of the VP7mt177 gene; and reverse primer 5'd(GAACCGTGGTCTAGCGATC), which binds at position 847 of the VP7mt177 gene). The PCR product was sequenced using eGFP specific primers (Forward primer 5'd(GCAAGCTTATGGTGAGCAAGGGCGAG) and reverse primer 5'd(GCGTCGACCTTGTACAGCTCGTC). Sequences were analysed using the ClustalX 2.0 software for Microsoft Windows (Thompson et al., 1997). Sequences for AHSV serotype 9 VP7 (gi|2149607) and eGFP (gi|186703059), obtained from NCBI (PubMed), were used as reference sequences in alignments.

2.2.8. Restriction endonuclease digestion and preparation of plasmid for subcloning

Restriction endonucleases were used in preparation of DNA prior to cloning, as well as after cloning, to confirm the insertion of the correct fragment. To prepare the plasmid pFastBac1-VP7mt177 for the insertion of the eGFP gene into site 177, the plasmid was digested in a two step reaction as follows: First, the plasmid was digested with *Hin*dIII for 4 hours according to the manufacturer's instructions. Following this step, a small portion was analysed by agarose gel

electrophoresis to confirm that the sample contained only linearized plasmid. This sample was then purified using the GFX Gel Purification Kit (Amersham Bioscience) and re-eluted in the original volume of ddH_2O. A second digestion step was performed using *Sal*I for 12 hours, followed by another column purification step, and elution in ddH_2O at ¼ of the original volume. The concentration, salt content and purity of the double-digested plasmid were verified using a spectrophotometer (NanoDrop Technologies, Wilmington, DE) prior to ligation.

2.2.9. Ligation of insert and vector

Sticky end ligations were performed in 20 µl reactions using 1.5U T4 DNA ligase (Boehringer – Mannheim) and a 10X reaction buffer. Reactions were left overnight at 16ºC for 14 hours. The final plasmid: insert concentration ratio was 1: 6.

2.2.10. Preparation of competent cells and transformation

E. coli XLIBlue cells were used for all transformations except during baculovirus expression, in which DH10Bac cells were used. XLIBlue Cells were made chemically competent using $CaCl_2$ as described by Sambrook and Russel (2001). In the case of making competent DH10Bac E. coli cells competent, the DMSO method was used (Chung and Miller 1988).

2.2.11. Transposition of recombinant VP7mt177-eGFP from pFastBac to Baculovirus genome

The Bac-To-Bac^{TM} Baculovirus expression system (Life Technologies) utilizes a site-specific transposition of an expression cassette into a shuttle vector (the bacmid bMON14272, 135Kb), which is a recombinant *Autographa californica* nuclear polyhedrosis viral (AcNPV) genome that can be replicated in *E.coli* cells. The bacmid contains a Kan^R site, a mini-F replicon and a LacZ *α* gene. Within the LacZ gene is a mini-att Tn7 site, which is the attachment site for the bacterial transposon Tn7. This transposon is contained in the pFastBac1 plasmid, into which the gene to be expressed is initially cloned. The recombinant pFastBac1-VP7mt177-eGFP plasmid was added to competent DH10Bac cells, left on ice for 30 minutes, followed by a heat-shock step for 45 seconds at 42℃. Thereafter, the mixture was left on ice for 3 minutes, and 750 ml TSBG/S.O.C. (1.6% Peptone, 1% yeast extract, 0.5% NaCl, 10% polyethyleneglycol, 1M $MgCl_2$, 1M $MgSO_4$, 0.02M glucose) medium added. The cells were left to grow for 4 hours at 37℃ to allow for the transposition of the recombinant gene into the baculovirus genome, then plated out on agar plates containing 100 µg/ml X-Gal, 40 µg/ml IPTG, 50 µg/ml Gentomycine, 10 µg/ml Kanamycine and 10 µg/ml Tetracycline, and allowed to grow for 48 hours at 37℃. Colonies containing putative bacmid recombinants were identified via blue-white selection. Several colonies were selected for DNA extraction and identification of the eGFP gene by PCR using eGFP specific primers.

2.2.12. Isolation of Recombinant Bacmid DNA

Candidate colonies containing recombinant bacmid DNA were re-streaked onto agar plates containing 100 µg/ml X-Gal, 40 µg/ml IPTG, 50 µg/ml Gentomycine, 10 µg/ml Kanamycine and 10µg/ml Tetracycline, and allowed to grow for 48 hours at 37℃ to verify the white phenotype. Once confirmed, single candidate colonies were picked and grown in 4 ml LB medium containing 50µg/ml Gentomycine, 10 µg/ml Kanamycine and 10 µg/ml Tetracycline for 12-16 hours. The protocol for isolating bacmid DNA was followed according to the manufacturer's instructions. DH10Bac cells containing recombinant bacmid were collected by centrifugation at 14 000 xg for 1 minute, resuspended simultaneously in 300 µl Solution I (50 mM glucose, 10 nM EDTA, 25 mM Tris) and 300 µl Solution II (0.2 M NaOH, 1% vol/vol SDS) and incubated at room temperature for 5 minutes. Thereafter, 300 µl ice-cold Solution III (3 M KAc pH 5.5) was added to precipitate proteins and genomic DNA, the mixture centrifuged at 14 000 xg for 15 minutes and the supernatant collected. The bacmid DNA was precipitated and collected by mixing this supernatant with 800 µl Propan-2-ol (isopropanol), incubating on ice for 15 minutes, followed by a centrifugation (14 000 g) for 15 minutes. The pellet containing plasmid DNA was washed twice with 500 µl 70% EtOH, dried and resuspended in ddH_2O.

2.2.13. Sf9 Cell culture

Spodoptera frugiperda (Sf9) cells (ATCC cells purchased from the American Type Cell Collection) were maintained in 50-100ml cultures in Pyrex flasks at manufacturer-recommended conditions. At all times Sf9 cells were kept at 27℃, maintained in TC100 Insect Medium (Highveld biological, Lyndhurst, Sandton) supplemented with 10% (vol/vol) foetal calf serum (FCS – Highveld Biological), 1.2% penicillin, streptomycin and Fungizone (Highveld Biological), as well as 0.8% pleuronic (Highveld Biological). Cultures were regularly maintained prior to transfection or infection, and their growth rate was closely followed and compared with expected growth rate, to ensure optimal viral replication and/or protein expression conditions.

2.2.14. Transfection of SF9 cells with recombinant Bacmid DNA

Transfections took place in 6 well plates according to the manufacturers instructions. 35 mm wells were each seeded with 1 X 10^6 cells, obtained from a suspension culture in mid-log phase, along with 2 ml TC100 Insect Medium (Highveld biological) supplemented with 10% (vol/vol) foetal calf serum (FCS – Highveld Biological), 1.2% penicillin, streptomycin and Fungizone (Highveld Biological). The cells were allowed to attach for 1 hr at 27℃, and their confluence confirmed. Two solutions were prepared separately, Solution A (approximately 100µg recombinant Bacmid DNA diluted in 100 µl pure TC100 medium) and Solution B (6 µl CellFECTIN™ Reagent -Invitrogen Life Technologies) diluted in 100 µl pure TC100 medium. Solutions A and B were mixed gently and incubated at room temperature for 45 minutes. The TC100 medium from the confluent Sf9 monolayers was aspirated, the cells washed twice with 2 ml clean TC100 medium, and overlayed with 1 ml of the diluted Bacmid DNA-CellFECTIN

mixture. These cells were left for approximately 16 hours for the Bacmid DNA to be transfected into the Sf9 cells. After 16 hours, the transfection mixture was removed and replaced with 2 ml TC100 Insect Medium (Highveld biological) supplemented with 10% (vol/vol) foetal calf serum (FCS – Highveld Biological), 1.2% penicillin, streptomycin and Fungizone (Highveld Biological), and left for a further 72 hours to generate recombinant baculoviruses. At this stage recombinant baculovirus socks were harvested and titred, and the cells assayed for recombinant protein production by means of SDS-PAGE, Western blotting and Fluorescence analysis.

2.2.15. Recombinant virus stock amplification

Prior to infection of Sf9 cells for recombinant protein production, recombinant baculovirus stocks of known titre were amplified in 50ml suspension cultures by infecting at a multiplicity of infection (M.O.I.) of 0.1, the maximum M.O.I. recommended by baculovirus manual for baculovirus amiplification. Cells from an Sf9 suspension culture of 50 ml (1 X 10^6 cells/ml) were collected by centrifugation for at 500 xg for 30 minutes, and resuspended in 2 ml viral stock for an MOI of 0.1. Viruses were harvested and titred 48 hours post infection (p.i.), and the cells analysed for fluorescence to confirm expression of recombinant eGFP proteins.

2.2.16. Sf9 cells Infections

Baculovirus infections of Sf9 cells Infections took place either in confluent monolayer cultures (6 well plates (1 X 10^6 cells), 25 cm^3 (3.5 X 10^6 cells) or 75 cm^3 (1 X 10^7 cells)), or suspension cultures (50 ml (5 X 10^7 cells) or 100 ml (1 X 10^8 cells)), depending on the nature of the experiment. Cells were counted using a haemocytometer under a light microscope. For all protein expression experiments cells were infected at an M.O.I. of 5-10 p.f.u/cell. Cells were harvested at different times after infection depending on the nature of the experiment. Expression of eGFP recombinant proteins was confirmed by SDS-PAGE, Western blotting and Fluorescence analysis.

2.2.17. Fluorescence analysis

Fluorescence measurements were taken either using a fluorometer or a Fluoroskan™ Ascent FL Type 374 (Thermo Lab Systems). For the purpose of measuring fluorescence in fractions of sucrose after gradient sedimentation experiments (see below), either of these fluorometers was used. While the absolute values obtained from readings differed, a simple experiment confirmed that the relative proportion of fluorescence in each fraction of the sum total fluorescence in all fractions was comparable (within 0.5%, results not shown). To observe fluorescence in the cells using epifluorescent microscopy, 6-well plates were infected (1 x 10^6 cells per well, M.O.I. of 5-10 p.f.u.) and observed 48 hours post infection under a Zeiss Axiovert 200 Fluorescent microscope.

2.2.18. Sodium dodecyl sulphate polyacrylamide gel electrophoresis (SDS-PAGE)

For protein analysis directly from SF9 cells, samples were mixed vol/vol with protein solvent buffer (PSB – 4% SDS, 20% glycerol, 10% 2-mercaptoethanol, 0.005% Bromophenol Blue, 0.125 Tris-HCl pH 6.8) and incubated at approximately 95% for 10 minutes for denaturation. These samples were then analysed on a 12% polyacrylamide gel (12% polyacrylamide; 0.375 M Tris-HCl, pH 8.8; 0.1% SDS; 0.01% TEMED; 0.1% ammonium persulphate) with a 5% stacking gel (5% polyacrylamide; 0.125 M Tris-HCl, pH 8.8; 0.1% SDS; 0.01% TEMED; 0.1% ammonium persulphate). To estimate the molecular weight of proteins, an appropriate marker was used alongside the samples (Rainbow Marker™, RPN 756, Amersham biosciences). Gels were electrophoresed at 140V using a Hoefer™ II SE 250 mini-vertical gel electrophoresis unit (Amersham Biosciences) for 2-3 hours. Proteins on the gel were visualized by staining with Coomassie Blue staining solution (0.125% Coomassie blue, 50% methanol, 10% acetic acid) for 30-45 minutes, followed by destaining at room temperature for 16-48 hours in 5% methanol, 5% acetic acid. For experiments involving proteins purified from a sucrose gradient, protein solvent buffer was prepared as stated above, with the exception of glycerol. This was done to minimize the distortion of samples on a gel caused by too much glycerol and sucrose in the sample.

2.2.19. Sucrose sedimentation gradients, analysis-scale

For general recombinant protein analysis, 50 X 10^6 cells expressing VP7-eGFP were collected 48 hours post infection by centrifugation at 5000 rpm for 5 minutes, discarding the supernatant. The cells were re-suspended in 400 µl STE (0.01M NaCl, 0.01M Tris, 0.05M EDTA) containing 0.5% non-ionic detergent (Triton X100 or NP40) as well as protease inhibitors (Pepstatin and Pefabloc, maximum amounts recommended by manufacturer) and left on ice for 30 minutes. The cells were then lysed mechanically by means of a dounce. A discontinuous sucrose gradient was prepared from bottom to top containing equal volumes (4.8 ml total) of 70%, 65%, 60%, 55% and 50% sucrose, upon which all of the cell lysate was loaded. The sucrose gradients were then centrifuged (Beckman Ultracentrifuge) using a Beckman SW55 rotor at 40 000 rpm (151 000 xg) for 18 hours. 19-21 fractions of approximately 250 µl (descending density) were collected and samples from these fractions were analysed using a fluorometer as well as by SDS-PAGE.

2.2.20. Sucrose sedimentation gradients, purification-scale

For large scale recombinant protein purification experiments, 100 X 10^6 Sf9 cells expressing VP7-eGFP were collected 48 hours post infection by centrifugation at 5000 rpm for 5 minutes, discarding the supernatant. The cells were re-suspended in 4ml STE (0.01 M NaCl, 0.01 M Tris, 0.05 M EDTA) containing 0.5% non-ionic detergent (Triton X100 or NP40) as well as protease inhibitors (Pepstatin and Pefabloc, maximum amounts recommended by manufacturer) and left on ice for 30 minutes. The cells were then lysed mechanically by means of a dounce. A

discontinuous sucrose gradient was prepared from bottom to top containing equal volumes (20 ml total) of 70%, 65%, 60%, 55% and 50% sucrose, upon which all of the cell lysate was loaded. The sucrose gradients were then centrifuged using a Beckman SW28 rotor at 20 000 rpm (53 000 xg) for 18 hours. 30-33 fractions of approximately 750 µl (descending density) were collected using a, which were analysed using a fluorometer and/or by SDS-PAGE.

2.2.21. Time trial analysis of the Kinetics of VP7 trimer / particle formation.

Two separate suspension cultures of 50 X 10^6 Sf9 cells were infected 12 hours apart with equal amounts of recombinant baculovirus expressing VP7-eGFP. 1 X 10^6 cells were collected at 18 hours post infection and every representative 6 hours thereafter, up to 90 hours post infection. Cells were collected by centrifugation at 200 g for 5 minutes, after which the TC100 medium in which the cells were growing was separated and kept, and the cells were resuspended in 1 ml STE (0.01 M NaCl, 0.01 M Tris, 0.05 M EDTA) containing protease inhibitors (Pepstatin and Pefabloc). The medium and cells were frozen and kept at -80℃ until all representative samples were collected. Each sample of cells was treated with NP40 for 30 minutes, the cells lysed mechanically by means of a dounce, and collected by centrifugation for 10 minutes at 16 200 xg (benchtop centrifuge) to separate soluble and insoluble components. The insoluble component (pellet) was re-suspended in 1 ml STE (0.01 M NaCl, 0.01 M Tris, 0.05 M EDTA). Thereafter, fluorescent measurements of each component (soluble, insoluble, medium) were taken for each representative sample. To account for background fluorescence, samples were also taken pre-infection, as well as at 0 hours (immediately after infection).

2.3 Results

2.3.1. *In silico* analysis of VP7-177-eGFP

The amino acid sequences of WT-VP7, VP7mt177 and VP7-177-eGFP proteins were compared in terms of hydrophobicity using Protscale (2.2.1). The results can be seen in Fig. 2.1. The insertion of eGFP in the modified VP7mt177 protein (Fig. 2.1. C) results in the VP7-177-eGFP protein having a lower predicted overall hydrophobicity as compared to WT-VP7 or VP7mt177 proteins.

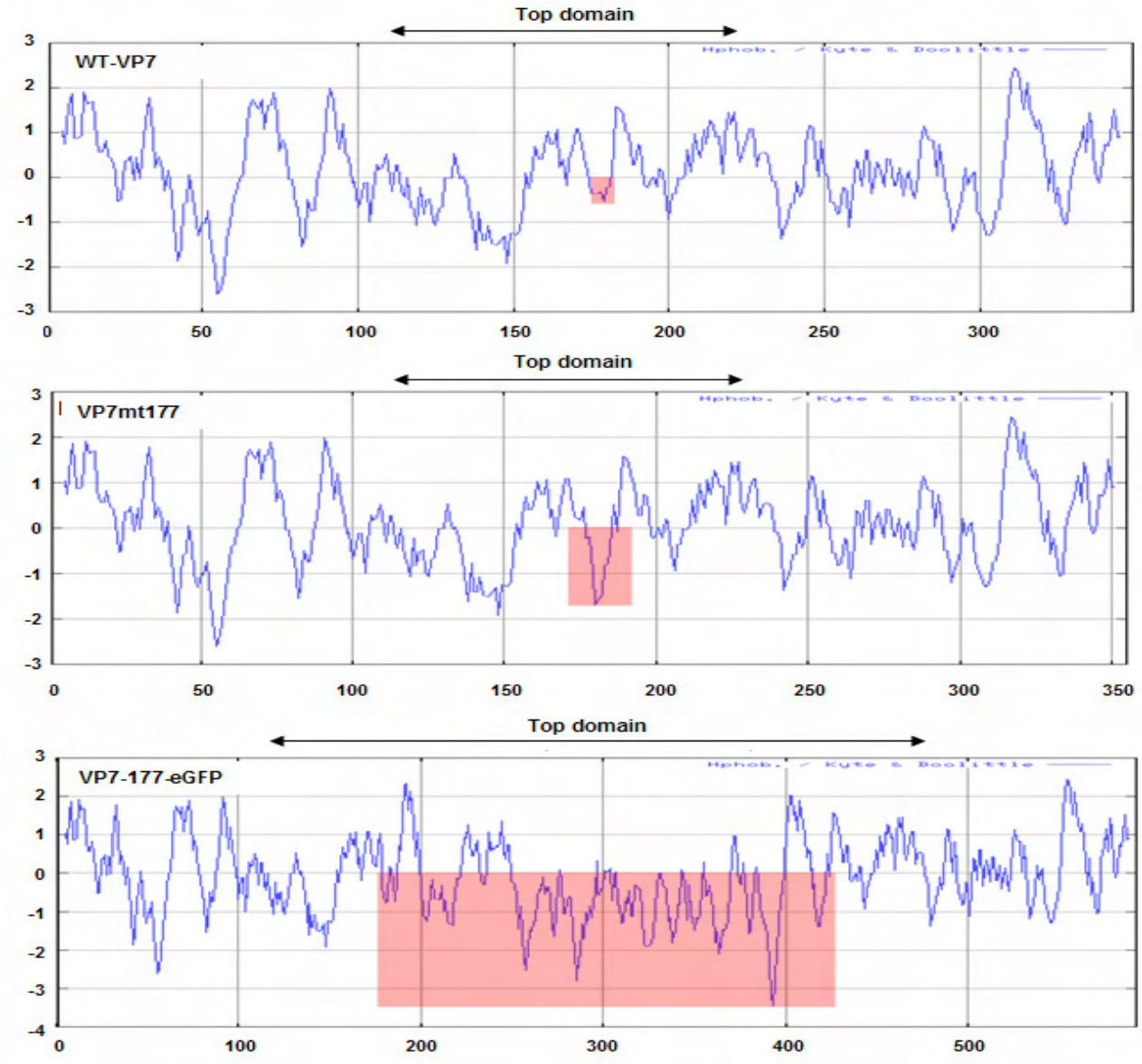

Figure 2.1. Hydrophobicity plots (Kyte and Doolittle, 1982) were generated for amino acid sequences of AHSV serotype 9 WT-VP7 (A), VP7mt177 (B) and VP7-177-eGFP (C). Negative values on the Y-axis indicate relative hydrophilicity, while positive values indicate relative hydrophobicity. The amino acid positions are indicated on the X-axis. The RGD loop present in WT-VP7 is highlighted in A. The modified and extended loop in site 177 (Maree, 2000), showing higher hydrophilicity in the modified VP7mt177 protein is highlighted in B. For VP7-177-eGFP (C), the eGFP insertion in the modified VP7mt177 protein is highlighted. It is apparent that eGFP represents a highly hydrophilic insertion.

In addition to hydrophobicity plots, the protein VP7-177-eGFP was modelled using the predicted sequence of VP7-177-eGFP and previously determined structures of BTV VP7 (PDB code: 1BVP) and a variant of eGFP (PDB code: 1CV7). Fig. 2.2 shows the structure of BTV trimers (left half) and the predicted structure of VP7-177-eGFP (right half). The modelled structure of VP7-177-eGFP (Fig. 2.2, right half) indicates that the displayed epitope, eGFP, does not interfere with the contact sites required for trimer formation.

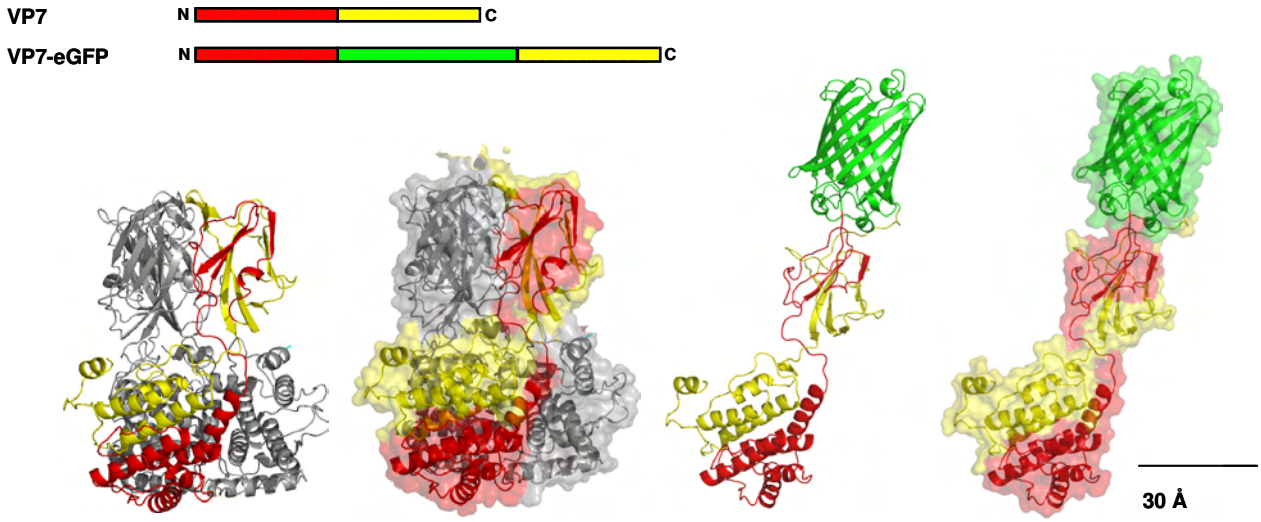

Figure 2.2. A comparison of BTV VP7 trimers and the modelled structure of a VP7-177-eGFP monomer. Trimers of BTV VP7 (PDB code: 1BVP) are shown in the left half, with and without a surface representation of the proteins. The modelled VP7-177-eGFP is represented analogously in the right half. One VP7 monomer is highlighted in each representation, with the N-terminal region preceding aa 178 shown in red and the C-terminal region following aa 177 shown in yellow. EGFP is represented in green. Primary structures of VP7 proteins are represented (top left), with colours corresponding to the structures. Images were generated using PyMOL v0.99 (Delano, 2002).

2.3.2.1. Construction of recombinant bacmid containing VP7-177-eGFP gene

The first aim of the project was to recombinantly insert the eGFP coding region into the coding region of one of the previously constructed VP7 insertion vectors, and express the resulting fusion protein by means of a baculovirus recombinant. The resulting chimeric protein would be expressed in such a way that the eGFP is displayed on the top domain of VP7. Three different insertions sites at amino acid positions 144, 177 and 200 of the VP7 protein were available from previously created vectors. It was decided that the VP7mt177 protein will be used for insertion because of promising results observed previously.

The cloning strategy of the gene VP7-177-eGFP is summarized in Fig. 2.1. Briefly, the strategy involved sub-cloning the eGFP coding sequence into a previously constructed pFastBac1 plasmid (Invitrogen) containing AHSV 9 VP7mt177 gene (Maree, 2000). This recombinant plasmid, designated pFB-VP7mt177, contains the modified AHSV-9 VP7 gene, 1168 nucleotides in length, with unique restriction enzyme sites *Hin*dIII, *Xba*I and *Sal*I incorporated at positions 548, 554 and 560, respectively. To facilitate directional subcloning of the eGFP gene into the VP7mt177 gene present in the plasmid pFB-VP7mt177, primers were designed to include the restriction endonuclease sites *Hin*dIII at the 5' end and and *Sal*I at the 3' end of the eGFP gene. The cloning procedure is summarized in Fig. 2.3.

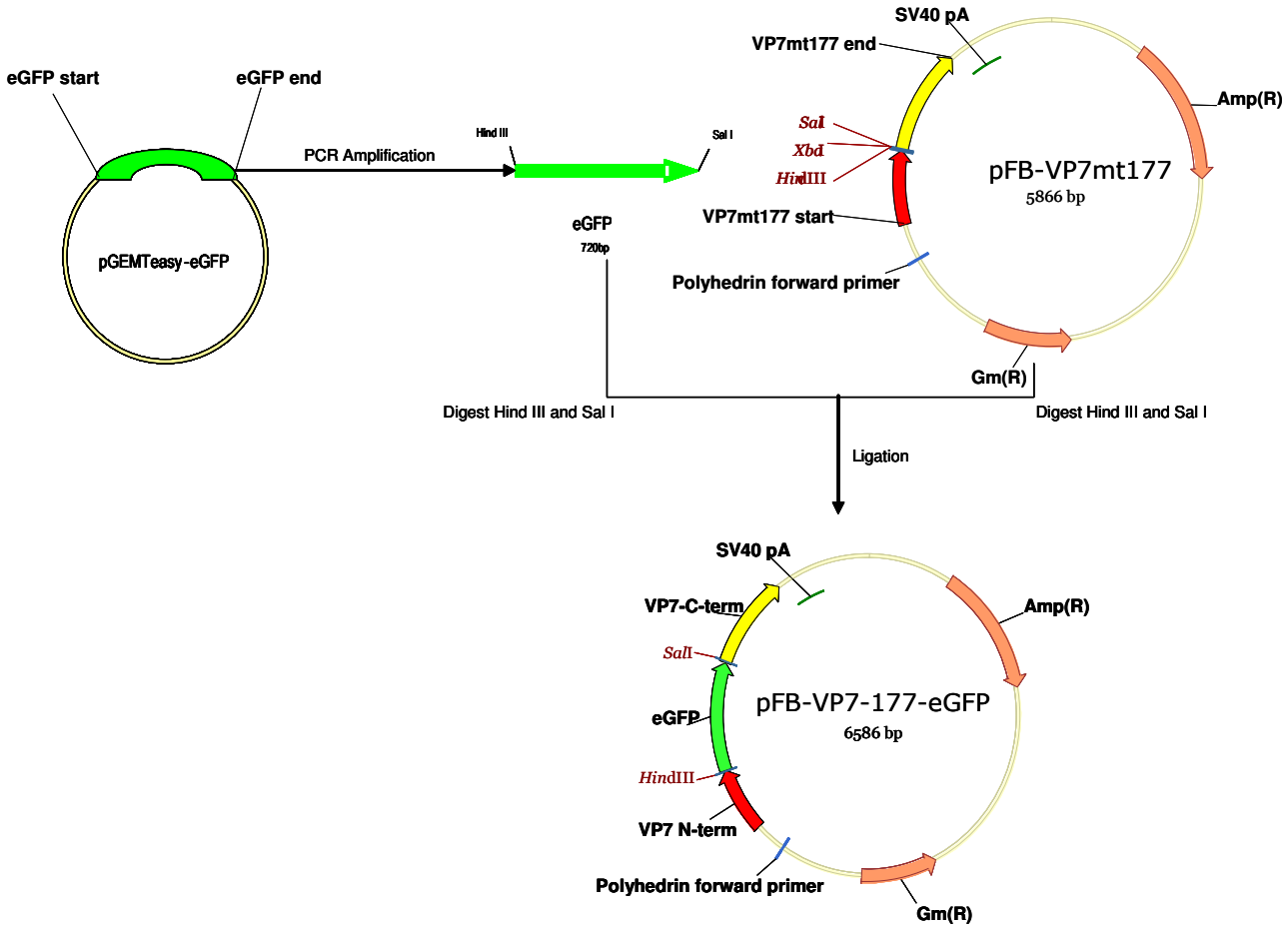

Figure 2.3. Strategy summarizing the cloning procedure resulting in the pFastBac plasmid containing the gene VP7-177-eGFP. The eGFP gene was amplified by PCR from pGEM-TEasy-eGFP, a plasmid containing the eGFP gene, using primers that include the endonuclease recognition sites *Hin*dIII (forward primer) and *Sal*I (reverse primer). The PCR amplicon as well as the target vector pFB-VP7mt177 were digested using *Hin*d III and *Sal*I, and ligated to each other, resulting in the recombinant plasmid pFB-VP7-177-eGFP. The VP7mt177 gene is shown as two halves, coding for the N-terminal half and the C-terminal half of the protein (VP7 N-term and VP7-C-term, respectively). The coding region is divided by the cloning sites 5' – *Hin*dIII, *Xba*I and *Sal*I – 3'.

The eGFP gene was amplified by PCR (2.2.6) from a pGem-TEasy plasmid containing the eGFP gene as a template. The eGFP-specific forward primer 5'GCAAGCTTATGG-TGAGCAAGGGCGAG, containing a *Hin*dIII recognition site (underlined) was used, along with the reverse primer 5'GCGTCGACCTTGTACAGCTCGTC, containing a *Sal*I recognition site (underlined). A DNA fragment of the expected size, 720 base pairs (bp), was amplified and identified by agarose gel electrophoresis (results not shown). Subsequently, this fragment was purified by agarose gel excision and column purification, and prepared for cloning by a double endonuclease digestion using *Hin*dIII and *Sal*I. Simultaneously, the plasmid pFB-VP7mt177 was prepared by endonuclease digestion using *Hin*dIII and *Sal*I. This was followed by the directional ligation of the prepared vector and insert molecules, and transformation into competent *E. coli* (XLI Blue) cells.

The transformed *E. coli* (XLI Blue) cells containing putative recombinant plasmids were grown and selected using appropriate antibiotics, followed by plasmid isolation (2.2.4). Putative recombinant plasmids were selected on the basis of molecular weight (expected size 6450 bp), and confirmed by screening for the eGFP gene by PCR using eGFP-specific primers. One recombinant plasmid was selected from which a fragment of the expected size (720 bp, Fig.2.4, lane 2) was amplified, and this plasmid was subsequently designated pFB-VP7-177-eGFP.

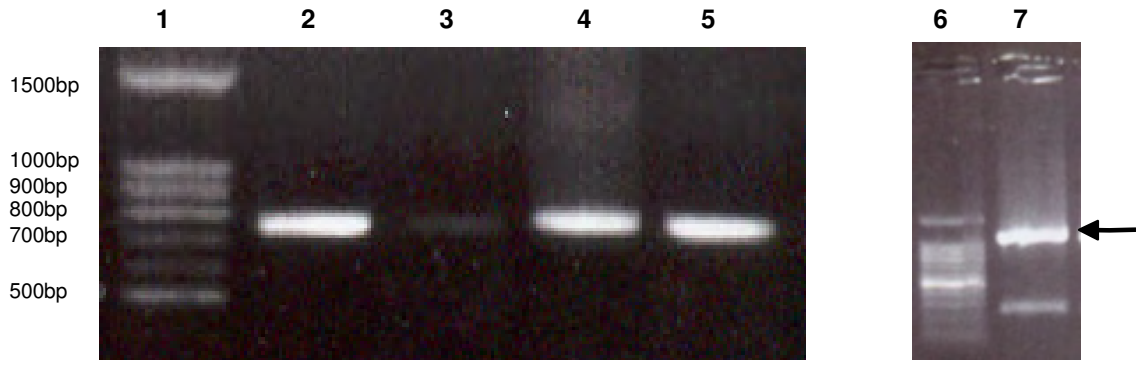

Figure 2.4. The presence of the eGFP gene (720bp) was confirmed by PCR. Lanes 1 and 6: 100bp ladder (Fermentas). eGFP-specific primers were used to amplify a 720bp fragment from plasmids pFB-VP7-177-eGFP (lane 2) and pGEM-TEasy-eGFP (lane 4), as well as from recombinant bacmid DNA (lanes 3 and 5). VP7-specific primers were used to amplify a 1100bp fragment (lane 7) from the same bacmid sample used in lanes 3 and 5.

Following this confirmation the recombinant VP7-177-eGFP gene was transposed into the Baculovirus genome (2.2.11). Putative DH10Bac cells containing recombinant baculovirus genomes were identified by blue-white selection of the DH10Bac colonies, and confirmed by PCR amplification of a 720bp fragment using eGFP-specific primers (Fig. 2.4, lane 5). One white colony was selected and further characterized to confirm the recombinant Baculovirus plasmid DNA contained the eGFP gene in the correct site within VP7mt177. VP7-specific internal primers flanking the cloning site within the VP7mt177 gene were used for a PCR amplification of a fragment 1100bp in size (fig. 2.4, lane 7) from recombinant bacmid DNA. The size of this fragment corresponds to the expected size of a 720bp insert (eGFP gene), as the primers are approximately 380 bp apart in the VP7 gene.

This fragment was subsequently used as a template for automated sequencing, using eGFP specific primers. DNA sequencing confirmed the correct sequence of the eGFP gene, as well as its flanking regions specific to the VP7mt177 gene (results not shown). Translation of the nucleotide sequence into amino acid sequence verified the presence of a single open reading frame. Once the sequence had been confirmed, the bacmid DNA was transfected in Sf9 cells (2.2.14.) to obtain recombinant baculoviruses.

2.3.2.2 Expression of VP7-177-eGFP protein

Sf9 cells were transfected with recombinant bacmids in order to produce recombinant baculoviruses expressing VP7-177-eGFP, VP7mt177 and eGFP. Epifluorescent microscopy and western blot detection were used to analyse expression of recombinant proteins. *Sf*9 cells expressing VP7-177-eGFP (Fig. 2.5 C) were fluorescent when viewed at 489nm using a fluorescent microscope (Fig. 2.5 D and E). Fluorescence was distributed throughout the cells, with randomly situated fluorescent clusters present in the cytoplasm of some of the cells. The fluorescence of VP7-177-eGFP was a positive indicator of correct structural conformation of the eGFP protein. Cell lysates were also analysed by SDS-PAGE, followed by Coomassie staining (Fig. 2.5 A). Bands were clearly visible at the expected positions in lanes 4, 5 and 6, corresponding to the sizes of VP7mt177 (39kDa), VP7-177-eGFP (67kDa) and eGFP (27kDa), respectively. To confirm that these bands were indeed representative of these proteins, a Western blot was performed with an anti-eGFP primary antibody (Fig. 2.5 B). The serum reacted with VP7-177-eGFP and eGFP (Fig. 2.5 B, lanes 5 and 6, respectively) and not with VP7mt177 (lane 4).

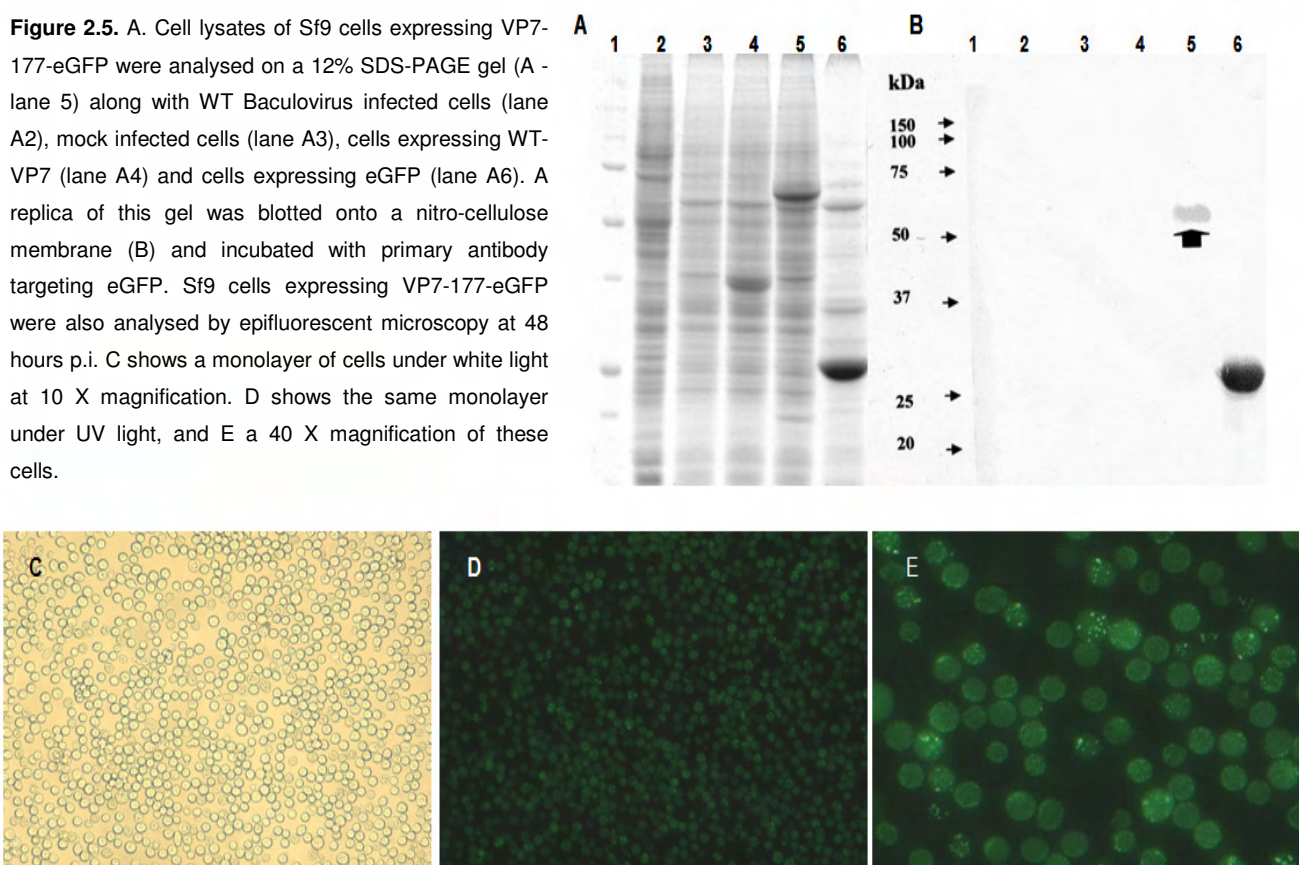

Figure 2.5. A. Cell lysates of Sf9 cells expressing VP7-177-eGFP were analysed on a 12% SDS-PAGE gel (A - lane 5) along with WT Baculovirus infected cells (lane A2), mock infected cells (lane A3), cells expressing WT-VP7 (lane A4) and cells expressing eGFP (lane A6). A replica of this gel was blotted onto a nitro-cellulose membrane (B) and incubated with primary antibody targeting eGFP. Sf9 cells expressing VP7-177-eGFP were also analysed by epifluorescent microscopy at 48 hours p.i. C shows a monolayer of cells under white light at 10 X magnification. D shows the same monolayer under UV light, and E a 40 X magnification of these cells.

Following these observations, supernatant from transfected cells containing recombinant baculoviruses was harvested and baculovirus stocks were amplified in suspension cultures.

VP7-177-eGFP baculovirus stocks were then titred. In addition, amplified and titred baculovirus stocks expressing VP7-C-eGFP were obtained (L. Burger, University of Pretoria) and expressed in *Sf*9 cells to use in comparative analysis to VP7-177-eGFP. Fig. 2.6 shows fluorescent micrographs of Sf9 cells expressing VP7-C-eGFP (A), VP7-177-eGFP (B), and eGFP (C). VP7-C-eGFP had a similar fluorescence pattern to VP7-177-eGFP, while in cells expressing eGFP fluorescence was uniformly distributed within cells. The heterologous display of fluorescence evident in the cytoplasm of cells expressing VP7-C-eGFP and VP7-177-eGFP may be related to VP7-mediated aggregation.

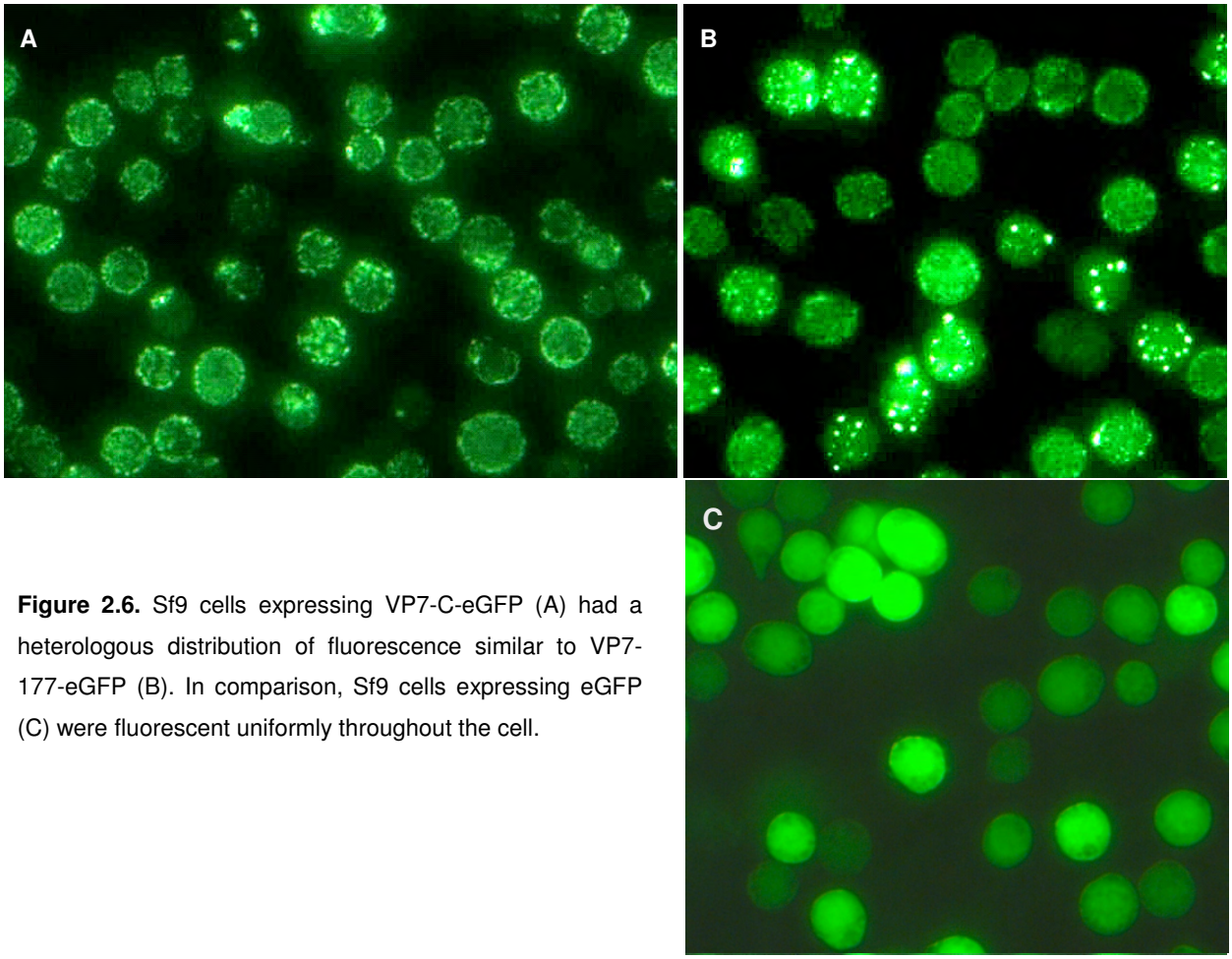

Figure 2.6. Sf9 cells expressing VP7-C-eGFP (A) had a heterologous distribution of fluorescence similar to VP7-177-eGFP (B). In comparison, Sf9 cells expressing eGFP (C) were fluorescent uniformly throughout the cell.

2.3.3. Sucrose sedimentation analysis of VP7-177-eGFP

In order to characterize the expression of VP7-177-eGFP, the protein was analysed via a discontinuous sucrose sedimentation gradient. This method had been used previously in AHSV VP7 vector research to partially purify VP7 particles. Total cell lysates of 1 X 10^8 Sf9 cells expressing VP7-177-eGFP were loaded on top of a 50%-70% discontinuous sucrose gradient (Equal proportions descending in 5% increments, top to bottom), and centrifuged at 53 000 xg for 18 hours. The cells were treated chemically with a non-ionic detergent as well as lysed mechanically by means of a dounce prior to differential centrifugation (2.2.20).

After differential centrifugation, the sucrose gradient was fractionated from the bottom into 34 fractions of approximately 750 µl each. Since the protein VP7-177-eGFP had already been shown to be fluorescent in cells where it is expressed, an equal proportion of each fraction was measured using a fluorometer. The proportion of fluorescence in each fraction was then calculated out of the combined fluorescence of all fractions, and the values were plotted as a line graph (Fig. 2.7). This experiment was performed to determine if fluorescence would be accurately representative of the amount of VP7-177-eGFP, to be used in subsequent sucrose sedimentation profiles. Two general peaks were observed, indicating differential centrifugation patterns of total VP7-177-eGFP proteins. A major peak accounting for 55% of total fluorescence was localized at the top part of the gradient, representing the soluble protein fraction of infected cells (Fig. 2.7, fractions 25-30). The second peak, accounting for 19% of the total fluorescence was localized at the lower third of the gradient, representing the insoluble protein fraction of infected cells (fractions 6-13).

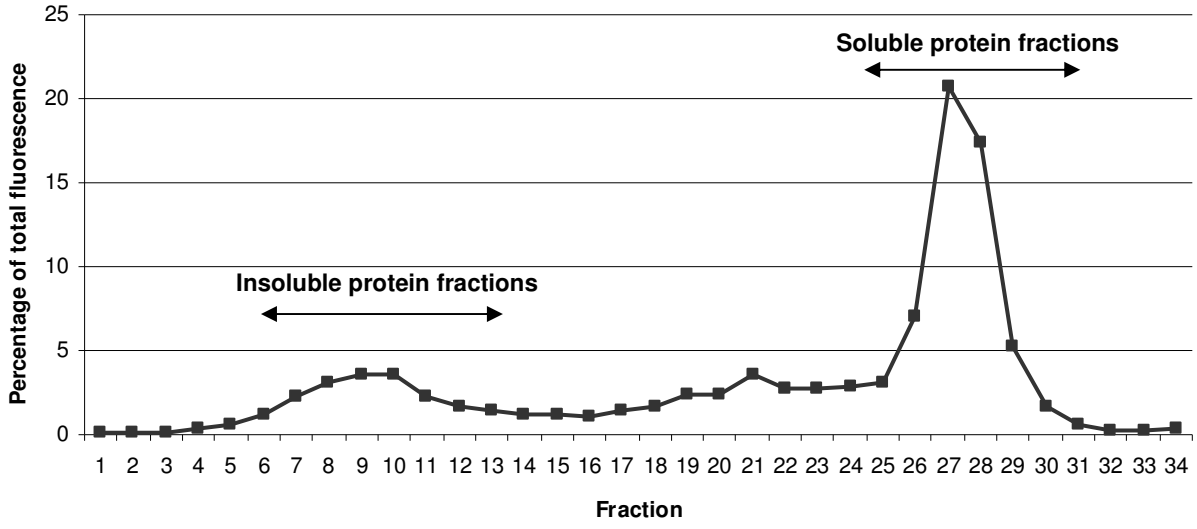

Figure 2.7. Graph showing the relative proportion of VP7-177-eGFP fluorescence in each fraction collected from a large scale sucrose sedimentation gradient. Two peaks of fluorescence were identified at fractions 6-13 and 25-30.

Each of the fractions was also analysed by SDS-PAGE analysis (Fig. 2.8). A band corresponding to the predicted size of VP7-177-eGFP (69kDa) occurred almost throughout the entire gradient, in fractions 5-30. The absolute quantities of VP7-177-eGFP were measured in each lane on the gel using SigmaGel™, and the proportion from each fraction was calculated as a percentage from the total (Fig. 2.9 B). Of the total VP7-177-eGFP protein, 91% was localized to three groups fractions: fractions 6-13 (46%), fractions 17-24 (26%) and fractions 25-30 (19%). The relative proportion of VP7-177-eGFP in each fraction on SDS-PAGE was very different from that indicated by fluorescence, suggesting that there were differences in the fluorescence/unit of VP7-177-eGFP protein.

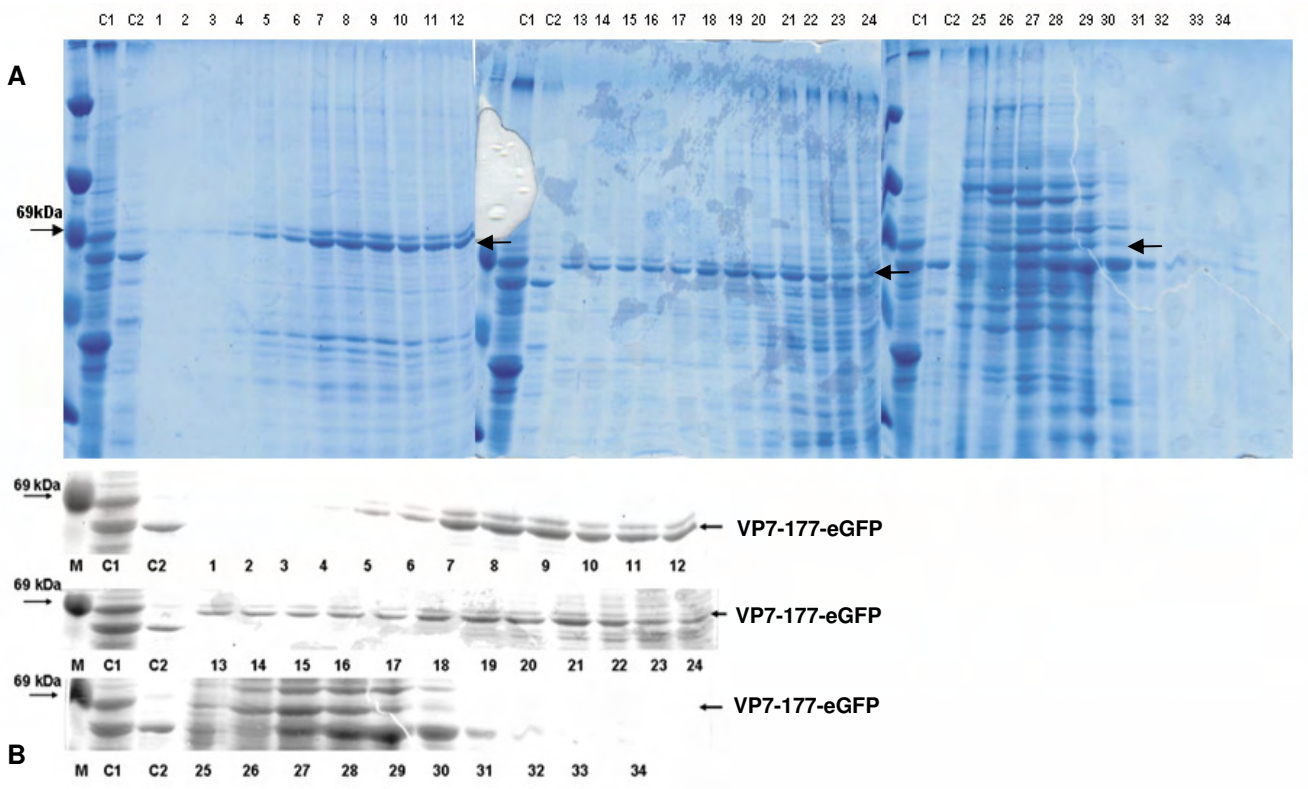

Figure 2.8. A. SDS-PAGE profiles of a large scale sucrose gradient sedimentation of Sf9 cells expressing VP7-177-eGFP. M – molecular weight marker. C1, total cell lysate of Sf9 cells expressing VP7-177-eGFP. C2, WT Baculovirus infected cells. Fractions were numbered 1 (highest density collected from the bottom) to 34, and an equal proportion of each fraction was analysed. Arrows indicate the position of VP7-177-eGFP. The protein occurred almost throughout the gradient, from fraction 5-30, although it was prominently found in the bottom third (higher density) of the gradient, consistent with previous chimeric AHSV VP7 research. B. The region of the SDS-PAGE gel in A where VP7-177-eGFP is found.

Figure 2.9 C shows the combined profiles of proportion of protein in each fraction as measured by fluorescence (solid line) or SDS-PAGE quantification (dashed line). It is evident that VP7-177-eGFP's sedimentation profile as determined by fluorescence was distinctly different from that determined by total protein quantification. Only 19% of the fluorescence was accounted for in fractions 6-13 as compared to 43% of total protein calculated for these fractions. In contrast, 55% of fluorescence is represented in the major peak at the top third of the gradient (fractions 25-30), where only 19% of total protein was present, shown by SDS-PAGE analysis.

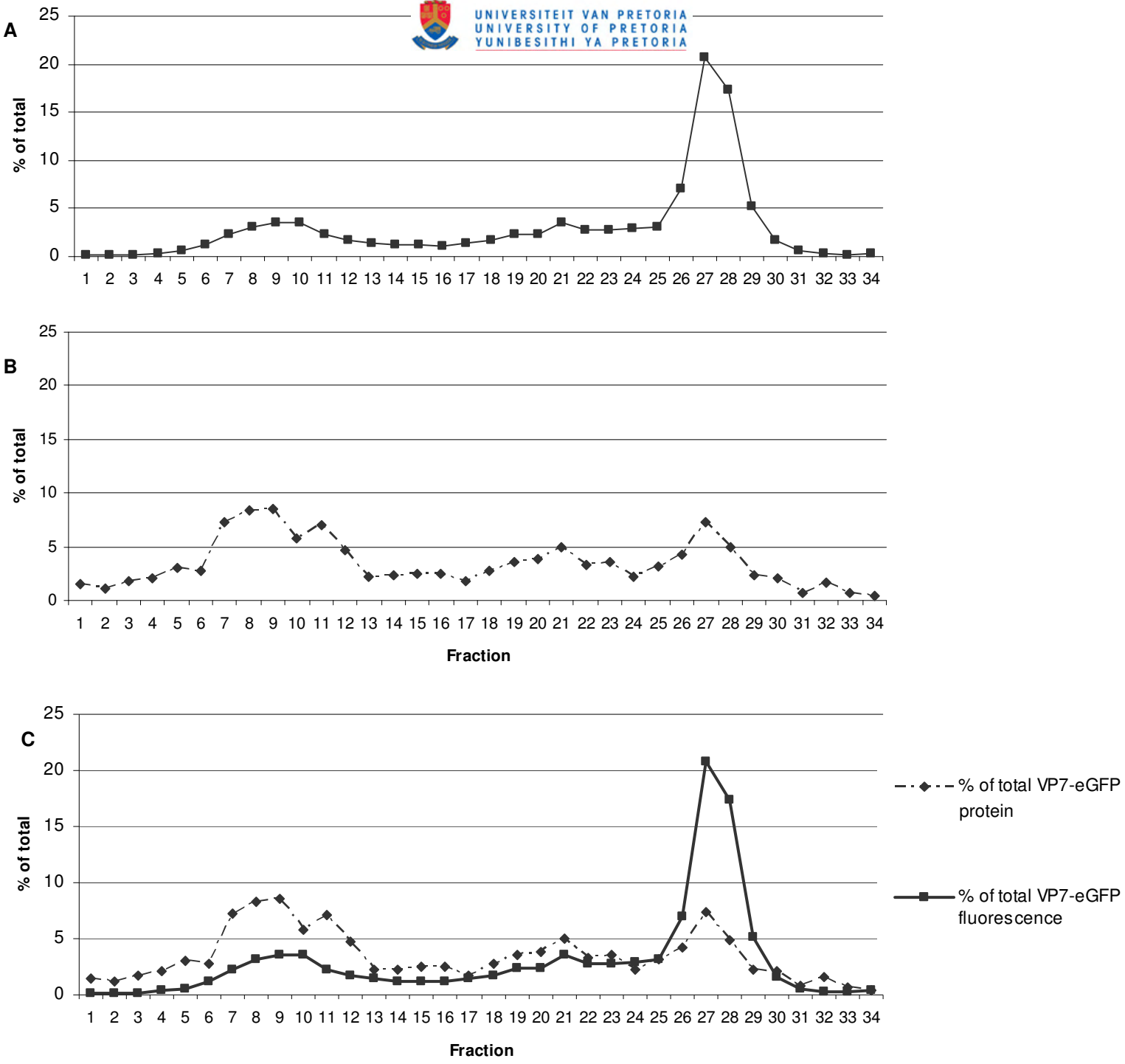

Figure 2.9. Graphs showing the proportion of VP7-177-eGFP protein in each fraction of a sucrose gradient as measured by fluorescence (A) and SDS-PAGE analysis (B). C shows the two patterns on the same graph. Results according to fluorescence indicated that most of the VP7-177-eGFP protein was present in the top third of the gradient, while the opposite was indicated by SDS-PAGE analysis.

A peak at the bottom third of the density gradient (Fractions 6-13) has been shown in previous studies to represent chimeric AHSV VP7 particles. The peak around fractions 26-29 contained the bulk of the cellular soluble proteins and presumably therefore also soluble VP7-177-eGFP, possibly representing protein monomers, dimers or trimers. It is clear from Fig. 2.9 C that the ratio of fluorescence to VP7-177-eGFP concentration changes significantly in the region of the

soluble protein fraction from the particulate fraction. To quantify this, the ratio of fluorescence/unit of VP7-177-eGFP was calculated for each fraction using absolute values of fluorescence and protein concentration, and the resulting values are depicted in Fig. 2.10. The ratio value remains more or less the same until between fractions 6-18, after which there is a slow increase in the ratio between fractions 18-24, followed by a sharp increase until the maximum is reached at the top fractions 26-29. The decrease in ratio calculated after fraction 29 probably occurred because of low absolute values of fluorescence.

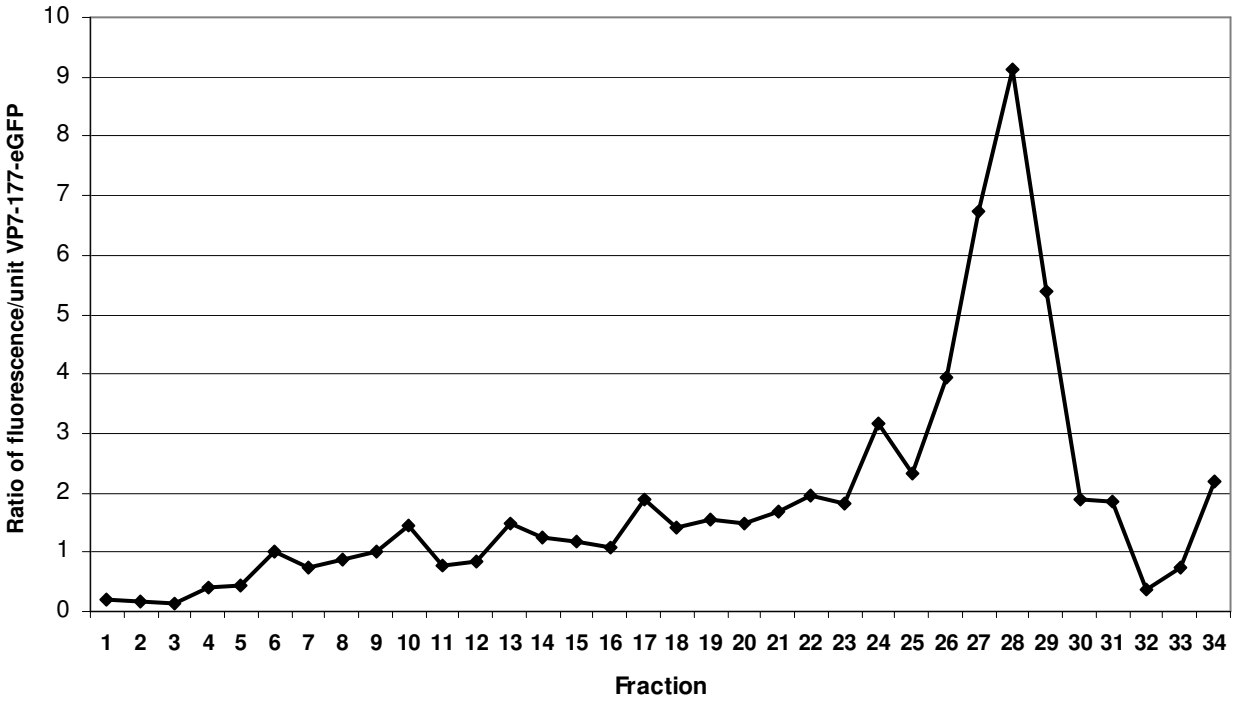

Figure. 2.10. The ratio of fluorescence/unit protein of VP7-177-eGFP was calculated for each fraction of a sucrose sedimentation gradient (shown in Fig. 2.8) using absolute values of fluorescence and protein concentrations. Fractions 25-29 display up to a nine-fold increase in fluorescence/unit protein as compared to fractions representing insoluble VP7-177-eGFP (6-13).

There was an unexpected variation in the ratio of fluorescence relative to the form of the protein, with the soluble fractions of VP7-177-eGFP (26-29) fluorescing between 4-9 (calculated average 7.5) times better than the particulate protein fractions (6-13). It appears as if the soluble forms of VP7-177-eGFP have an improved fluorescence/unit protein value relative to the larger insoluble aggregates of the protein. The soluble fraction therefore probably represents the largest concentration of correctly folded protein. The heterologous fluorescence pattern of the different forms of VP7-177-eGFP prompted further investigation into the nature of the protein found in the soluble and insoluble fractions.

2.3.4. Investigation of Heterologous VP7 chimeric protein profiles

2.3.4.1. Analysis of fractions containing insoluble VP7-177-eGFP

Previous studies have shown that WT-VP7 proteins that sediment in the lower third of a 70%-50% discontinuous sucrose gradient form unique hexagonal crystals with a diameter of about 6-8 µm. However, fusion proteins of WT-VP7 with a C-terminal-attached eGFP (VP7-C-eGFP) sedimenting in the same fractions do not form the typical hexagonal structures. Rather, the aggregates are larger (approximately 11 µm in diameter), more rounded and dense. This raised the question of the nature of the particles or aggregates that would be formed by VP7-177-eGFP.

To investigate this, fractions representing the largest quantity of insoluble VP7-177-eGFP (Fig. 2.9, fractions 6-13) were selected and analysed by S.E.M. Micrographs are shown in Fig. 2.11 (D-F). The morphology of the aggregates is compared to that of WT-VP7 (Maree, 2000; Fig. 2.11 A.), VP7mt177 (Maree, 2000; Fig. 2.11 B.) and VP7-C-eGFP (Burger, 2005; Fig. 2.11 C.). Both WT-VP7 and VP7mt177 have the typical flat, smooth hexagonal particle structure with a diameter of between 6-8µm. The VP7-C-eGFP aggregates are larger (10-12 µm) and display a dense circular appearance with a rough surface. The aggregates formed by VP7-177-eGFP range in size from approximately 1 µm to 15 µm and do not have a distinct shape. In addition these aggregates appear more loosely packed than those formed by VP7-C-eGFP. The surface of these aggregates is on the whole uneven, appearing stringy and porous, with clustered particles connected by proteinaceous fibers.

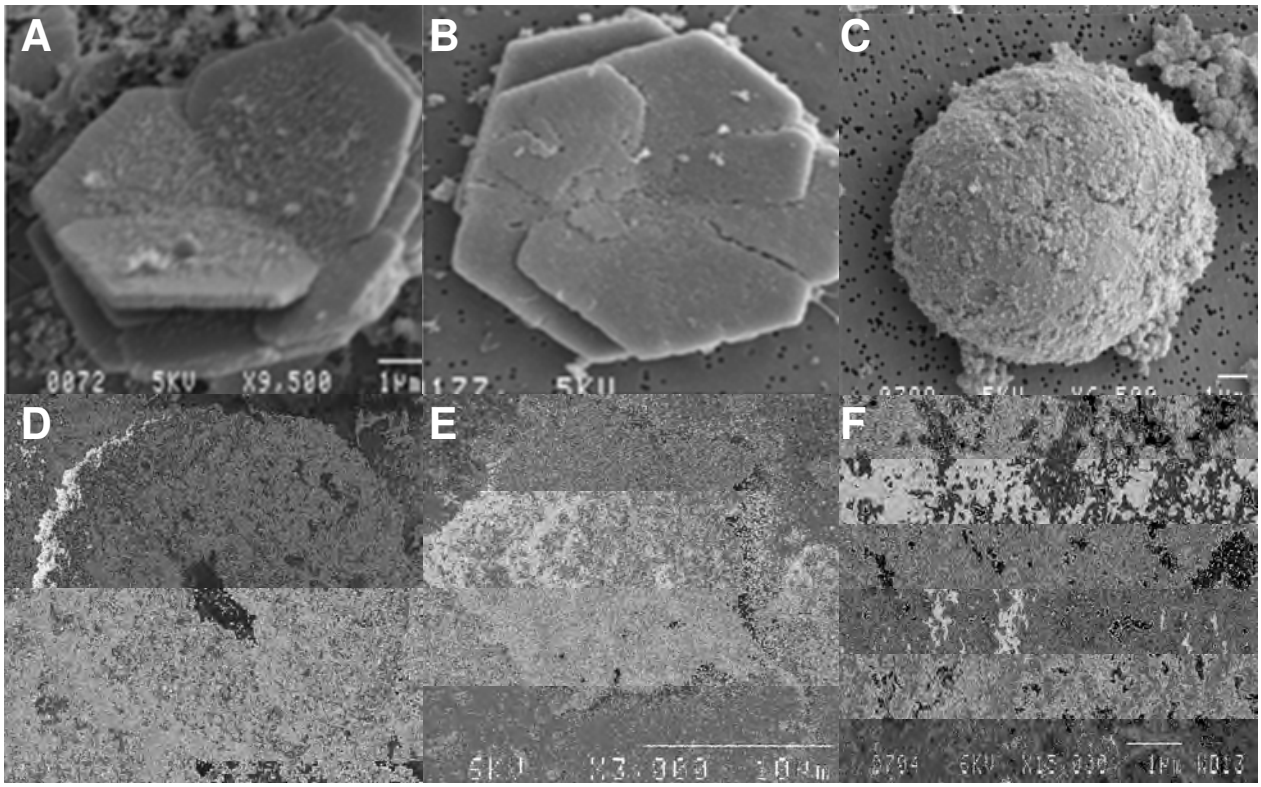

Figure 2.11. Scanning electron microscope images showing aggregates formed by WT-VP7 (A), VP7mt177 (B), VP7-C-eGFP (C) and VP7-177-eGFP (D-F).

2.3.4.2. Analysis of fractions containing soluble VP7-177-eGFP

Previous studies have shown that any soluble form of AHSV WT-VP7 expressed in cells represents the protein in trimer form. It was hypothesized that soluble VP7-177-eGFP proteins observed through sucrose sedimentation gradients may be in the form of trimers. However, the non-particulate, soluble VP7-177-eGFP protein observed could also have represented monomers or dimers.

To investigate the nature of the non-particulate component of VP7mt177-eGFP, an experiment was conducted to determine the molecular weight of the protein in its native state. Samples from fractions containing soluble VP7-177-eGFP were collected and loaded again on top of a 70%-50% sucrose gradient, and centrifuged for 18 hours at 151 000 xg. This protein sample was combined with proteins of known sizes to act as size markers – Bovine Serum Albumin (BSA - 67kDa), Aldolase (158 kDa) and Catalase (232 kDa). A 66kDa VP7-177-eGFP monomer was expected to co-migrate with BSA, whereas a 198 kDa trimer was expected to migrate in a position between the aldolase and catalase markers.

Once the fractions had been collected, samples of each fraction were analysed by SDS-PAGE (results not shown). The three size markers were distributed in distinct fractions as follows: catalase (fractions 14 and 15), aldolase (15-16) and BSA (16-17). In addition, fluorescence measurements of each fraction were taken and the proportion of VP7-177-eGFP in each fraction calculated. The fluorescence results were plotted on a graph, taking into consideration the position of the size marker proteins (Fig. 2.12). The fluorescence peaks appeared in fractions 15 and 16, with the primary peak located between the 158 kDa and 232 kDa protein size markers. This result provided evidence that these non-particulate fluorescence peaks represented VP7-177-eGFP in the form of trimers.

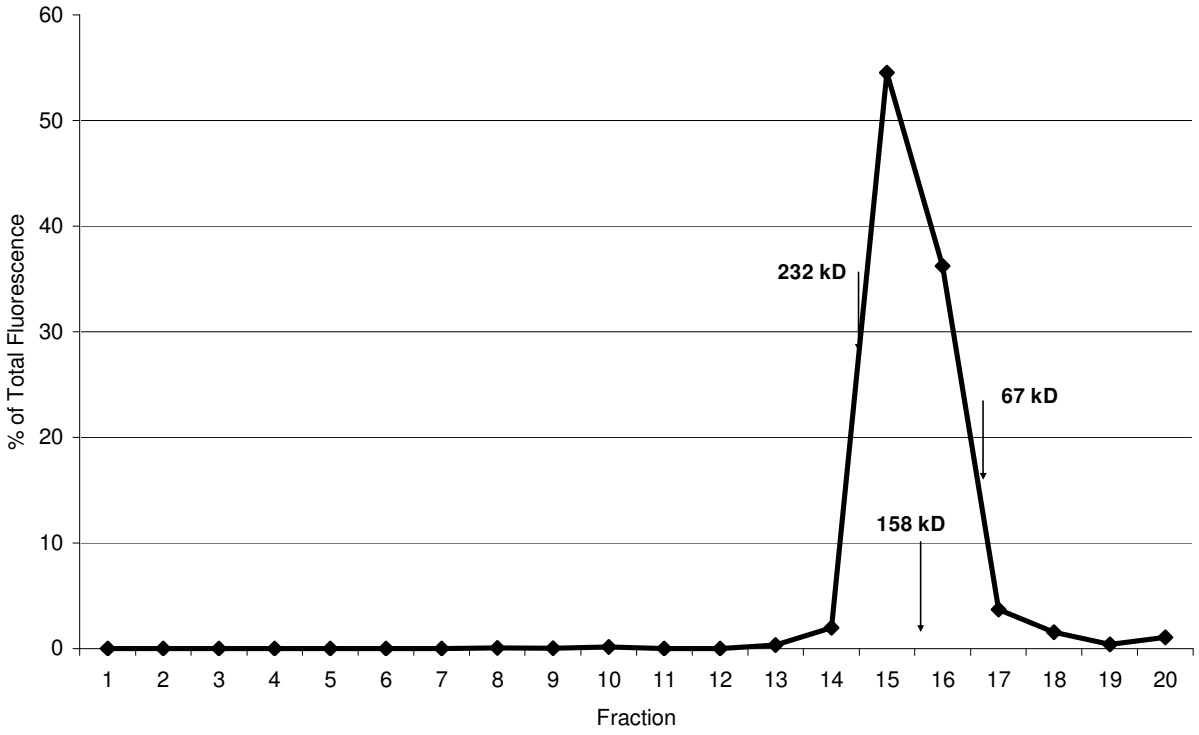

Figure 2.12. The sedimentation profile of soluble fractions of VP7-177-eGFP combined with the sedimentation profiles of pure soluble proteins of known sizes BSA (67 kDa), Aldolase (158 kDa) and Catalase (232 kDa). The major peak lies in the region between 158kDa and 232 kDa, the expected region for VP7-177-eGFP trimers (198 kDa).

Thus, it was demonstrated that VP7-177-eGFP is able to form soluble trimers. These trimers fluoresce significantly better than the aggregated particles. Since trimers represent a stable and consistent structure, these results raised for the first time the option of using soluble trimers of VP7 fusion proteins for the immune display of foreign peptides, rather than particles. In order for a VP7-trimer-based peptide display strategy to be viable, a high yield of trimers would be necessary. Therefore, the yield of trimers that can be obtained when they are recombinantly

expressed in Sf9 cells was investigated, and a series of experiments followed to test the kinetics of trimer/aggregate formation during Baculovirus expression of the protein.

2.3.5. Kinetics of VP7-177-eGFP and VP7-C-eGFP expression.

Previous studies have shown that AHSV WT-VP7 is primarily found in aggregated form when expressed in large quantities in Sf9 cells, consisting of a very small portion (approximately 8%) of soluble protein. However most of these studies were performed on Sf9 cells harvested 72 hours post infection (p.i.), in order to maximize the quantity of aggregated recombinant VP7 protein. Since AHSV VP7mt177 soluble trimers may represent an improved display of peptides, it was important to determine when the maximum amount of soluble trimers is synthesized. The presence of eGFP allowed quantitative assays of VP7-177-eGFP expression in *Sf*9 cells over time. These results were compared to VP7-C-eGFP, where the fluorescent protein is on the C-terminus of WT-VP7.

2.3.5.1. The kinetics of VP7-177-eGFP expression.

A preliminary experiment was carried out to determine if the proportion of soluble to aggregated VP7-177-eGFP changed with time post-infection. Cell lysates of cells harvested at 36 and 48 hours p.i. were prepared, analysed by sucrose density gradient sedimentation (2.2.19), and the amount of VP7-177-eGFP quantified in each fraction by fluorescence. These results were compared to the previous results obtained with cells harvested at 72 hours p.i. (Fig. 2.9 A). The results can be seen in Fig 2.13. At 36 hours p.i., 93% of the total fluorescence was detected in fractions containing soluble trimers. This is reduced to 74% at 48 hours p.i. and 42% at 72 hours p.i. This indicated that the proportion of soluble to aggregated VP7-177-eGFP protein decreases throughout the infection cycle.

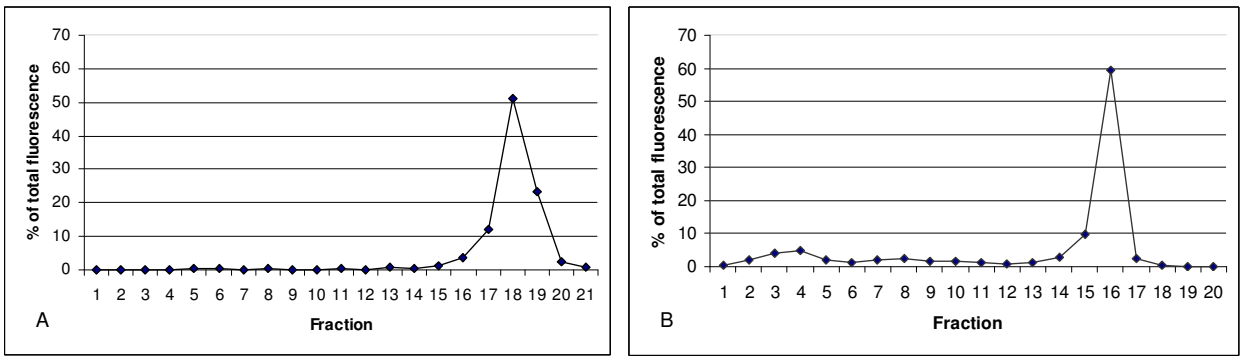

Figure 2.13. Sedimentation profiles of Sf9 cells lysates of VP7-177-eGFP by fluorescence. Samples were harvested 36 hours p.i. (A) and 48 hours p.i. (B). The results from these were compared with the values obtained from the experiment shown in Fig. 2.9 A. The trend over time shows a transition of the proportion of fluorescence from fractions containing soluble protein to those containing insoluble protein.

To characterize the kinetics of VP7-177-eGFP aggregation in more detail and to determine the optimal time for harvesting soluble or particulate VP7-177-eGFP proteins, a time-trial experiment was conducted using shorter time intervals. Samples of Sf9 cells expressing VP7-177-eGFP were collected at 6 hour intervals within the period 18 – 90 hours p.i. Samples before infection, as well as samples immediately after infection were treated as controls to account for background fluorescence of Sf9 cells and the baculovirus stock used for infection, respectively. The cells of a 1 ml sample (representing 1 x 10^6 cells out of a culture of 1 x 10^8 cells) were collected in a centrifugation step (200 xg), and fluorescence of the medium was measured. This measured the soluble VP7-177-eGFP released from the cells through cell lysis at late times in the Baculovirus infection cycle. The cells of each sample were lysed by means of a dounce after treatment with NP-40. The cell lysates were then separated into soluble and non-soluble components in a high speed (16 000 xg) centrifugation step. The absolute fluorescence values of soluble and insoluble components were measured for each time point and compared to one another.

Fig. 2.14 shows the trends of soluble VP7-177-eGFP fluorescence within and outside the cells, as well as total insoluble VP7-177-eGFP fluorescence, over a 90 hour period post infection. Fluorescence representing soluble VP7-177-eGFP present in the cells (solid squares) is observed from 18 hours p.i., increases steadily and reaches a maximum at 48 hours p.i., after which it declines. Fluorescence in the medium in which the cells are cultured (triangles) begins to increase after 36 hours p.i., and increases throughout the 90 hour period. Fluorescence representing insoluble VP7-177-eGFP (solid diamonds) reaches 90% of its maximum around 54 hours p.i.

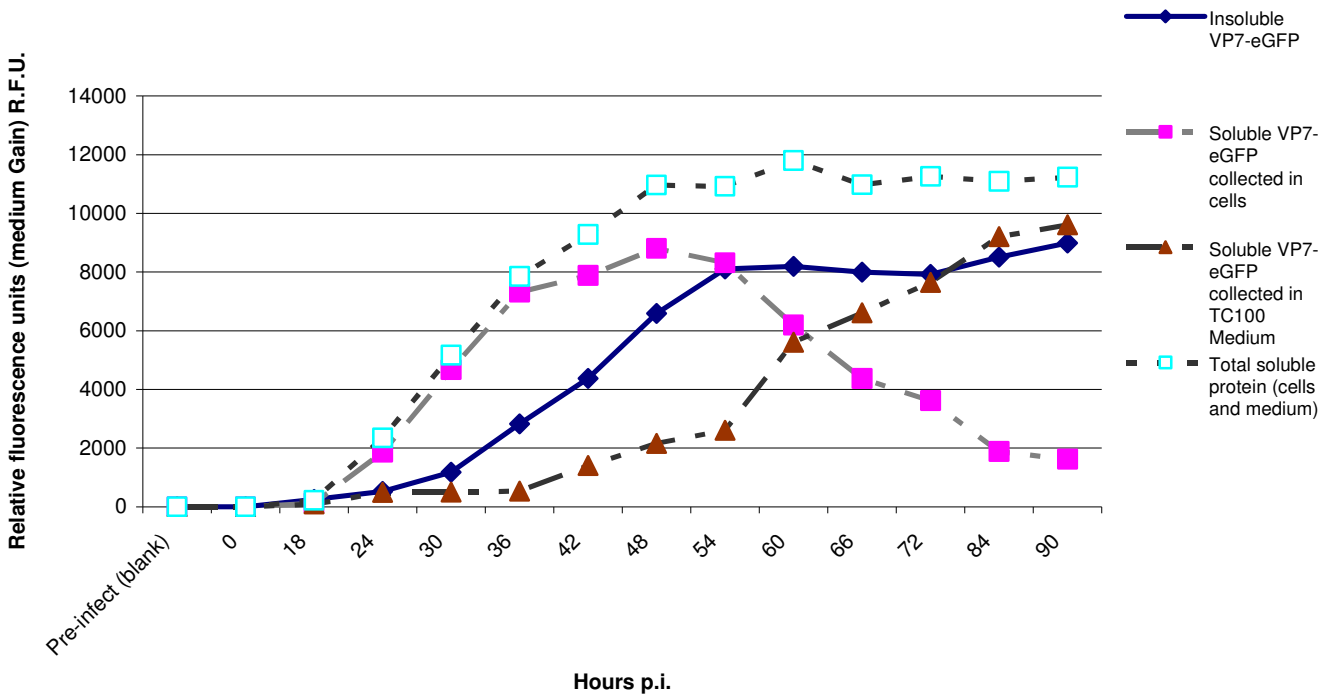

Figure 2.14. VP7-177-eGFP expression over a 90 hour period. Representative samples were collected 18 hours p.i. and every 6 hours thereafter and separated into soluble components in the medium, soluble components in the cells and insoluble components in the cells. A line representing total soluble protein indicates that expression of soluble protein reaches a plateau around 48 hours p.i.

After 48 hours p.i., the decrease in the soluble cell-associated VP7-177-eGFP coincides with an equal increase in the soluble medium-associated VP7-177-eGFP. This result suggests that the decline in the cell-associated soluble fraction is mainly due to cell lysis and release of soluble fluorescing protein into the cellular medium. Therefore, the sum of cell- and medium-associated soluble protein (Fig 2.14, hollow squares) is a more accurate representation of total soluble VP7-177-eGFP synthesis. The amount of soluble protein increases steadily and reaches a plateau after 48 hours p.i. The maximum amount of soluble protein is attained at 48 hours p.i. The maximum amount of insoluble protein is observed at 90 hours p.i.

To determine the optimal time for harvesting soluble VP7-177-eGFP protein from recombinant Baculovirus infected cells, the proportion of soluble protein collected at each interval was calculated as a percentage of the maximum (48 hours p.i.). Similarly, the proportion of insoluble VP7-177-eGFP collected at each time interval was calculated as a percentage of the maximum (90 hours p.i. – Fig. 2.15). This comparison highlights the fact that harvesting cells expressing VP7-177-eGFP at 72 hours p.i. represents only 40% of the soluble trimers than can potentially be harvested.

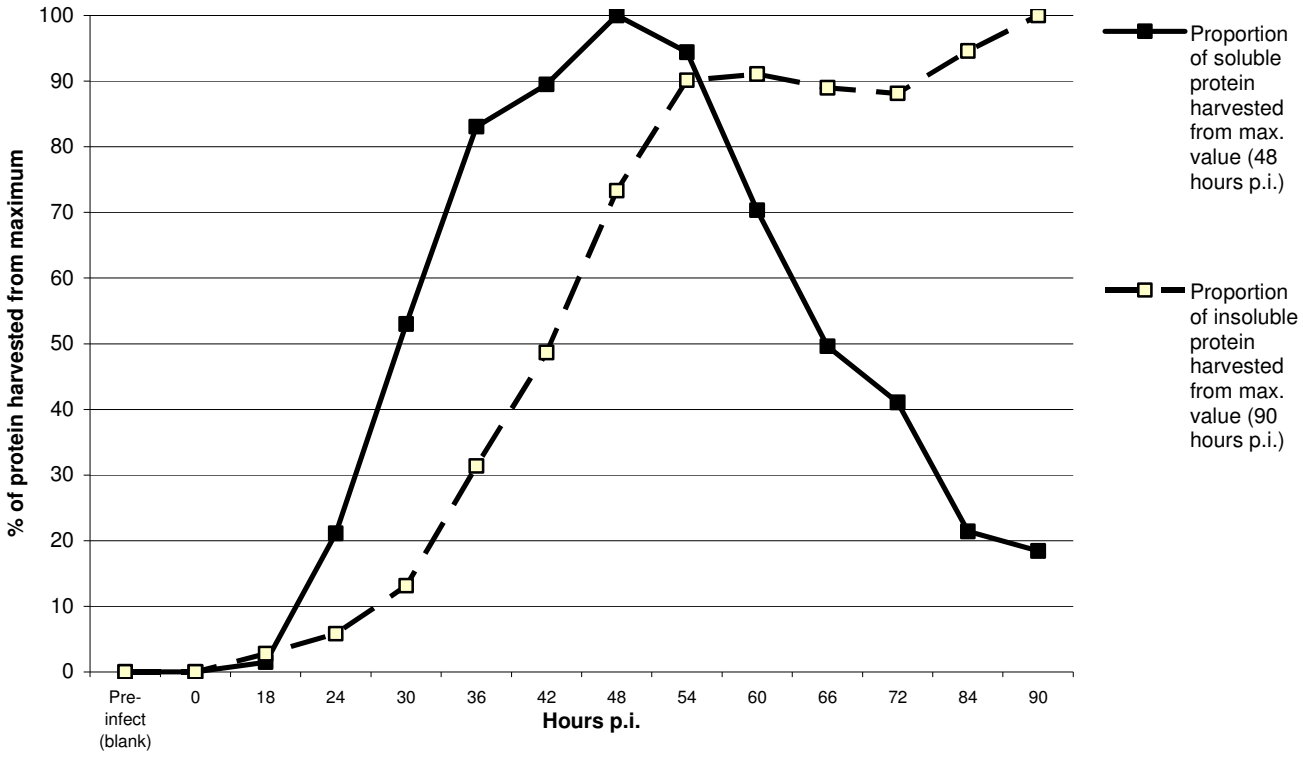

Figure 2.15. Graph showing the proportions of harvested soluble and insoluble VP7-177-eGFP at each time interval post infection, as calculated from the respective maxima.

It is notable that these results are based only on fluorescence readings. To obtain a more accurate representation of actual protein proportion in relation to fluorescence, the values of insoluble VP7-177-eGFP (Fig. 2.14) were increased 7-fold. This represents a conservative estimate of fluorescence / unit protein with regards to aggregates, ascertained in section 2.3.2. The comparison is illustrated in Fig. 2.16. At 60 hours p.i., where total protein expression reaches a maximum, 20% of VP7-177-eGFP accounts for total soluble protein.

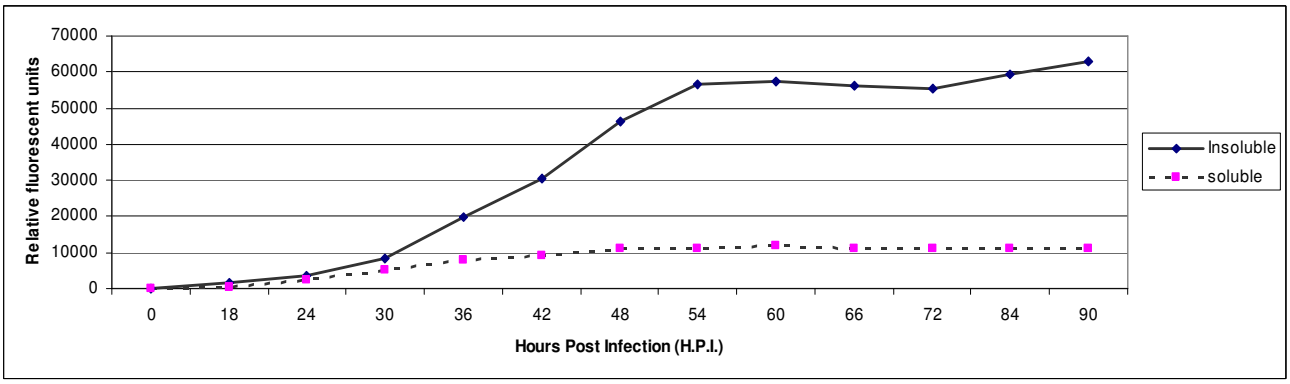

Fig. 2.16. Fluorescence values from figure 2.14 corresponding to insoluble protein were multiplied by a factor of 7 to give a more accurate representation of insoluble VP7-177-eGFP quantity.

2.3.5.2. The kinetics of VP7-C-eGFP expression.

An analogous kinetics assay was performed on the protein VP7-C-eGFP (refer to Fig. 2.6 A and Fig. 2.11 C). A comparison between the two proteins would serve to highlight the differences and similarities between an eGFP protein displayed on the top domain of an AHSV VP7 chimeric protein (VP7-177-eGFP) and an AHSV WT-VP7 with a C-terminal-linked eGFP. The time trial experiment described in 2.3.5.1. (Fig. 2.14) was replicated with Sf9 cells expressing VP7-C-eGFP (Fig. 2.17).

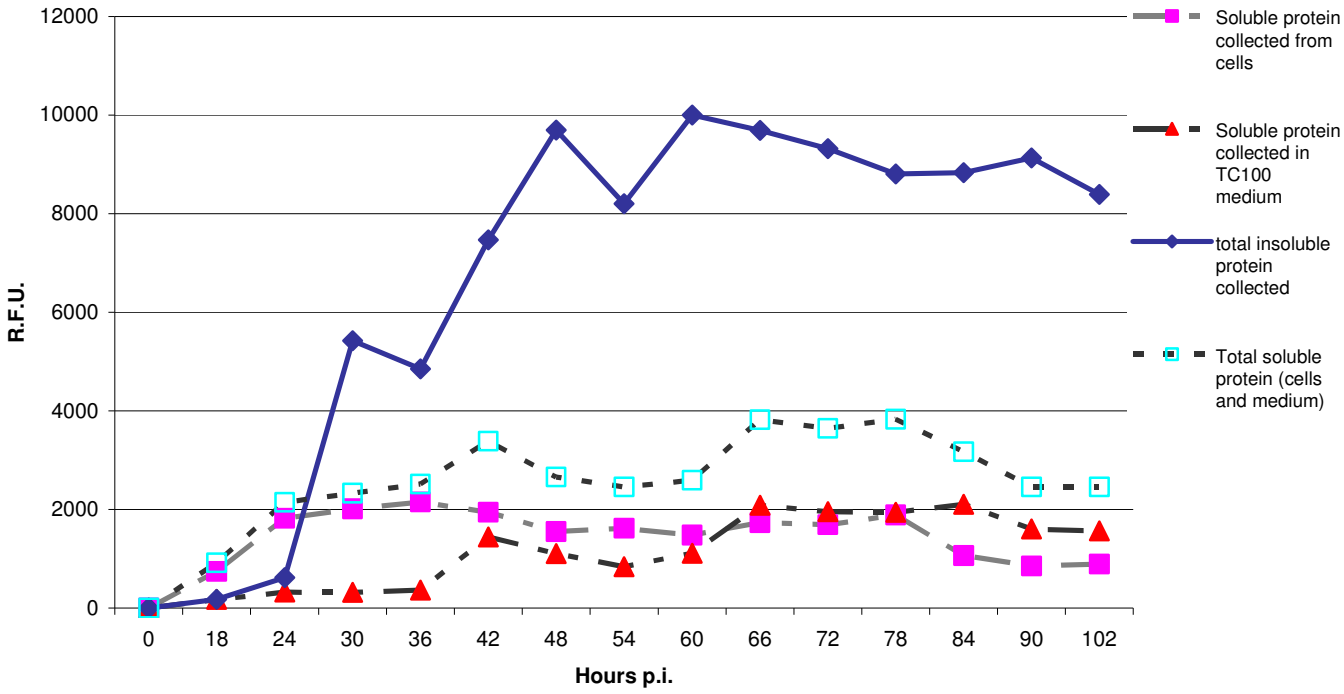

Figure 2.17. VP7-C-eGFP expression over a 90 hour period. Representative samples were collected 18 hours p.i. and every 6 hours thereafter and separated into soluble components in the medium, soluble components in the cells and insoluble components in the cells. A line representing total soluble protein indicates that expression of soluble protein reaches a plateau around 24 hours p.i.

The amount of soluble VP7-C-eGFP form (Fig. 2.17, hollow squares) only exceeds the insoluble form (Fig. 2.17, solid diamonds) up to 24 hours p.i., after which most of the newly synthesized VP7-C-eGFP is observed in the insoluble form. This is in contrast to the profile of VP7-177-eGFP (Fig. 2.14), where the fluorescence of the combined soluble fractions exceeds that of the particulate fraction throughout the entire infection cycle.

2.3.6. Stability of VP7-177-eGFP trimers

The option of using chimeric VP7 soluble trimers as peptide display vectors raised the question about the stability of such trimers. Specifically, this refers to adherence to structural conformation (in the case of VP7-177-eGFP – maintaining fluorescence) and retaining solubility after exposure to a variety of treatments including detergents, salts, freezing and thawing and dialysis. These experiments were also designed to provide information on whether the trimers formed by VP7-177-eGFP were likely to spontaneously aggregate into larger particles *in vitro* after partial purification by sucrose gradient sedimentation.

2.3.6.1. The effect of detergent on VP7-177-eGFP trimers

The effect of detergent on cells prior to differential centrifugation was tested by dividing a sample of infected cells into 4 samples comparable in the amount of VP7-177-eGFP by fluorescence, and observing the effect of removal of the nuclei, as well as treatment with detergent (Table 2.1). An initial low speed centrifugation (3000 xg step to remove the nuclei from the sample showed fluorescence in the pellet, indicating some insoluble VP7mt177-eGFP precipitated in this step. However, the treated and untreated samples of mechanically lysed cells, with or without removal of the nuclei, all showed similar fluorescence results with regards to soluble VP7mt177-eGFP in the supernatant following a high speed (16 000 xg for 10 minutes) centrifugation step.

Table 2.1. Fluorescence [F] analysis of cells expressing VP7-177-eGFP prior to sucrose gradients

Sample	Initital [F] readings	Remove nuclei	[F] supernatant	[F] pellet	Detergent	Centrifuge 16 000g 10 minutes	[F] supernatant	[F] Pellet
A1	14100	no			yes	yes	10410	5850
A2	14600	no			no	yes	9680	5580
B1	14600	yes	13110	1700	yes	yes	8320	2590
B2	15200	yes	12950	1910	no	yes	9570	4450

To observe the effect of detergent treatment on the sedimentation profile of VP7-177-eGFP, whole cell lysates of cells expressing VP7-177-eGFP were mechanically lysed and divided into 2 samples with equal fluorescence values. Only one was treated with a detergent (0.05% NP-40). Following this, both samples were lysed mechanically by means of a dounce. This experiment was carried out on cell lysates 72 hours p.i. to specifically observe the effect of detergent on insoluble VP7-177-eGFP. The distribution of fluorescence for both samples can be

seen in fig. 2.18. However, the distribution of fluorescence through the rest of the gradient shifts towards the lower fractions in the sample treated with detergent. This provided evidence that treatment of cell lysates with detergent prior to differential sedimentation affected only the fractions representing particulate forms of V7mt177-eGFP, while the soluble trimers appeared to remain unaffected.

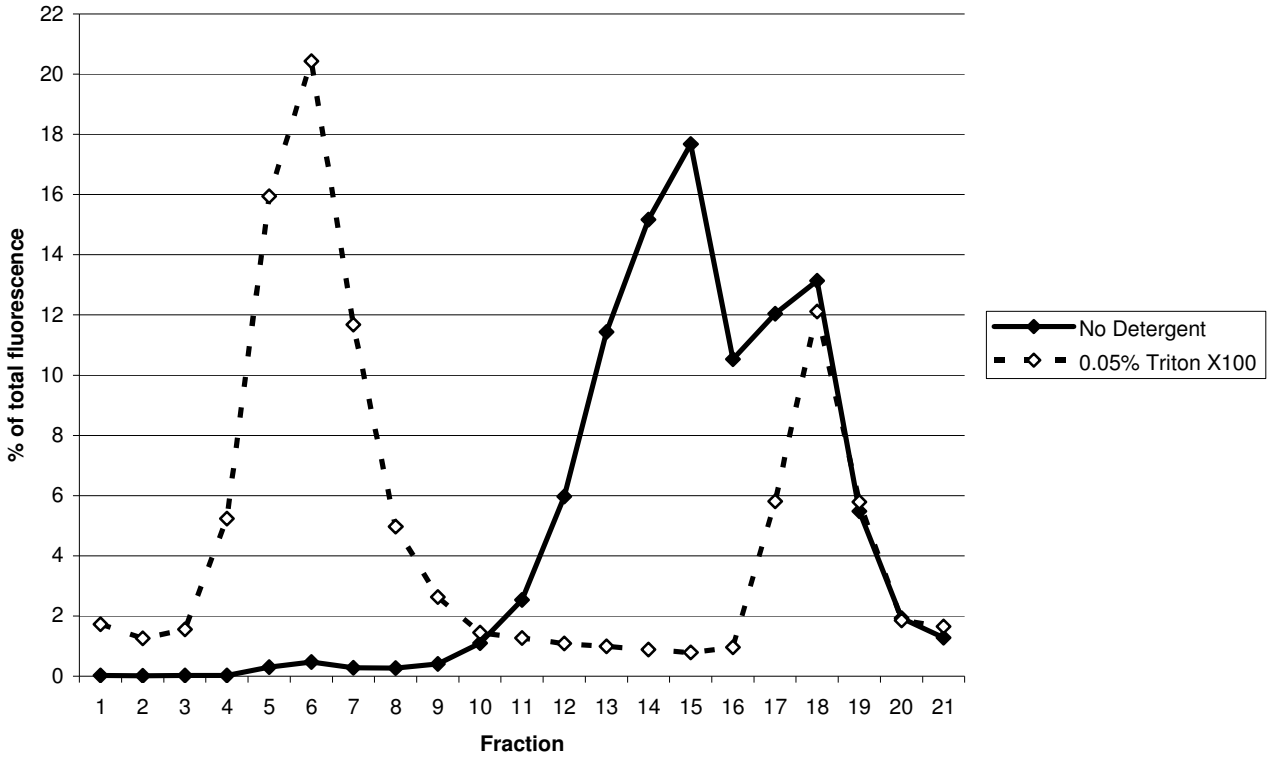

Figure 2.18. Sucrose sedimentation gradient of VP7-177-eGFP total Sf9 cell lysates in the presence/absence of non-ionic detergent. Fractions representing soluble trimers (18-20) remain unchanged in both cases. For the sample not treated with detergent, the migration of particles is restricted to the top half of the gradient.

To further test the effect of treatment with a non-ionic detergent on the soluble trimer fractions, fractions containing V7-177-eGFP trimers from a previous sedimentation analysis (Fig. 2.7, Fractions 25-32) were isolated, split into two equal parts comparable by fluorescence, and analysed on a new sucrose gradient under the same conditions (2.2.20), where one sample was treated with 0.05% detergent and the other was not prior to centrifugation. The resulting distribution was alike between the two samples (Fig 2.19), and it was concluded that further treatment with detergent did not affect soluble VP7-177-eGFP migration in the sucrose gradient.

A

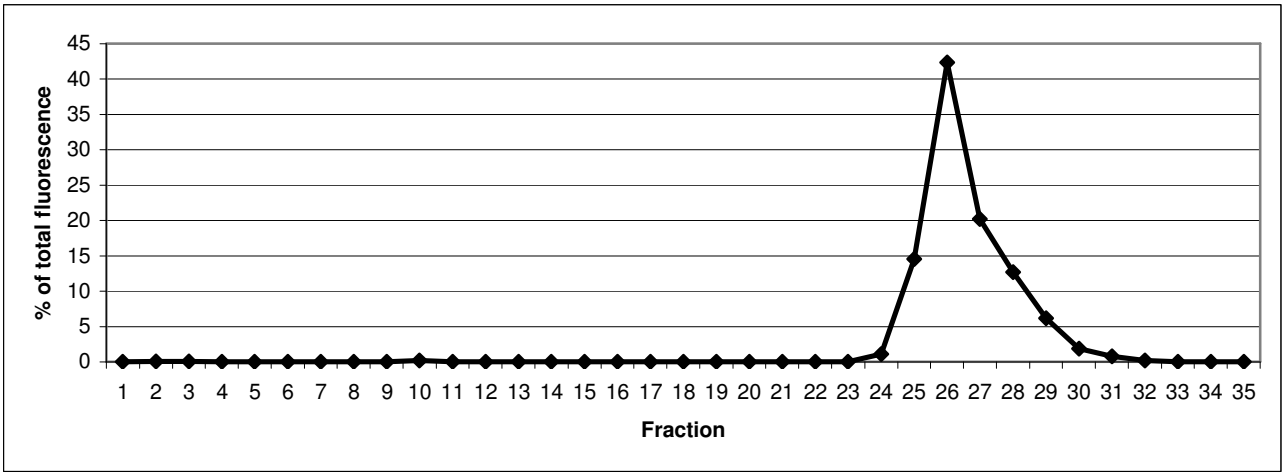

B

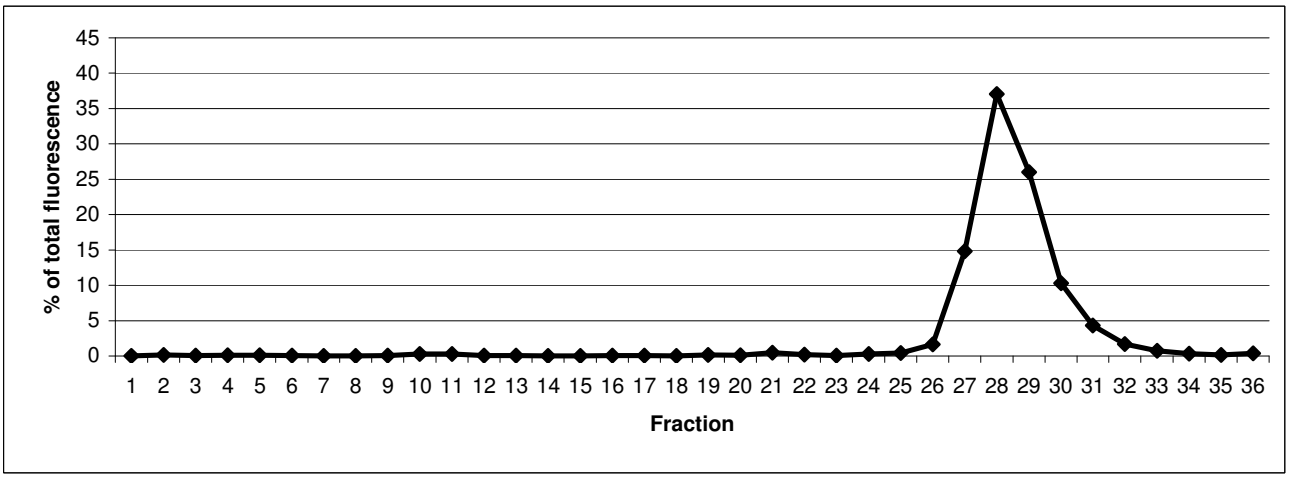

Figure 2.19. Sucrose sedimentation profile of soluble VP7-177-eGFP trimer fractions after additional treatment with 0.05% Triton X100 (A) as compared to no additional treatment (B). The additional detergent did not have an effect on the migration pattern of the trimers.

2.3.6.2. The effect of ionic concentration on VP7-177-eGFP trimers

To observe if a high ionic concentration has an effect on the solubility of VP7-177-eGFP, a sample of soluble VP7-177-eGFP, obtained by high-speed centrifugation of total cell lysates and collection of the supernatant, was divided into 5 samples equivalent in their VP7-177-eGFP content by their fluorescence. Increasing amounts of NaCl were added to the samples as indicated in Table 2.2. The samples (column A) were incubated at 4℃ for 30 minutes, then centrifuged (16 200 xg for 20 minutes), whereafter the supernatant was removed, fluorescence measured (column B) and the loss of soluble fluorescence calculated. Column C shows the fluorescence readings from column B as a percentage of column A. These results indicate a negligible effect of increasing molarities of NaCl on the solubility of VP7-177-eGFP trimers, where at least 94% of soluble trimers were recovered up to a NaCl concentration of 1M, and 89.6% was recovered at 5M, an extreme saline solution.

Table 2.2. The effect of NaCl concentration on soluble VP7-177-eGFP trimers.

NaCl [M]	A (Pre-incubation)	B (post-incubation)	C (% soluble)
0.01	8814	8360	94.85
0.1	9154	9020	98.54
0.5	9473	9377	98.99
1	8645	8532	98.69
5	7429	6658	89.62

2.3.6.3. The effect of dialysis and freeze drying on VP7-177-eGFP trimers

VP7-177-eGFP trimers would have to remain stable and soluble during dialysis, as well as freeze drying, if they were to be used for vaccination purposes. An experiment was designed that utilized fluorescence as an indicator of structural integrity of soluble trimers before and after such treatments. Soluble VP7-177-eGFP trimers were obtained by means of a single high speed centrifugation step of cell lysates (16 400 xg for 10 minutes) and collection of the supernatant (Fig. 2.20 A). The sample was dialysed against a 0.1M NaCl T.E. buffer (Fig. 2.20 B), then centrifuged as above, and the fluorescence of the supernatant measured (Fig. 2.20 C). This supernatant was then freeze dried, resuspended in 0.1M NaCl TE buffer (Fig. 2.20 D). The solubility of VP7-177-eGFP trimers following freeze drying was then tested by centrifugation and measurement of fluorescence in the supernatant (E). A 5 % discrepancy was observed between fluorescent values, which was considered a reasonable variation in readings due to low absolute fluorescence values. No significant loss of fluorescence was observed after dialysis (Fig. 2.20 B), with all the protein remaining soluble (Fig. 2.20 C). Approximately 28% of the fluorescence was lost after freeze drying (Fig. 2. 20 D), but fluorescence analysis of this sample after a high speed centrifugation showed it still consisted of only soluble protein (Fig. 2.20 E).

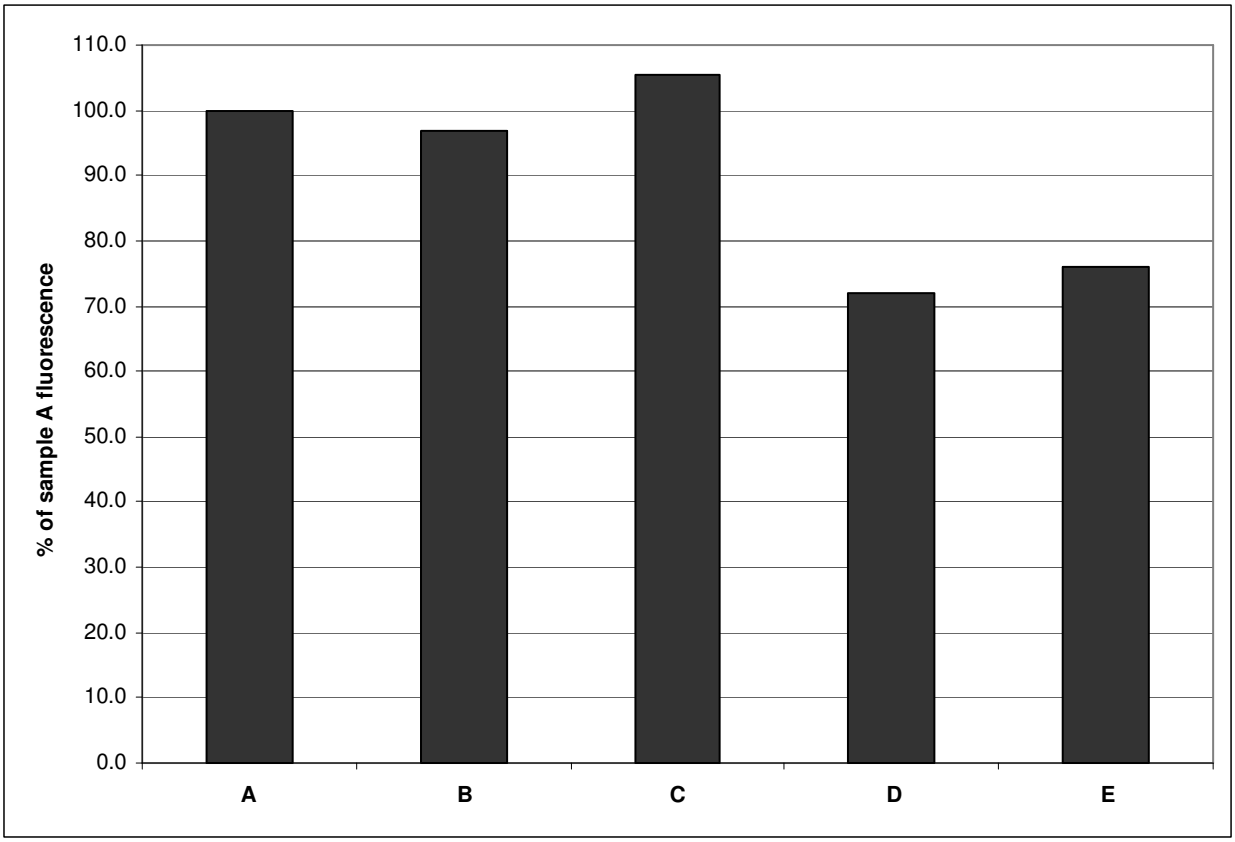

Figure 2.20. An analysis of the effects of dialysis and freeze drying on the solubility and stability of VP7-177-eGFP trimers. Lysates of VP7-177-eGFP expressing cells were centrifuged, and the fluorescence in the supernatant measured as an indicator of soluble VP7-177-eGFP trimers present in the sample (A). This supernatant was dialyzed against 0.1M NaCl TE buffer (B). The solubility of VP7-177-eGFP trimers in the dialyzed sample was tested by centrifugation and measurement of fluorescence in the supernatant (C). Subsequently, this sample was freeze-dried and resuspended in an equal volume of 0.1M NaCl TE buffer as in A (D), after which the solubility of VP7-177-eGFP trimers was tested by centrifugation and measurement of fluorescence in the supernatant (E). All values are expressed as a percentage of the fluorescence of sample A.

Thus, soluble VP7-177-eGFP trimers could be recovered after partial purification and freeze drying (with an approximate 30% loss in recovery) while maintaining their fluorescence, and thus their structural stability. There was no evidence of spontaneous aggregation of trimers into particles when the protein is freeze-dried. These results provided further evidence that soluble AHSV VP7 chimeric protein trimers represent a stable system to be used in epitope presentation.

2.3.7. Immune response against VP7-177-eGFP

The increased fluorescence of soluble chimeric VP7-177-eGFP as compared to the chimeric VP7-177-eGFP particles implied that the trimers had an advantage with respect to the display of a peptide insert to the aqueous environment – a fact that may reflect display to the immune system as well. Furthermore, trimers could be partially purified and remained stable after purification, making them a viable option. To test the hypothesis of an improved display of

epitopes using trimers as opposed to particles, guinea pigs were injected with soluble or particulate forms of the VP7-177-eGFP protein.

Particulate and soluble fractions of VP7-177-eGFP were purified from their corresponding fractions in a sucrose sedimentation gradient by dialysis in a low salt (0.01M NaCl) TE buffer, followed by two repeated dialysis steps. The sample was then freeze-dried overnight and re-suspended in a smaller volume of 0.01M NaCl TE buffer to facilitate injection into guinea pigs. A small proportion was analysed by SDS-PAGE to quantify the amount of protein in each sample to be injected (results not shown).

Each guinea pig was injected with approximately 25µg of partially purified protein, distributed over an initial immunization, followed by two booster immunizations. Three animals (group A) were injected with particulate VP7-177-eGFP, and another three (group B) were injected with soluble VP7-177-eGFP trimers. Serum from immunized guinea pigs was obtained, and equal proportions of serum from each animal within a group were combined, resulting in serum of guinea pigs injected with insoluble aggregates (serum A), and serum of guinea pigs injected with VP7-177-eGFP trimers (serum B). The efficiency of recognition of eGFP was tested by Western blot analysis. In this case, the protein detected was another chimeric protein, AHSV NS1-eGFP (Lacheiner, 2006). This protein was selected to ensure any recognition of peptides by the serum is specific to eGFP and not AHSV VP7. The use of this protein over eGFP was due to its molecular weight, which was more convenient to observe, and because purified fractions of the protein were available. A control Western blot analysis (Fig. 2.21. lanes 1-3) showed that NS1 (lane 1) did not react with a commercial eGFP primary antibody, while NS1-eGFP (lane 2) and eGFP (lane 3) reacted very well. To obtain an overview of the efficiency of recognition of eGFP by sera derived from group A and group B, a dilution series of each type of serum was tested against a constant concentration of NS1-eGFP by western blot analysis to observe if there is a relative difference in the level of eGFP antibody response.

The results (Fig. 2.21 and Fig. 2.22) show a different endpoint recognition of NS1-eGFP by the two sera, where no detection of eGFP occurred beyond a dilution factor of 1:200 in the case of serum A, obtained from injection of aggregated VP7-177-eGFP. In contrast, serum B, derived from the injection of soluble VP7-177-eGFP trimers, recognized NS1-eGFP up to a dilution of 1:1500. These preliminary results indicate an approximate 7.5-fold improved antibody recognition in serum obtained from animals injected with soluble VP7-177-eGFP, as compared to aggregated VP7-177-eGFP.

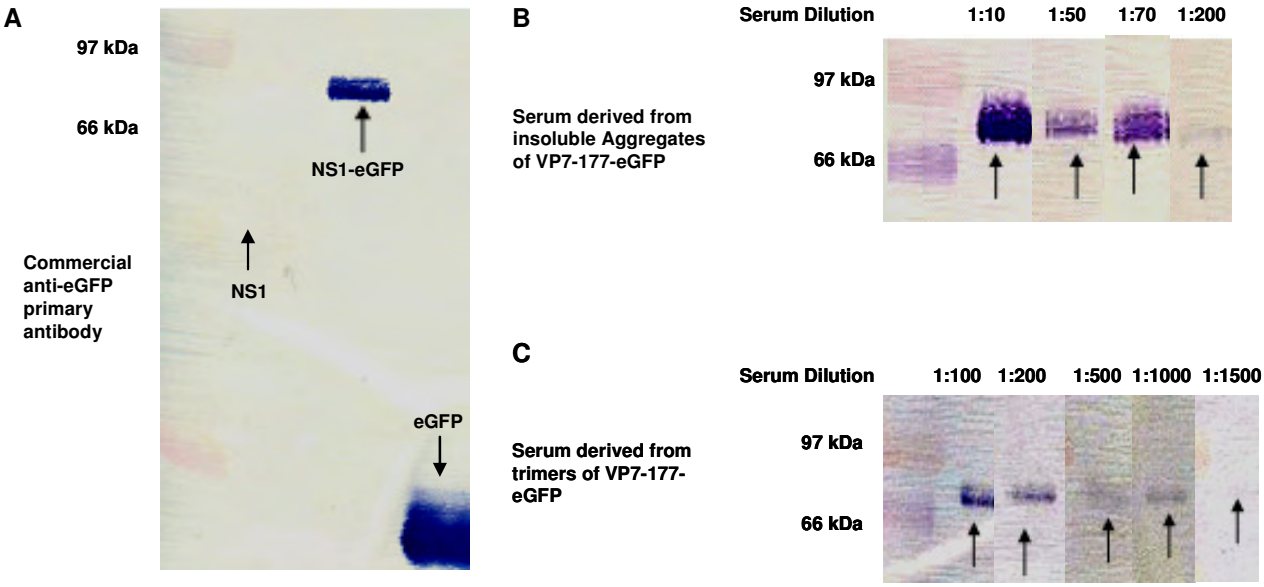

Figure 2.21. Western blot analysis of serum raised against soluble and aggregated forms of VP7-177-eGFP. A. Western blot using a commercial anti-eGFP primary antibody, used as a positive control. Purified AHSV NS1 protein was not recognized by the antibody, while NS1-eGFP, as well as eGFP, were recognized. B. Recognition of NS1-eGFP by Serum derived from guinea pigs injected with aggregated VP7-177-eGFP was tested in dilutions 1:10, 1:50, 1:70 and 1:200 (arrows). C. Serum derived from guinea pigs injected with VP7-177-eGFP trimers (group B) was tested in dilutions 1:100, 1:200, 1:500, 1:1000 and 1:1500 (arrows). Dilutions of sera further than those indicated in either group, respectively, failed to recognize NS3-eGFP in a Western blot assay.

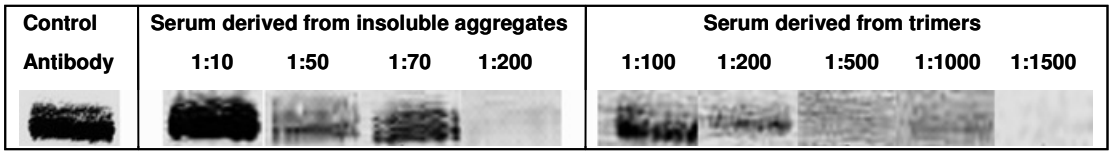

Figure 2.22. Summary of data from Fig. 2.21. Western blot analysis showed that serum derived from aggregated VP7-177-eGFP recognized the target protein, NS1-eGFP to an endpoint dilution of 1:200, whereas serum derived from trimers recognized the target protein NS1-eGFP to an endpoint dilution of 1:1500.

2.4 Discussion

Three key aspects are crucial for VP7 to be considered as an effective scaffold for the immune display of foreign peptides. These are the consistent and predictable arrangement of peptides on the scaffold presenting them, the efficient presentation of these peptides to the immune system, and the efficiency of their production and purification.

With the above requirements in mind, this project aimed to evaluate the efficacy of a modified AHSV VP7 protein, VP7mt177, as a peptide presentation vector. The VP7mt177 protein contains a modified extended loop possessing the RGD motif at amino acid sites 175-180 (Maree, 2000), where immunologically relevant peptides can be expressed on the top domain as fusions of VP7. In this study, eGFP was selected as a prototypal peptide in order to show by functional integrity whether structural conformation of an inserted peptide is maintained when expressed in site 177. In addition, eGFP would serve as a fluorescent marker to study the assembly process and physical properties of VP7 chimeras. Of particular relevance is the solubility and particle formation of VP7mt177 chimeras, as well as immunogenicity of inserted epitopes displayed on the top domain of VP7mt177 chimeras.

This investigation has contributed to the overall research programme by shedding light on some pertinent issues regarding the use of AHSV VP7 chimeras as peptide display vectors. Primarily, the structure of the inserted peptide was deemed to be correct. Additionally, the use of fluorescence indeed allowed critical qualitative and quantitative analysis from sucrose sedimentation profiles, giving insight into the kinetics of VP7 chimeric protein assembly and aggregation and contributing to optimization of chimeric VP7 purification. Perhaps most significantly, the results of this investigation highlighted the advantage of a soluble trimer-based display over that of a particulate one.

EGFP has been used in investigations analogous to this one, to examine the tolerance of insertion and efficacy of display of a subunit peptide display system. For example, in Hepatitis B CLPs (Kratz et al., 1999) the GFP protein was inserted within the flexible c/e1 loop of the core protein and retained functional integrity. Another case of note is display using Tobacco Mosaic Virus (TMV), where eGFP was attached to the C-terminal of the core protein and successfully displayed on TMV cores (Smith et al., 2006). It is, however, the first time that a complete protein has been expressed as a fusion on the top domain of a modified AHSV VP7 peptide display vector, and one of only a few cases where eGFP has been successfully expressed as a fusion within another peptide chain.

EGFP represents a significant insertion into the top domain of VP7 (eGFP is almost three quarters of the size of a VP7 monomer), and therefore the formation of VP7-177-eGFP trimers is a testimony in itself to the structural integrity of higher order structures formed by VP7 proteins. Clearly, as was predicted by the model of VP7-177-eGFP (Fig. 2.2), the insertion of a large peptide into site 177 did not abrogate trimer formation of the VP7 scaffold (Fig. 2.12), In addition, fluorescence of VP7-177-eGFP indicated the structural integrity of the inserted peptide (Fig. 2.5 E and Fig. 2.6 B).

The sedimentation pattern of VP7-177-eGFP could be used for analysis of multimeric units as well as for partial purification of soluble or particulate fractions. Once expression of the VP7-177-eGFP protein had been confirmed (Fig. 2.5), cell lysates of SF9 cells expressing the protein were analysed on a sucrose sedimentation gradient under conditions that had been previously determined (Maree, 2000; Meyer, 2002). The sedimentation pattern of VP7-177-eGFP was heterologous, with protein peaks observed in both the top fractions of the gradient, co-sedimenting with soluble cellular proteins, and the bottom fractions of the gradient (Fig. 2.9). Previous studies have shown that VP7 chimeras sedimenting in the lower fractions of the gradient represent particles/aggregations of VP7 proteins. S.E.M. analysis of partially purified VP7-177-eGFP from these fractions (Fig. 2.9, fractions 6-13 and Fig. 2.11, D-F) showed that the aggregated form of this protein represents a non-specific aggregation pattern when compared to the structures formed by WT-VP7 or VP7mt177 proteins.

Co-sedimentation of VP7-177-eGFP with the soluble cellular proteins (Fig. 2.8) indicated that a portion of VP7-177-eGFP expressed was soluble. The availability of a fluorescent marker provided a convenient manner in which to observe the level of oligomerization while the protein is in its native state. After isolation of the soluble fraction from a sucrose gradient identified by fluorescence, the sample was loaded onto a new sucrose gradient (50%-70% density) along with pure bovine seum albumin (BSA), Aldolase and Catalase. The results (Fig. 2.12) show that the primary VP7 peak occurred in the range expected for the trimeric form of the protein. This experiment supported the hypothesis that the soluble VP7-177-eGFP is a trimer, and provided further evidence that chimeric VP7 proteins form stable trimeric oligomers.

The rest of VP7-177-eGFP (i.e. any particulate form) migrated lower than the soluble trimers through the gradient and showed a broad distribution. The proportion of particulate protein per fraction was not consistent in repeated experiments, sometimes showing more than one major peak. It was hypothesized that this variability could be accounted for by three possibilities:

1. If the cells expressing VP7 chimeras are mechanically lysed, some particles may become entangled with lipids that are derived from internal membrane components during mechanical lysis. Therefore, if the cells are not treated with an optimal amount of non-ionic detergent to break up these complexes, the particles are found in higher up in the sucrose gradient (Fig. 2.16).
2. If aggregation of VP7-177-eGFP into particles is distorted by the steric strain of certain peptides displayed on the top domain of VP7-177-eGFP trimers, not all aggregated forms may be homologous in the pattern of their aggregation and thus may differ in their relative densities (See Fig. 2.11 D-F for examples of heterogenous assemblies formed by VP7-177-eGFP).
3. Since it was confirmed that VP7-177-eGFP trimers migrate as soluble proteins (i.e. their resulting sedimentation position is consistent with soluble proteins – Fig. 2.8 and Fig. 2.12), the intermediate fluorescent peaks may represent particles of a homologous aggregation pattern with a common density, but at different stages of assembly. Thus, there would be a variation in the size of the particles dependent on the heterogeneity of aggregation of a VP7 chimer. These varied particles would migrate at different rates according to their molecular weight.

These possibilities were investigated through the sedimentation of VP7-177-eGFP in the presence/absence of detergent, as well as analysis of the aggregated protein by S.E.M. It is apparent that the use of detergent to chemically lyse the cells had the greatest effect on the distribution pattern of non-soluble components. As can be seen in Fig. 2.16, a shift of aggregated VP7-177-eGFP to lower fractions was caused by the addition of non-ionic detergent to the mechanically lysed samples (Fig. 2.16, compare solid line, fractions 10-17 to dashed line, fractions 3-10). When considering the nature of aggregated VP7-177-eGFP as seen by S.E.M. (Fig. 2.11 D-F) there is evidence of aggregation into random shapes and sizes. This would affect the migration of particles that differ in molecular weight. Furthermore, the surface of the aggregates is varied with loosely packed regions, possibly a result of the increased overall hydrophilicity of VP7-177-eGFP as compared to WT-VP7, and tightly packed regions manifesting in a flat, compact surface (Fig. 2.11 E). This may lead to a variation in the density of aggregates. It is therefore likely that while the amount of detergent had the most drastic effect on the sedimentation pattern of particles, all three factors should be taken into account, as none of them can be ruled out.

The amount of soluble and insoluble VP7-177-eGFP synthesized in recombinant Baculovirus infected cells was monitored at different times post infection (Fig 2.12). Initially, the amount of soluble protein increases rapidly until it reaches a plateau. Aggregates are observed later in the

expression cycle, and also increase until a plateau is reached. If the proportion of soluble to insoluble VP7-177-eGFP, as measured by fluorescence, is taken into account (Fig. 2.14.), at 30 hours p.i. the ratio of fluorescence of soluble to insoluble protein is 4:1. This decreases to 2.7:1 (36 hours p.i.), 2:1 (42 hours p.i.) and an average of 1.4:1 from 48 hours p.i. onwards. There is no evidence to support active transport of VP7 out of intact cells, thus it is assumed any soluble protein outside the cells is a reflection of cell degradation, likely the effect of Baculovirus on the cells later in the infection. An analogous study of VP7-C-eGFP resulted in a similar pattern of fluorescence in soluble and insoluble protein observed (Fig. 2.16), with two main differences. First, the maximum level of soluble protein expression is reached at an earlier time (24 hours p.i.) than that of VP7-177-eGFP. Second, the proportion of soluble to insoluble VP7-C-eGFP, as measured by fluorescence, when maximum expression is reached, is approximately 0.3:1, almost 5 times lower than VP7-177-eGFP. In the case of VP7-177-eGFP, 90% of total insoluble protein is expressed by 54 hours p.i., but it is the finding of this investigation that to obtain maximum soluble VP7 chimeras, cells should be harvested 48 hours p.i. (Fig. 2.19). This represented the maximum amount of expressed soluble VP7-177-eGFP that could be collected in intact cells.

The results obtained with VP7-177-eGFP suggest that early in the infection cycle when the protein is expressed at low levels, the VP7-177-eGFP is largely soluble, and monomers will assemble to form soluble trimers. Later in the infection cycle the rate of recombinant protein synthesis accelerates, resulting in either aggregation of the soluble VP7-177-eGFP trimers or aggregation of misfolded newly-expressed monomers. In WT-VP7, the crystals observed by S.E.M. represent an ordered aggregation of trimers that form a regular structure (a hexagonal crystal) after the cells have been broken up (Burroughs et al., 1994; Maree, 2000). Previous research on chimeric VP7 proteins shows that recombinant expression of any chimeric VP7 vector that is modified with inserted peptides results in a form of insoluble aggregates, which can be collected via differential sucrose sedimentation in the lower fractions and observed by S.E.M (Maree, 2000; Meyer, 2002; Rutkowska, 2003; van Rensburg, 2005). The morphology of these aggregates is generally more similar to that observed in VP7-C-eGFP (compact, relatively amorphous aggregates, Fig. 2.11 C) rather than the ordered crystal formed by WT-VP7 (Fig. 2.11 A).

Optimal folding of proteins is a complex process that is dependent on several variables within a cell and the expression system, and modifications such as codon usage (Hatfield et al., 2007) or pH (Topilina et al., 2007) can greatly influence not only optimal expression rates, but efficiency of protein folding as well as solubility. The insoluble aggregates collected when VP7-177-eGFP is heterologously expressed may represent one of several phenomena. One

possibility is that the aggregations of VP7-177-eGFP represent VP7-177-eGFP trimers with the appropriate tertiary and quaternary structure that interact with each other via the sites that usually interact to form crystals observed in WT-VP7 proteins. However as a result of the presence of a hydrophilic peptide (eGFP) these inter-trimer interactions are interrupted (sterically or chemically) and the result is a disordered association of trimers. Alternatively, once a critical amount of soluble VP7-177-eGFP trimers are present in the cell, the changes in chemistry in the cytoplasm due to the surrounding number of hydrophobic domains may interfere with the correct folding of newly expressed VP7-177-eGFP proteins. Another reason for incorrect folding could be the lack of chaperones available for the number of VP7-177-eGFP proteins that are expressed. This has been observed in insect cells previously, as the AcNPV-promoter driven expression exceeds the level of chaperones available in the insect cell (Ailor and Betenbaugh, 1998). In these cases, newly synthesized peptides may not correctly fold into their tertiary structure and will therefore probably aggregate into “aggresomes” (Johnston et al., 1998). Aggresomes represent the eukaryotic cellular response to an overabundance of misfolded proteins, whose levels exceed the capacity of the cell’s ubiquitination pathway (Johnston et al., 1998). In aggresomes, misfolded proteins are encased in a “cage” of intermediate filaments made up of the vimentin protein (García-Mata et al., 1999). The peptides in these aggresomes may represent a mixture of completely misfolded, partially folded and correctly folded proteins, not unlike the cases observed in bacterial inclusion bodies (Clarck, 2004; Ventura and Villaverde, 2006).

In the case of VP7-177-eGFP, the initial folding of the protein, as well as the formation of trimers, was not affected by the insertion of a large peptide. The insoluble component observed may represent overloading of the cell’s ability to produce correctly folded proteins. However, it has not yet been determined if the soluble fluorescent proteins in VP7-C-eGFP-expressing cells represent correctly folded VP7 proteins. In the event that the VP7 protein in VP7-C-eGFP does not fold correctly, there is still the possibility that the attached eGFP will autonomously fold. In this case, the eGFP acts as a fluorescent tag of an improperly folded protein rather than an indicator of overall structure. Thus, the “spots” of brighter fluorescence observed in VP7-C-eGFP expressing proteins may represent aggresomes, whose location and formation is indicated in cells by eGFP, as has been demonstrated previously (García-Mata et al., 1999). It is clear that several issues regarding the nature of the insoluble components of chimeric VP7 proteins remain unresolved.

One method of overcoming hydrophobicity-mediated aggregation is the addition of L-arginine to cell lysates (Buchner and Rudolph, 1991; Tsumoto et al., 2003). Indeed, recent evidence in VP7 chimeric protein research has shown that the addition of arginine increases the proportion of

soluble trimers for a specific VP7 chimera, whether the arginine is added to the lysed cells or the partially purified aggregated form (Huismans, personal communication). This does not necessarily imply that aggregates represent groups of correctly folded trimers, but certainly lends support for the strength and homogeneity of the trimer as a peptide presenting vector. It is likely that aggregations of VP7-177-eGFP contain both incorrectly-folded proteins that interact with each other through non-specific hydrophobic contacts *as well as* trimers, which become entangled in these aggregations. While there was no evidence for this in this investigation, an appropriate assay would be to measure R.F.U. values of soluble components that are released if fluorescent VP7-177-eGFP aggregations could be disrupted using a solubilizing agent such as L-arginine. Thus, the total R.F.U. values of insoluble VP7-177-eGFP could be compared to the total R.F.U. values of soluble and insoluble VP7-177-eGFP after treatment with L-arginine. If the values are equivalent, then fluorescence of aggregations represent correctly folded soluble trimers that co-aggregate with aggresomes. If the total R.F.U. value after treatment is higher, the aggregations represent clusters of polypeptides where the displayed eGFP was buried.

Results indicating that the exposure of the displayed peptide was more effective in the soluble trimers than the particle aggregates prompted an investigation into the stability of chimeric VP7 trimers through purification and storage processes. Several experiments (Table 2.1, Fig. 2.18 and 2.19) provided evidence that treatment of cell lysates or purified protein with a non-ionic detergent such as Triton X 100 or NP-40 had no effect on the soluble trimers. An experiment to test the effect of high NaCl concentration showed that at least 90% of VP7-177-eGFP trimers remain soluble in a saline solution of up to 5M (Table 2.2). This eliminates for the most part the possibility of trimer-trimer interactions in high salt concentrations to aggregate. To simulate partial purification and storage of epitope-presenting VP7 trimers, soluble VP7 trimers were dialysed repeatedly in a low salt buffer, freeze dried and re-hydrated in a series of steps. There was no significant loss of protein through dialysis (Fig. 2.20 A-C), while freeze-drying resulted in a loss of approximately 30% (Fig. 2.20 D). This loss however likely represents protein degradation and not aggregation into particles, as all protein recovered was shown to comprise soluble trimers (Fig 2.20 E).

This study elucidated several key aspects about chimeric VP7 proteins. First, the VP7 protein can tolerate the insetion of a large peptide to its top domain and still form trimers. Second, the inserted peptide, eGFP, folds correctly and fluoresces. Finally, the most predictable and stable exposure of a peptide to the aqueous environment occurs when the protein is in trimeric form. An uncertainty which was highlighted in this study is the exact nature of the insoluble protein aggregates that form when chimeric VP7 proteins are heterologously expressed. The difference in fluorescence readings per unit protein between soluble trimers and insoluble aggregates can

be ascribed to either a “masking” effect in the aggregate form of the protein – due to the tendency of the hydrophobic VP7 trimers to aggregate in layers that are packed on top of one another – or due to the “trapping” of soluble trimers in insoluble aggregations of partially or totally incorrectly folded VP7-177-eGFP (discussed above). This finding led to the hypothesis that the fluorescence / unit protein value may well represent a proportional indicator of the level of exposure of the epitope on the surface of either soluble trimers or insoluble aggregates of VP7 chimeras, which could be informative about immune display of such an insert. To test this hypothesis, guinea pigs were injected with either soluble or particulate VP7-177-eGFP, partially purified by sucrose gradient sedimentation. The response was tested by Western blot analysis, confirming recognition specific to linear epitopes of eGFP (Fig. 2.21 and 2.22). Moreover, dilutions of tested sera indicate that response to the soluble trimer form of the chimeras was more effective than the response to insoluble aggregates. In this sense, eGFP acted as a reliable indicator of peptide display. These results, however, represent a crude estimation, and a more accurate quantification could be obtained by an indirect Enzyme-Linked ImmunoSorbent Assay (ELISA). The significance of this cannot be underestimated: in the past, subunit peptide display strategies with chimeric VP7 proteins have focused on the insoluble components. The results from this investigation indicate that soluble trimers represent a display platform that is more reliable in structure and presentation of a peptide.

When considering the implication of using eGFP as a model or prototype for any other peptide, it is important to consider the structure and stability of the eGFP protein. Fluorescent proteins based on the monomeric GFP structure are highly stable proteins, resistant to proteolytic degradation as well as maintaining structural stability across a range of pH conditions (Zimmer, 2002). In addition, the extended and unstructured N- and C-terminal regions, which are proximal to one another in the tertiary structure of eGFP, make it extremely amenable to insertion within a loosely structured peptide chain of another protein. Thus, using function (fluorescence) to deduce in-tact structure is a feature that is highly applicable in the case of eGFP, but the rule should be regarded with a degree of scepticism when applied to other peptides. Ideally, the selection of epitopes should be based on known tertiary structure (or at lease the structural integrity of regions surrounding the epitope if the epitope is highly hydrophilic and/or unstructured), and modelled appropriately as a fusion of VP7. Other factors that can be added or modified include linker regions (Nagai and Miyawaki, 2004) to spatially separate an autonomously structured epitope from the VP7 scaffold, or modifications to the peptide sequence itself to make it more resistant to proteolysis. These modifications can be made by the inclusion of non-natural amino acids such as β- amino acids, where the amino group is bonded to the β-carbon instead of the α-carbon (Seebach et al., 1996; Steer et al.,

2002), backbone reduction or partial retro-inversion (Purcell et al., 2007; Webb et al., 2003), all of which have shown improved resistance to proteolytic degradation.

A recent review by Reichel et al. (2006) points out some of the recent progress of VLPs in acting as epitope presentation platforms. Most progress has been made using HBsAg-based vaccines (the only CLP/VLP vaccine available on the market is Engerix-B® produced by GlaxoSmithKline™) and HPV based vaccines (with several vaccines in phase 3 or approved upon publication of the manuscript). The limited success in VLP/CLP-based vaccines does not reflect the overall progress in subunit vaccines in general, and many other approaches are being used for display of short peptides to the immune system (see Purcell et al., 2007 and references therein for more examples of licensed subunit vaccines).

Despite the advantages of VLP/CLP based vectors, optimization of stability of the tertiary substructure of epitopes presented on the surface of these structures still remains a major challenge, with limited solutions being utilized in cases such as chimeric HPV VLPs (Xu et al 2006). The investigations by Kratz et al. (1999) and Smith et al. (2006), also using eGFP as a prototypal displayed peptide, concluded that although the recombinant CLPs produced satisfactory B-cell response, antigen loading was compromised to a degree, due to the necessity of facilitating subunits to interact with one another to form a higher order CLP structure. These results support the conclusions made by Chackerian et al. (2002) in the investigating the immunogenicity of recombinant Papillomavirus VLPs as compared to the subunit pentamers. Those results indicated that while immune response generated by core protein pentamers was lower than that generated by VLPs, it was still relatively efficient and viable, and could be adjusted by the addition of an adjuvant. Furthermore, there is evidence that it is the correct localized display of the immunogen and not the higher order structure in which it is presented, which determines generation of efficient immune response (Chackerian et al., 2002). Thus, the use of the virus like- or core like-particles' *subunits* or building blocks, can accommodate the challenge of acting as the presentation vector. However in order for this to succeed the subunit in question must be able to tolerate peptide insertions, where the antigenic peptide can be presented to the immune system in a (spatially) regular and consistent manner.

In this sense, orbivirus VP7 proteins represent ideal candidates for acting as peptide display vectors for several reasons: First, the use of trimers as peptide display platforms abrogates the requirement of the formation of a higher order structure (e.g. as would be the case in the formation of an Orbivirus CLP by interactions of chimeric VP7 trimers and a subcore made up of VP3 proteins). The benefits of this are twofold – antigenic loading does not need to be compromised, and there is no danger of sub-optimal higher order assembly due to "bulk" or

charge of the inserted peptide (for examples of suboptimal formation of AHSV CLPs, see Maree et al., 1998a; Maree et al., 1998b). Second, the formation of trimers is a tightly regulated interaction, due to the arrangement of the bonds and number of sites (Grimes et al., 1995) connecting VP7 monomers to form trimers, therefore the nature of the trimeric structure forces the epitope into a formation that is evenly spaced and ordered when compared to the freestanding antigenic subunit. Finally, the shape of the trimeric VP7 structure is flexible in terms of the bulk and shape of peptides that can be tolerated in the top domain by loops that face away from one another. The extent of the "bulk" of the peptide that is tolerated by recombinant AHSV VP7mt177, as well as the peptide's correct tertiary structure was demonstrated by this investigation.

Chapter 3: Concluding remarks

This investigation has demonstrated that a full length, functional protein can be inserted into the top domain of the peptide presentation vector VP7mt177, and retain its structural and functional integrity. In addition, chimeric VP7-177-eGFP proteins were demonstrated to form soluble trimers, which could be partially purified and used to elicit immunogenic response to the displayed peptide, eGFP. The fluorescence of eGFP was successfully used as a tool to study the kinetics of expression of the chimeric protein.

Previous strategies with chimeric VP7 proteins involved the use of the particulate forms as epitope display platforms (Maree, 2000; Meyer, 2002; Riley, 2003; Rutkowska, 2003, Van Rensburg, 2005), or as subunits in the in vivo assembly of CLPs (Maree, 2000; Maree et al., 1998a; Maree et al., 1998b). A trimer- based display strategy, however, has not been adequately explored. This investigation has highlighted two main advantages of using chimeric soluble VP7 trimers over larger insoluble aggregations: First, the display of an epitope to its surrounding aqueous environment is more efficient when displayed on the surface of trimers. Second, the display of an epitope mounted on a platform is arguably more homologous using VP7 trimers as opposed to particles. This is illustrated in the inconsistent aggregation pattern and nature of particulate VP7-177-eGFP.

With regards to the viability of AHSV VP7 chimeric proteins as epitope presentation vectors, it is the conclusion of this investigation that since VP7 trimers were shown to be more effective than insoluble aggregates, and since VP7 proteins of AHSV is specifically so innately hydrophobic and tend to form insoluble aggregates, AHSV VP7 vectors may not represent the most optimal system. Nonetheless, a strong argument can still be made for the use of *Orbivirus* VP7 trimers, and with this in mind the focus of AHSV vector-based research should shift towards optimizing solubility of a VP7-based vector. Indeed, as a result of this investigation all existing VP7 vectors were re-analysed to select for solubility as a criterion for potential candidates (H. Huismans, personal communication). In addition, new analogous vectors are currently being developed that are based on BTV VP7 rather than AHSV VP7 (H. Huismans, personal communication). The use of a BTV-based vector should resolve the solubility issue, as WTBTV VP7 trimers are almost 100% soluble when expressed in Sf9 cells, while still maintaining the rigorous predictable tendency to form trimers from monomers.

References

Ailor, E. and M.J. Betenbaugh 1998. Overexpression of a cytosolic chaperone to improve solubility and secretion of a recombinant IgG protein in insect cells. Biotechnol. Bioeng. 58, 196-203.

Antonis, A.F.G., C.J.M. Bruschke, P. Rueda, L. Maranga, J.I. Casal, C. Vela, L.A.T. Hilgers, P.B.G.M. Belt, K. Weerdmeester, M.J.T. Carrondo and J.P.M. Langeveld 2006. A novel recombinant virus-like particle vaccine for prevention of porcine parvovirus-induced reproductive failure. Vaccine. 24, 5481-5490.

Arakawa, T., D. Ejima, K. Tsumoto, N. Obeyama, Y. Tanaka, Y. Kita and S.N. Timasheff 2007a. Suppression of protein interactions by arginine, A proposed mechanism of the arginine effects. Biophys. Chem. 127, 1-8.

Arakawa, T., K. Tsumoto, Y. Kita, B. Chang and D. Ejima 2007b. Biotechnology applications of amino acids in protein purification and formulations. Amino Acids. 33, 587-605.

Aucoin, M.G., D. Jacob, P.S. Chahal, J. Meghrous, A. Bernier and A.A. Kamen 2007. Virus-like particle and viral vector production using the baculovirus expression vector system/ insect cell system, Adeno-associated virus-based products. *In* Methods in Molecular Biology, pp. 281-296.

Bachmann, M.F., R.M. Zinkernagel and A. Oxenius 1998. Cutting edge commentary, Immune responses in the absence of costimulation, Viruses know the trick. J. Immunol. 161, 5791-5794.

Bamford, D.H. 2000. Virus structures, those magnificent molecular machines. Curr. Biol. 10, 558-61.

Baneyx, F. 1999. Recombinant protein expression in Escherichia coli. Curr. Opin. Biotechnol. 10, 411-421.

Bansal, O.B., A. Stokes, A. Bansal, D. Bishop and P. Roy 1998. Membrane organization of bluetongue virus nonstructural glycoprotein NS3. J Virol. 72, 3362-9.

Basak, A.K., P. Gouet, J. Grimes, P. Roy and D. Stuart 1996. Crystal structure of the top domain of African horse sickness virus VP7, comparisons with bluetongue virus VP7. J Virol. 70, 3797-806.

Basak, A.K., J.M. Grimes, P. Gouet, P. Roy and D.I. Stuart 1997. Structures of orbivirus VP7, implications for the role of this protein in the viral life cycle. Structure. 5, 871-83.

Basak, A.K., D.I. Stuart and P. Roy 1992. Preliminary crystallographic study of bluetongue virus capsid protein, VP7. J. Mol. Biol. 228, 687-9.

Beaton, A.R., J. Rodriguez, Y.K. Reddy and P. Roy 2002. The membrane trafficking protein calpactin forms a complex with bluetongue virus protein NS3 and mediates virus release. Proc Natl Acad Sci U S A. 99, 13154-9.

Beljelarskaya, S.N. 2002. A baculovirus expression system for insect cells. Mol. Biol. 36, 281-292.

Benguric, D.R., B. Dungu, F. Thiaucourt and D.H. du Plessis 2001. Phage displayed peptides and anti-idiotype antibodies recognised by a monoclonal antibody directed against a diagnostic antigen of Mycoplasma capricolum subsp. capripneumoniae. Vet Microbiol. 81, 165-79.

Berg, R.H. and R.N. Beachy 2008. Fluorescent Protein Applications in Plants. *In* Methods in Cell Biology, pp. 153-177.

Bhattacharya, B., R.J. Noad and P. Roy 2007. Interaction between Bluetongue virus outer capsid protein VP2 and vimentin is necessary for virus egress. Virology Journal. 4

Biondi, R.M., P.J. Baehler, C.D. Reymond and M. Véron 1998. Random insertion of GFP into the cAMP-dependent protein kinase regulatory subunit from *Dictyostelium discoideum*. Nucleic Acids Res. 26, 4946-4952.

Blachere, N.E., Z. Li, R.Y. Chandawarkar, R. Suto, N.S. Jaikaria, S. Basu, H. Udono and P.K. Srivastava 1997. Heat shock protein-peptide complexes, reconstituted in vitro, elicit peptide-specific cytotoxic T lymphocyte response and tumor immunity. J. Exp. Med. 186, 1315-1322.

Bottcher, B., S.A. Wynne and R.A. CroWTher 1997. Determination of the fold of the core protein of hepatitis B virus by electron cryomicroscopy. Nature. 386, 88-91.

Boyce, M., J. Wehrfritz, R. Noad and P. Roy 2004. Purified recombinant bluetongue virus VP1 exhibits RNA replicase activity. J. Virol. 78, 3994-4002.

Buchner, J. and R. Rudolph 1991. Renaturation, purification and characterization of recombinant F(ab)-fragments produced in Escherichia coli. Bio/Technology. 9, 157-162.

Burrage, T.G., R. Trevejo, M. Stone-Marschat and W.W. Laegreid 1993. Neutralizing epitopes of African horsesickness virus serotype 4 are located on VP2. Virology. 196, 799-803.

Burroughs, J.N., J.M. Grimes, P.P. Mertens and D.I. Stuart 1995. Crystallization and preliminary X-ray analysis of the core particle of bluetongue virus. Virology. 210, 217-20.

Burroughs, J.N., R.S. O'Hara, C.J. Smale, C. Hamblin, A. Walton, R. Armstrong and P.P. Mertens 1994. Purification and properties of virus particles, infectious subviral particles, cores and VP7 crystals of African horsesickness virus serotype 9. J. Gen. Virol. 75, 1849-57.

Butan, C., H. Van Der Zandt and P.A. Tucker 2004. Structure and assembly of the RNA binding domain of bluetongue virus non-structural protein 2. J. Biol. Chem. 279, 37613-37621

Campbell, R.E., O. Tour, A.E. Palmer, P.A. Steinbach, G.S. Baird, D.A. Zacharias and R.Y. Tsien 2002. A monomeric red fluorescent protein. Proc. Natl. Acad. Sci. U.S.A. 99, 7877-7882.

Castellino, F., P.E. Boucher, K. Eichelberg, M. Mayhew, J.E. Rothman, A.N. Houghton and R.N. Germain 2000. Receptor-mediated uptake of antigen/heat shock protein complexes results in major histocompatibility complex class I antigen presentation via two distinct processing pathways. Journal of Experimental Medicine. 191, 1957-1964.

Cha, H.J., N.G. Dalal, M.Q. Pham, V.N. Vakharia, G. Rao and W.E. Bentley 1999. Insect larval expression process is optimized by generating fusions with green fluorescent protein. Biotechnol. Bioeng. 65, 316-324.

Cha, H.J., N.N. Dalal and W.E. Bentley 2005. Secretion of human interleukin-2 fused with green fluorescent protein in recombinant Pichia pastoris. Appl. Biochem. Biotech. 126, 1-11.

Chackerian, B. 2007. Virus-like particles, flexible platforms for vaccine development. Exp. Rev. Vacc. 6, 381-390.

Chackerian, B., P. Lenz, D.R. Lowy and J.T. Schiller 2002. Determinants of autoantibody induction by conjugated papillomavirus virus-like particles. J. Immunol. 169, 6120-6126.

Chalfie, M., Y. Tu, G. Euskirchen, W.W. Ward and D.C. Prasher 1994. Green fluorescent protein as a marker for gene expression. Science. 263, 802-805.

Chapman, S., K.J. Oparka and A.G. Roberts 2005. New tools for in vivo fluorescence tagging. Curr. Opin. Plant Bio. 8, 565-573.

Cherish Babu, P.V., V.K. Srinivas, V. Krishna Mohan and E. Krishna 2008. Renaturation, purification and characterization of streptokinase expressed as inclusion body in recombinant E. coli. J. Chromatogr. B, Analytical Technologies in the Biomedical and Life Sciences. 861, 218-226.

Chianese-Bullock, K.A., J. Pressley, C. Garbee, S. Hibbitts, C. Murphy, G. Yamshchikov, G.R. Petroni, E.A. Bissonette, P.Y. Neese, W.W. Grosh, P. Merrill, R. Fink, E.M.H. Woodson, C.J. Wiernasz, J.W. Patterson and C.L. Slingluff Jr 2005. MAGE-A1-, MAGE-A10-, and gp100-derived peptides are immunogenic when combined with granulocyte-macrophage colony-stimulating factor and montanide ISA-51 adjuvant and administered as part of a multipeptide vaccine for melanoma. J. Immunol. 174, 3080-3086.

Chudakov, D.M., S. Lukyanov and K.A. Lukyanov 2005. Fluorescent proteins as a toolkit for in vivo imaging. Trends Biotechnol. 23, 605-613.

Chuma, T., H. Le Blois, J.M. Sanchez-Vizcaino, M. Diaz-Laviada and P. Roy 1992. Expression of the major core antigen VP7 of African horsesickness virus by a recombinant baculovirus and its use as a group-specific diagnostic reagent. J. Gen. Virol. 73, 925-31.

Clarke, B.E., S.E. NeWTon, A.R. Carroll, M.J. Francis, G. Appleyard, A.D. Syred, P.E. Highfield, D.J. Rowlands and F. Brown 1987. Improved immunogenicity of a peptide epitope after fusion to hepatitis B core protein. Nature. 330, 381-383.

Cody, C.W., D.C. Prasher, W.M. Westler, F.G. Prendergast and W.W. Ward 1993. Chemical-Structure of the Hexapeptide Chromophore of the Aequorea Green-Fluorescent Protein. Biochemistry. 32, 1212-1218.

Coetzer, J.A.W. and A.J. Guthrie 2004. African horse sickness. Infectious diseases of livestock, 1231-1246.

Condreay, J.P. and T.A. Kost 2007. Baculovirus expression vectors for insect and mammalian cells. Current Drug Targets. 8, 1126-1131.

Conway, J.F., N. Cheng, A. Zlotnick, S.J. Stahl, P.T. Wingfield, D.M. Belnap, U. Kanngiesser, M. Noah and A.C. Steven 1998. Hepatitis B virus capsid, localization of the putative immunodominant loop (residues 78 to 83) on the capsid surface, and implications for the distinction between c and e-antigens. J. Mol. Biol. 279, 1111-1121.

Cormack, B.P., R.H. Valdivia and S. Falkow 1996. FACS-optimized mutants of the green fluorescent protein (GFP). Gene. 173, 33-38.

CroWTher, R.A., N.A. Kiselev, B. Böttcher, J.A. Berriman, G.P. Borisova, V. Ose and P. Pumpens 1994. Three-dimensional structure of hepatitis B virus core particles determined by electron cryomicroscopy. Cell. 77, 943-950.

D'Apice, L., R. Sartorius, A. Caivano, D. Mascolo, G. Del Pozzo, D.S. Di Mase, E. Ricca, G.L. Pira, F. Manca, D. Malanga, R. De Palma and P. De Berardinis 2007. Comparative analysis of new innovative vaccine formulations based on the use of procaryotic display systems. Vaccine. 25, 1993-2000.

De Berardinis, P., L. D'Apice, A. Prisco, M.N. Ombra, P. Barba, G. Del Pozzo, S. Petukhov, P. Malik, R.N. Perham and J. Guardiola 1999. Recognition of HIV-derived B and T cell epitopes displayed on filamentous phages. Vaccine. 17, 1434-1441.

De Berardinis, P., R. Sartorius, C. Fanutti, R.N. Perham, G. Del Pozzo and J. Guardiola 2000. Phage display of peptide epitopes from HIV-1 elicits strong cytolytic responses. Nat. Biotechnol. 18, 873-876.

De Waal, P.J. and H. Huismans 2005. Characterization of the nucleic acid binding activity of inner core protein VP6 of African horse sickness virus. Arch. Virol. 150, 2037-2050.

DeLano, W.L. The PyMOL Molecular Graphics System (2002) DeLano Scientific, Palo Alto, CA, USA. http, //www.pymol.org

Devaney, M.A., J. Kendall and M.J. Grubman 1988. Characterization of a nonstructural phosphoprotein of two orbiviruses. Virus Res. 11, 151-64.

Diprose, J.M., J.N. Burroughs, G.C. Sutton, A. Goldsmith, P. Gouet, R. Malby, I. Overton, S. Zientara, P.P. Mertens, D.I. Stuart and J.M. Grimes 2001. Translocation portals for the substrates and products of a viral transcription complex, the bluetongue virus core. Embo J. 20, 7229-39.

Diprose, J.M., J.M. Grimes, G.C. Sutton, J.N. Burroughs, A. Meyer, S. Maan, P.P. Mertens and D.I. Stuart 2002. The core of bluetongue virus binds double-stranded RNA. J Virol. 76, 9533-6.

Dixit, R., R. Cyr and S. Gilroy 2006. Using intrinsically fluorescent proteins for plant cell imaging. Plant J. 45, 599-615.

Doerfler, W. 1986. Expression of the Autographa californica nuclear polyhedrosis virus genome in insect cells, homologous viral and heterologous vertebrate genes--the baculovirus vector system. Curr. Top. Microbiol. 131, 51-68.

Domingo, G.J., S. Orru and R.N. Perham 2001. Multiple display of peptides and proteins on a macromolecular scaffold derived from a multienzyme complex. J. Mol. Biol. 305, 259-267.

Du Plessis, M., M. Cloete, H. Aitchison and A.A. Van Dijk 1998. Protein aggregation complicates the development of baculovirus- expressed African horsesickness virus serotype 5 VP2 subunit vaccines [In Process Citation]. Onderstepoort J Vet Res. 65, 321-9.

du Plessis, M. and L.H. Nel 1997. Comparative sequence analysis and expression of the M6 gene, encoding the outer capsid protein VP5, of African horsesickness virus serotype nine. Virus Res. 47, 41-9.

Eaton, B.T., A.D. Hyatt and J.R. White 1988. Localization of the nonstructural protein NS1 in bluetongue virus- infected cells and its presence in virus particles. Virology. 163, 527-37.

Feng, G., R.H. Mellor, M. Bernstein, C. Keller-Peck, Q.T. Nguyen, M. Wallace, J.M. Nerbonne, J.W. Lichtman and J.R. Sanes 2000. Imaging neuronal subsets in transgenic mice expressing multiple spectral variants of GFP. Neuron. 28, 41-51.

Fillmore, G.C., H. Lin and J.K. Li 2002. Localization of the single-stranded RNA-binding domains of bluetongue virus nonstructural protein NS2. J Virol. 76, 499-506.

Fiser, A. and A. Šali 2003. MODELLER, Generation and Refinement of Homology-Based Protein Structure Models. Method Enzymol, pp. 461-491.

Forzan, M., M. Marsh and P. Roy 2007. Bluetongue virus entry into cells. J. Virol. 81, 4819-4827.

Forzan, M., C. Wirblich and P. Roy 2004. A capsid protein of nonenveloped Bluetongue virus exhibits membrane fusion activity. Proc Natl Acad Sci U S A. 101, 2100-2105.

French, T.J., J.J. Marshall and P. Roy 1990. Assembly of double-shelled, viruslike particles of bluetongue virus by the simultaneous expression of four structural proteins. J Virol. 64, 5695-700.

French, T.J. and P. Roy 1990. Synthesis of bluetongue virus (BTV) corelike particles by a recombinant baculovirus expressing the two major structural core proteins of BTV. J Virol. 64, 1530-1536.

García-Mata, R., Bebök, Z., Sorscher, E. J., Sztul, E. S. Characterization and dynamics of aggresome formation by a cytosolic GFP- chimera. J. Cell Biol. 146, 1239-1254.

Gasteiger E., H.C., Gattiker A., Duvaud S., Wilkins M.R., Appel R.D., Bairoch A. 2005. Protein Identification and Analysis Tools on the ExPASy Server. *In* The Proteomics Protocols Handbook Ed. J.M. Walker. Humana Press, pp.571-607.

Ghosh, M.K., M.V. Borca and P. Roy 2002a. Virus-derived tubular structure displaying foreign sequences on the surface elicit CD4+ Th cell and protective humoral responses. Virology. 302, 383-92.

Ghosh, M.K., E. Deriaud, M.F. Saron, R. Lo-Man, T. Henry, X. Jiao, P. Roy and C. Leclerc 2002b. Induction of protective antiviral cytotoxic T cells by a tubular structure capable of carrying large foreign sequences. Vaccine. 20, 1369-77.

Giraldez, T., T.E. Hughes and F.J. Sigworth 2005. Generation of functional fluorescent BK channels by random insertion of GFP variants. J. Gen. Physiol. 126, 429-438.

Gouet, P., J.M. Diprose, J.M. Grimes, R. Malby, J.N. Burroughs, S. Zientara, D.I. Stuart and P.P. Mertens 1999. The highly ordered double-stranded RNA genome of bluetongue virus revealed by crystallography. Cell. 97, 481-90.

Gould, A.R. and A.D. Hyatt 1994. The orbivirus genus. Diversity, structure, replication and phylogenetic relationships. Comp Immunol Microbiol Infect Dis. 17, 163-88.

Grimes, J., A.K. Basak, P. Roy and D. Stuart 1995. The crystal structure of bluetongue virus VP7. Nature. 373, 167-70.

Grimes, J.M., J.N. Burroughs, P. Gouet, J.M. Diprose, R. Malby, S. Zientara, P.P. Mertens and D.I. Stuart 1998. The atomic structure of the bluetongue virus core. Nature. 395, 470-8.

Grimes, J.M., J. Jakana, M. Ghosh, A.K. Basak, P. Roy, W. Chiu, D.I. Stuart and B.V. Prasad 1997. An atomic model of the outer layer of the bluetongue virus core derived from X-ray crystallography and electron cryomicroscopy. Structure. 5, 885-93.

Hassan, S.H., C. Wirblich, M. Forzan and P. Roy 2001. Expression and functional characterization of bluetongue virus VP5 protein, role in cellular permeabilization. J Virol. 75, 8356-67.

Hassan, S.S. and P. Roy 1999. Expression and functional characterization of bluetongue virus VP2 protein, role in cell entry. J Virol. 73, 9832-42.

Heim, R., A.B. Cubitt and R.Y. Tsien 1995. Improved green fluorescence [4]. Nature. 373, 663-664.

Heim, R., D.C. Prasher and R.Y. Tsien 1994. Wavelength mutations and posttranslational autoxidation of green fluorescent protein. Proc Natl Acad Sci U S A. 91, 12501-4.

Hewat, E.A., T.F. Booth, P.T. Loudon and P. Roy 1992a. Three-dimensional reconstruction of baculovirus expressed bluetongue virus core-like particles by cryo-electron microscopy. Virology. 189, 10-20.

Hewat, E.A., T.F. Booth and P. Roy 1992b. Structure of bluetongue virus particles by cryoelectron microscopy. J Struct Biol. 109, 61-9.

Hewat, E.A., T.F. Booth, R.H. Wade and P. Roy 1992c. 3-D reconstruction of bluetongue virus tubules using cryoelectron microscopy. J Struct Biol. 108, 35-48.

Hilleman, M.R. 2000. Overview of vaccinology with special reference to papillomavirus vaccines. J. Clin. Virol. 19, 79-90.

Hockney, R.C. 1994. Recent developments in heterologous protein production in Escherichia coli. Trends Biotechnol. 12, 456-463.

Hu, Y.C. 2005. Baculovirus as a highly efficient expression vector in insect and mammalian cells. Acta Pharm. Sinic. 26, 405-416.

Hughes, T.E., H. Zhang, D.E. Logothetis and C.H. Berlot 2001. Visualization of a Functional Gαq-Green Fluorescent Protein Fusion in Living Cells. Association with the plasma membrane is disrupted by mutational activation and by elimination of palmitoylation sites, but not by activation mediated by receptors or AlF4. J. Biol. Chem. 276, 4227-4235.

Huismans, H. 1979. Protein synthesis in bluetongue virus-infected cells. Virology. 92, 385-96.

Huismans, H. and B.J. Erasmus 1981. Identification of the serotype-specific and group-specific antigens of bluetongue virus. Onderstepoort J Vet Res. 48, 51-8.

Huismans, H., N.T. Van der Walt, M. Cloete and B.J. Erasmus 1987a. Isolation of a capsid protein of bluetongue virus that induces a protective immune response in sheep. Virology. 157, 172-9.

Huismans, H., N.T. Van der Walt and B.J. Erasmus 1985. Immune response against the purified serotype specific antigen of bluetongue virus and initial attempts to clone the gene that codes for the synthesis of this protein. Prog Clin Biol Res. 178, 347-53.

Huismans, H., A.A. Van Dijk and A.R. Bauskin 1987b. In vitro phosphorylation and purification of a nonstructural protein of bluetongue virus with affinity for single-stranded RNA. J Virol. 61, 3589-95.

Huismans, H., A.A. Van Dijk and H.J. Els 1987c. Uncoating of parental bluetongue virus to core and subcore particles in infected L cells. Virology. 157, 180-8.

Hyatt, A.D., Y. Zhao and P. Roy 1993. Release of bluetongue virus-like particles from insect cells is mediated by BTV nonstructural protein NS3/NS3A. Virology. 193, 592-603.

Hyung, J.C., S.S. Hwa, J.L. Hye, S.C. Hye, N.N. Dalal, M.Q. Pham and W.E. Bentley 2005. Comparative production of human interleukin-2 fused with green fluorescent protein in several recombinant expression systems. Biochem. Eng. J. 24, 225-233.

Iwata, H., M. Yamagawa and P. Roy 1992. Evolutionary relationships among the gnat-transmitted orbiviruses that cause African horse sickness, bluetongue, and epizootic hemorrhagic disease as evidenced by their capsid protein sequences. Virology. 191, 251-61.

Jahn, T.R. and S.E. Radford 2008. Folding versus aggregation, Polypeptide conformations on competing pathways. Arch. Biochem. Biophys. 469, 100-117.

Jegerlehner, A., A. Tissot, F. Lechner, P. Sebbel, I. Erdmann, T. Kündig, T. Bächi, T. Storni, G. Jennings, P. Pumpens, W.A. Renner and M.F. Bachmann 2002. A molecular assembly system that renders antigens of choice highly repetitive for induction of protective B cell responses. Vaccine. 20, 3104-3112.

Johnston, J.A., C.L. Ward and R.R. Kopito 1998. Aggresomes: A cellular response to misfolded proteins. J. Cell Biol. 143:1883-1898.

Kahlon, J., K. Sugiyama and P. Roy 1983. Molecular basis of bluetongue virus neutralization. J Virol. 48, 627-32.

Kain, S., P. Kitts, G. Zhang, V. Gurlu, T. Yang, B. Cormack, R. Valdivia and S. Falkow 1996. Enhanced green fluorescent protein vectors that provide stronger fluorescence intensities and higher expression in mammalian cells. FASEB J. 10

Kar, A.K. and P. Roy 2003. Defining the structure-function relationships of bluetongue virus helicase protein VP6. J Virol. 77, 11347-56.

Kersten, G.F.A. and D.J.A. Crommelin 2003. Liposomes and ISCOMs. Vaccine. 21, 915-920.

Kost, T.A., J.P. Condreay and D.L. Jarvis 2005. Baculovirus as versatile vectors for protein expression in insect and mammalian cells. Nature Biotechnol. 23, 567-575.

Kowalik, T.F. and J.K. Li 1989. Sequence analyses and structural predictions of double-stranded RNA segment S1 and VP7 from United States prototype bluetongue virus serotypes 13 and 10. Virology. 172, 189-95.

Kratz, P.A., B. Böttcher and M. Nassal 1999. Native display of complete foreign protein domains on the surface of hepatitis B virus capsids. Proc. Natl. Acad. Sci. U.S.A. 96, 1915-1920.

Kretzmann, H. 2006. The characterization of African horsesickness virus VP7 particles with foreign peptides inserted into site 200 of the VP7 protein top domain. MSc dissertation.

Kyte, J. and R.F. Doolittle 1982. A simple method for displaying the hydropathic character of a protein. J. Mol. Biol. 157, 105-132.

Lacheiner, K. 2006. Tubules composed of non-structural protein NS1 of african horsesickness virus as a system for the immune display of foreign peptides. MSc Dissertation.

Lalonde, S., D.W. Ehrhardt, D. Loque, J. Chen, S.Y. Rhee and W.B. Frommer 2008. Molecular and cellular approaches for the detection of protein-protein interactions, Latest techniques and current limitations. Plant J. 53, 610-635.

Le Blois, H., T. French, P.P. Mertens, J.N. Burroughs and P. Roy 1992. The expressed VP4 protein of bluetongue virus binds GTP and is the candidate guanylyl transferase of the virus. Virology. 189, 757-61.

Lechner, F., A. Jegerlehner, A.C. Tissot, P. Maurer, P. Sebbel, W.A. Renner, G.T. Jennings and M.F. Bachmann 2002. Virus-like particles as a modular system for novel vaccines. Intervirology. 45, 212-217.

Li, X., X. Wang, S. Xiong, J. Zhang, L. Cai and Y. Yang 2007. Expression and purification of recombinant nattokinase in Spodoptera frugiperda cells. Biotechnol. Lett. 29, 1459-1464.

Limn, C.K. and P. Roy 2003. Intermolecular interactions in a two-layered viral capsid that requires a complex symmetry mismatch. J Virol. 77, 11114-24.

Limn, C.K., N. Staeuber, K. Monastyrskaya, P. Gouet and P. Roy 2000. Functional dissection of the major structural protein of bluetongue virus, identification of key residues within VP7 essential for capsid assembly. J Virol. 74, 8658-69.

Livet, J., T.A. Weissman, H. Kang, R.W. Draft, J. Lu, R.A. Bennis, J.R. Sanes and J.W. Lichtman 2007. Transgenic strategies for combinatorial expression of fluorescent proteins in the nervous system. Nature. 450, 56-62.

Loudon, P.T. and P. Roy 1991. Assembly of five bluetongue virus proteins expressed by recombinant baculoviruses, inclusion of the largest protein VP1 in the core and virus-like proteins. Virology. 180, 798-802.

MacLachlan, N.J., U.B. Balasuriya, N.L. Davis, M. Collier, R.E. Johnston, G.L. Ferraro and A.J. Guthrie 2007. Experiences with new generation vaccines against equine viral arteritis, West Nile disease and African horse sickness. Vaccine. 25, 5577-5582.

Mäkelä, A.R. and C. Oker-Blom 2006. Baculovirus Display, A Multifunctional Technology for Gene Delivery and Eukaryotic Library Development. Adv. Virus Res, pp. 91-112.

Mäkelä, A.R. and C. Oker-Blom 2008. The baculovirus display technology - An evolving instrument for molecular screening and drug delivery. Com. Chem. High T. Scr . 11, 86-98.

Mancini, E.J., F. De Haas and S.D. Fuller 1997. High-resolution icosahedral reconstruction, fulfilling the promise of cryo-electron microscopy. Structure. 5, 741-750.

Maranga, L., P. Rueda, A. Antonis, C. Vela, J. Langeveld, J. Casal and M. Carrondo 2002. Large scale production and downstream processing of a recombinant porcine parvovirus vaccine. Appl. Microbiol. Biotech. . 59, 45-50.

March, J.C., G. Rao and W.E. Bentley 2003. Biotechnological applications of green fluorescent protein. Appl. Microbiol. Biotech. . 62, 303-315.

Maree, F.F. 2000. Multimeric protein structures of African horsesickness virus and their use as antigen delivery systems. PhD dissertation.

Maree, F.F. and H. Huismans 1997. Characterization of tubular structures composed of nonstructural protein NS1 of African horsesickness virus expressed in insect cells. J. Gen. Virol. 78, 1077-82.

Maree, S., S. Durbach and H. Huismans 1998a. Intracellular production of African horsesickness virus core-like particles by expression of the two major core proteins, VP3 and VP7, in insect cells. J. Gen. Virol. 79, 333-7.

Maree, S., S. Durbach, F.F. Maree, F. Vreede and H. Huismans 1998b. Expression of the major core structural proteins VP3 and VP7 of African horse sickness virus, and production of core-like particles. Arch. Virol. Suppl. 14, 203-9.

Martinez-Costas, J., G. Sutton, N. Ramadevi and P. Roy 1998. Guanylyltransferase and RNA 5'-triphosphatase activities of the purified expressed VP4 protein of bluetongue virus. J. Mol. Biol. 280, 859-66.

Martinez-Torrecuadrada, J.L., M. Diaz-Laviada, P. Roy, C. Sanchez, C. Vela, J.M. Sanchez-Vizcaino and J.I. Casal 1996. Full protection against African horsesickness (AHS) in horses induced by baculovirus-derived AHS virus serotype 4 VP2, VP5 and VP7. J. Gen. Virol. 77, 1211-21.

Mattion, N.M., P.A. Reilly, S.J. DiMichele, J.C. Crowley and C. Weeks-Levy 1994. Attenuated poliovirus strain as a live vector, expression of regions of rotavirus outer capsid protein VP7 by using recombinant Sabin 3 viruses. J. Virol. 68, 3925-33.

Mecham, J.O., V.C. Dean and M.M. Jochim 1986. Correlation of serotype specificity and protein structure of the five U.S. serotypes of bluetongue virus. J. Gen. Virol. 67, 2617-24.

Medin, J.A., L. Hunt, K. Gathy, R.K. Evans and M.S. Coleman 1990. Efficient, low-cost protein factories, Expression of human adenosine deaminase in baculovirus-infected insect larvae. Proc. Natl. Acad. Sci. U.S.A. 87, 2760-2764.

Medzhitov, R. and C.A. Janeway, Jr. 1997. Innate immunity, the virtues of a nonclonal system of recognition. Cell. 91, 295-8.

Mertens, P.P., J.N. Burroughs and J. Anderson 1987. Purification and properties of virus particles, infectious subviral particles, and cores of bluetongue virus serotypes 1 and 4. Virology. 157, 375-86.

Mertens, P.P. and J. Diprose 2004. The bluetongue virus core, a nano-scale transcription machine. Virus Res. 101, 29-43.

Meyer, Q.C. 2002. The presentation of an HIV-1 neutralizing epitope on the surface of major structural protein VP7 of African horse sickness virus. MSc dissertation.

Michel, M.L., P. Pontisso, E. Sobczak, Y. Malpiece, R.E. Streeck and P. Tiollais 1984. Synthesis in animal cells of hepatitis B surface antigen particles carrying a receptor for polymerized human serum albumin. Proc Natl Acad Sci U S A. 81, 7708-12.

Mikhailov, M., K. Monastyrskaya, T. Bakker and P. Roy 1996. A new form of particulate single and multiple immunogen delivery system based on recombinant bluetongue virus-derived tubules. Virology. 217, 323-31.

Miyawaki, A. 2003. Fluorescence imaging of physiological activity in complex systems using GFP-based probes. Curr. Opin Neurobiol. 13, 591-596.

Miyawaki, A., A. Sawano and T. Kogure 2003. Lighting up cells, Labelling proteins with fluorophores. Nature Rev. Mol. Cell Biol. 4

Morein, B., B. Sundquist and S. Hoglund 1984. Iscom, a novel structure for antigenic presentation of membrane proteins from enveloped viruses. Nature. 308, 457-460.

Morise, H., O. Shimomura, F.H. Johnson and J. Winant 1974. Intermolecular energy transfer in the bioluminescent system of Aequorea. Biochemistry. 13, 2656-2662.

Moss, B., O. Elroy-Stein, T. Mizukami, W.A. Alexander and T.R. Fuerst 1990. New mammalian expression vectors. Nature. 348, 91-92.

Moylett, E.H. and I.C. Hanson 2003. 29. Immunization. J Allergy Clin Immunol. 111, S754-65.

Mumtsidu, E., A.M. Makhov, M. Roessle, A. Bathke and P.A. Tucker 2007. Structural features of the Bluetongue virus NS2 protein. J. Struct. Biol. 160, 157-167.

Nagai, T. and A. Miyawaki 2004. A high-throughput method for development of FRET-based indicators for proteolysis. Biochem. Bioph. Res. Co. 319, 72-77.

Nagesha, H.S., L. Wang, B. Shiell, G. Beddome, J.R. White and R.A. Irving 2001. A single chain Fv antibody displayed on phage surface recognises conformational group-specific epitope of bluetongue virus. J. Virol. Methods. 91, 203-207.

Nason, E.L., R. Rothagel, S.K. Mukherjee, A.K. Kar, M. Forzan, B.V. Prasad and P. Roy 2004. Interactions between the inner and outer capsids of bluetongue virus. J. Virol. 78, 8059-67.

Natalello, A., R. Santarella, S.M. Doglia and A.d. Marco 2008. Physical and chemical perturbations induce the formation of protein aggregates with different structural features. Protein Expres. Purif. 58, 356-361.

Noessner, E., R. Gastpar, V. Milani, A. Brandl, P.J.S. Hutzler, M.C. Kuppner, M. Roos, E. Kremmer, A. Asea, S.K. Calderwood and R.D. Issels 2002. Tumor-derived heat shock protein 70 peptide complexes are cross-presented by human dendritic cells. J. Immunol. 169, 5424-5432.

Ormo, M., A.B. Cubitt, K. Kallio, L.A. Gross, R.Y. Tsien and S.J. Remington 1996. Crystal structure of the Aequorea victoria green fluorescent protein. Science. 273, 1392-5.

Owens, R.J., C. Limn and P. Roy 2004. Role of an arbovirus nonstructural protein in cellular pathogenesis and virus release. J. Virol. 78, 6649-56.

Petrovsky, N. 2006. Novel human polysaccharide adjuvants with dual Th1 and Th2 potentiating activity. Vaccine. 24

Prasad, B.V., S. Yamaguchi and P. Roy 1992. Three-dimensional structure of single-shelled bluetongue virus. J. Virol. 66, 2135-42.

Purcell, A.W., J. McCluskey and J. Rossjohn 2007. More than one reason to rethink the use of peptides in vaccine design. Nat. Rev. Drug Disc. 6, 404-414.

Purdy, M.A., G.D. Ritter and P. Roy 1986. Nucleotide sequence of cDNA clones encoding the outer capsid protein, VP5, of bluetongue virus serotype 10. J. Gen. Virol. 67, 957-62.

Ramadevi, N., N.J. Burroughs, P.P. Mertens, I.M. Jones and P. Roy 1998a. Capping and methylation of mRNA by purified recombinant VP4 protein of bluetongue virus. Proc. Natl. Acad. Sci. U.S.A. 95, 13537-42.

Ramadevi, N., J. Rodriguez and P. Roy 1998b. A leucine zipper-like domain is essential for dimerization and encapsidation of bluetongue virus nucleocapsid protein VP4. J. Virol. 72, 2983-90.

Riley, J.A. 2003. Construction of a new peptide insertion site in the top domain of major core protein VP7 of African horsesickness virus. MSc dissertation.

Roitt, I., J. Brostoff and D. Male 2001. Immunology. Mosby. 496 p.

Romanos, M. 1995. Advances in the use of Pichia pastoris for high-level gene expression. Curr. Opin. Biotechnol. 6, 527-533.

Romanos, M.A., C.A. Scorer and J.J. Clare 1992. Foreign gene expression in yeast, a review. Yeast. 8, 423-488.

Roy, P. 1996. Orbivirus structure and assembly. Virology. 216, 1-11.

Roy, P. 2008. Structure and Function of Bluetonge Virus and its Proteins. *In* Segmented Double-Sstranded RNA Viruses, Structural and Molecular Biology Ed. J. Patton. Caister Academic Press, Norfolk, UK.

Roy, P., D.H. Bishop, S. Howard, H. Aitchison and B. Erasmus 1996. Recombinant baculovirus-synthesized African horsesickness virus (AHSV) outer-capsid protein VP2 provides protection against virulent AHSV challenge. J. Gen. Virol. 77, 2053-7.

Roy, P., T. Hirasawa, M. Fernandez, V.M. Blinov and J.M. Sanchez-Vixcain Rodrique 1991. The complete sequence of the group-specific antigen, VP7, of African horsesickness disease virus serotype 4 reveals a close relationship to bluetongue virus. J. Gen. Virol. 72, 1237-41.

Roy, P., P.P. Mertens and I. Casal 1994. African horse sickness virus structure. Comp. Immunol. Microbiol. Infect. Dis. 17, 243-73.

Roy, P., T. Urakawa, A.A. Van Dijk and B.J. Erasmus 1990. Recombinant virus vaccine for bluetongue disease in sheep. J. Virol. 64, 1998-2003.

Rutkowska, D.A. 2003. The development of vaccine delivery systems based on presenting peptides on the surface of core protein VP7 of African horse sickness virus. MSc dissertation.

Sambrook, J. and Russell, D.W. 2001. Molecular Cloning, a laboratory manual. Third edition. Cold Spring harbor Laboratory Press.

Sanchez-Vizcaino, J.M. 2004. Control and eradication of African horse sickness with vaccine. Dev. Biol. (Basel). 119, 255-258.

Sanders, M.T., L.E. Brown, G. Deliyannis and M.J. Pearse 2005. ISCOM^{TM}-based vaccines, the second decade. Immunol. Cell Biol. 83, 119-128.

Schmidt, F.R. 2004. Recombinant expression systems in the pharmaceutical industry. Appl. Microbiol. Biotech. . 65, 363-372.

Schodel, F., D. Peterson, D.R. Milich, Y. Charoenvit, J. Sadoff and R. Wirtz 1997. Immunization with hybrid hepatitis B virus core particles carrying circumsporozoite antigen epitopes protects mice against *Plasmodium yoelii* challenge. Behring Inst Mitt, 114-9.

Schodel, F., R. Wirtz, D. Peterson, J. Hughes, R. Warren, J. Sadoff and D. Milich 1994. Immunity to malaria elicited by hybrid hepatitis B virus core particles carrying circumsporozoite protein epitopes. J. Exp. Med. 180, 1037-46.

Seebach, D., M. Overhand, F.N.M. Kühnle, B. Martinoni, L. Oberer, U. Hommel and H. Widmer 1996. β-peptides, Synthesis by Arndt-Eistert homologation with concomitant peptide coupling. Structure determination by NMR and CD spectroscopy and by X-Ray crystallography. Helical secondary structure of a β-hexapeptide in solution and its stability towards pepsin. Helv. Chim. Acta. 79, 913-941.

Sheridan, D.L., C.H. Herlot, A. Robert, F.M. Inglis, K.B. Jakobsdottir, J.R. Howe and T.E. Hughes 2002. A new way to rapidly create functional, fluorescent fusion proteins, Random insertion of GFP with an in vitro transposition reaction. BMC Neuroscience. 3

Sheridan, D.L. and T.E. Hughes 2004. A faster way to make GFP-based biosensors, two new transposons for creating multicolored libraries of fluorescent fusion proteins. BMC Biotechnology. 4

Shimomura, O. 1979. Structure of the Chromophore of Aequorea Green Fluorescent Protein. Febs. Lett. 104, 220-222.

Shimomura, O., F.H. Johnson and Y. Saiga 1962. Extraction, purification and properties of aequorin, a bioluminescent protein from the luminous hydromedusan, Aequorea. J. Cell. Comp. Physiol. 59, 223-239.

Shin, H.S., H.J. Lim and H.J. Cha 2003. Quantitative monitoring for secreted production of human interleukin-2 in stable insect Drosophila S2 cells using a green fluorescent protein fusion partner. Biotechnol. Progr. 19, 152-157.

Siegel, M.S. and E.Y. Isacoff 1997. A genetically encoded optical probe of membrane voltage. Neuron. 19, 735-741.

Silva, J.L., Y. Cordeiro and D. Foguel 2006. Protein folding and aggregation, two sides of the same coin in the condensation of proteins revealed by pressure studies. Biochimica et Biophysica Acta – Prot. Proteom. 1764, 443-451.

Smith, M.L., J.A. Lindbo, S. Dillard-Telm, P.M. Brosio, A.B. Lasnik, A.A. McCormick, L.V. Nguyen and K.E. Palmer 2006. Modified Tobacco mosaic virus particles as scaffolds for display of protein antigens for vaccine applications. Virology. 348, 475-488.

Soler, E. and L.M. Houdebine 2007. Preparation of recombinant vaccines. Biotechnol. Ann. Rev., pp. 65-94.

Sørensen, H.P. and K.K. Mortensen 2005. Advanced genetic strategies for recombinant protein expression in Escherichia coli. J. Biotechnol. 115, 113-128.

Spence, L., M. Fauvel, S. Bouchard, L. Babiuk and Saunders 1975. Letter, Test for reovirus-like agent. Lancet. 2, 322.

Stauber, N., J. Martinez-Costas, G. Sutton, K. Monastyrskaya and P. Roy 1997. Bluetongue virus VP6 protein binds ATP and exhibits an RNA-dependent ATPase function and a helicase activity that catalyse the unwinding of double-stranded RNA substrates. J. Virol. 71, 7220-6.

Stearns, T. 1995. Green fluorescent protein, The green revolution. Curr. Biol. 5, 262-264.

Steer, D.L., R.A. Lew, P. Perlmutter, A.I. Smith and M.I. Aguilar 2002. β-Amino acids, Versatile peptidomimetics. Curr. Med. Chem. 9, 811-822.

Stefani, M. and C.M. Dobson 2003. Protein aggregation and aggregate toxicity, new insights into protein folding, misfolding diseases and biological evolution. J. Mol. Med. 81, 678-699.

Stewart Jr, C.N. 2006. Go with the glow, fluorescent proteins to light transgenic organisms. Trends Biotechnol. 24, 155-162.

Stoltz, M.A., C.F. Van der Merwe, J. Coetzee and H. Huismans 1996. Subcellular localization of the nonstructural protein NS3 of African horsesickness virus. Onderstepoort J. Vet. Res. 63, 57-61.

Stone-Marschat, M.A., S.R. Moss, T.G. Burrage, M.L. Barber, P. Roy and W.W. Laegreid 1996. Immunization with VP2 is sufficient for protection against lethal challenge with African horsesickness virus Type 4. Virology. 220, 219-22.

Stuart, D.I. and J.M. Grimes 2006. Structural studies on orbivirus proteins and particles. *In* Curr. Top. Microbiol, pp. 221-244.

Suto, R. and P.K. Srivastava 1995. A mechanism for the specific immunogenicity of heat shock protein-chaperoned peptides. Science. 269, 1585-1588.

Sutton, G., J.M. Grimes, D.I. Stuart and P. Roy 2007. Bluetongue virus VP4 is an RNA-capping assembly line. Nat. Struct. Mol. Biol. 14, 449-451.

Szomolanyi-Tsuda, E. and R.M. Welsh 1998. T-cell-independent antiviral antibody responses. Curr. Opin. Immunol. 10, 431-5.

Tamura, Y., P. Peng, K. Liu, M. Daou and P.K. Srivastava 1997. Immunotherapy of tumors with autologous tumor-derived heat shock protein preparations. Science. 278, 117-120.

Tao, Y., D.L. Farsetta, M.L. Nibert and S.C. Harrison 2002. RNA synthesis in a cage--structural studies of reovirus polymerase lambda3. Cell. 111, 733-45.

Taïeb, J., N. Chaput and L. Zitvogel 2005. Dendritic cell-derived exosomes as cell-free peptide-based vaccines. Crit. Rev. Immunol. 25, 215-223.

Theron, J., H. Huismans and L.H. Nel 1996. Site-specific mutations in the NS2 protein of epizootic haemorrhagic disease virus markedly affect the formation of cytoplasmic inclusion bodies. Arch. Virol. 141, 1143-51.

Theron, J. and L.H. Nel 1997. Stable protein-RNA interaction involves the terminal domains of bluetongue virus mRNA, but not the terminally conserved sequences. Virology. 229, 134-42.

Thomas, C.P., T.F. Booth and P. Roy 1990. Synthesis of bluetongue virus-encoded phosphoprotein and formation of inclusion bodies by recombinant baculovirus in insect cells, it binds the single-stranded RNA species. J. Gen. Virol. 71, 2073-83.

Thompson, J.D., T.J. Gibson, F. Plewniak, F. Jeanmougin and D.G. Higgins 1997. The CLUSTAL X windows interface, flexible strategies for multiple sequence alignment aided by quality analysis tools. Nucleic Acids Res. 25, 4876-4882.

Traore, O., G. Belliot, C. Mollat, H. Piloquet, C. Chamoux, H. Laveran, S.S. Monroe and S. Billaudel 2000. RT-PCR identification and typing of astroviruses and Norwalk-like viruses in hospitalized patients with gastroenteritis, evidence of nosocomial infections. J. Clin. Virol. 17, 151-8.

Tsien, R.Y. 1998. The green fluorescent protein. Annu. Rev. Biochem. 67, 509-44.

Tsumoto, K., D. Ejima, K. Nagase and T. Arakawa 2007. Arginine improves protein elution in hydrophobic interaction chromatography. The cases of human interleukin-6 and activin-A. J. Chromat. A. 1154, 81-86.

Tsumoto, K., M. Umetsu, I. Kumagai, D. Ejima and T. Arakawa 2003. Solubilization of active green fluorescent protein from insoluble particles by guanidine and arginine. Biochem. Bioph. Res. Co. 312, 1383-1386.

Tsumoto, K., M. Umetsu, I. Kumagai, D. Ejima, J.S. Philo and T. Arakawa 2004. Role of arginine in protein refolding, solubilization, and purification. Biotech. Prog. 20, 1301-1308.

Urakawa, T., D.G. Ritter and P. Roy 1989. Expression of largest RNA segment and synthesis of VP1 protein of bluetongue virus in insect cells by recombinant baculovirus,. association of VP1 protein with RNA polymerase activity. Nucleic Acids Res. 17, 7395-401.

Van Dijk, A.A. 1993. Development of recombinant vaccines against bluetongue. Biotechnol. Adv. 11, 1-12.

Van Dijk, A.A. and H. Huismans 1980. The in vitro activation and further characterization of the bluetongue virus-associated transcriptase. Virology. 104, 347-56.

Van Dijk, A.A. and H. Huismans 1988. In vitro transcription and translation of bluetongue virus mRNA. J. Gen. Virol. 69, 573-81.

Van Niekerk, M., V. Van Staden, A.A. Van Dijk and H. Huismans 2001. Variation of African horsesickness virus nonstructural protein NS3 in southern Africa. J. Gen. Virol. 82, 149-58.

Van Rensburg, R. 2005. Construction and structural evaluation of viral protein 7 of African horsesickness virus as a particulate, multiple peptide vaccine delivery system. MSc dissertation. University of Pretoria, Pretoria.

Van Staden, V. and H. Huismans 1991. A comparison of the genes which encode non-structural protein NS3 of different orbiviruses. J. Gen. Virol. 72, 1073-9.

Van Staden, V., C.C. Smit, M.A. Stoltz, F.F. Maree and H. Huismans 1998. Characterization of two African horse sickness virus nonstructural proteins, NS1 and NS3. Arch. Virol. Suppl. 14, 251-8.

Van Staden, V., J. Theron, B.J. Greyling, H. Huismans and L.H. Nel 1991. A comparison of the nucleotide sequences of cognate NS2 genes of three different orbiviruses. Virology. 185, 500-504.

Ventura, S., and Villaverde, A 2006. Protein quality in bacterial inclusion bodies. Trends Biotechnol. 24, 179-185.

Vera, A., N. González-Montalbán, A. Arís and A. Villaverde 2007. The conformational quality of insoluble recombinant proteins is enhanced at low growth temperatures. Biotechnol. Bioeng. 96, 1101-1106.

Wade-Evans, A.M., L. Pullen, C. Hamblin, R. O'Hara, J.N. Burroughs and P.P. Mertens 1997. African horsesickness virus VP7 sub-unit vaccine protects mice against a lethal, heterologous serotype challenge. J. Gen. Virol. 78, 1611-6.

Wade-Evans, A.M., L. Pullen, C. Hamblin, R.S. O'Hara, J.N. Burroughs and P.P. Mertens 1998. VP7 from African horse sickness virus serotype 9 protects mice against a lethal, heterologous serotype challenge. Arch. Virol. Suppl. 14, 211-9.

Wan, Y., Y. Wu, J. Zhou, L. Zou, Y. Liang, J. Zhao, Z. Jia, J. Engberg, J. Bian and W. Zhou 2005. Cross-presentation of phage particle antigen in MHC class II and endoplasmic reticulum marker-positive compartments. European J. Immunol. 35, 2041-2050.

Ward, T.H. and F. Brandizzi 2004. Dynamics of proteins in Golgi membranes, comparisons between mammalian and plant cells highlighted by photobleaching techniques. Cell. Mol. Life Sci. 61, 172-185.

Webb, A.I., M.I. Aguilar and A.W. Purcell 2003. Optimisation of peptide-based cytotoxic T-cell determinants using non-natural amino acids. Lett. Pept. Sci. 10, 561-569.

Wehrfritz, J.M., M. Boyce, S. Mirza and P. Roy 2007. Reconstitution of bluetongue virus polymerase activity from isolated domains based on a three-dimensional structural model. Biopolymers. 86, 83-94.

Wong, S.L. 1995. Advances in the use of Bacillus subtilis for the expression and secretion of heterologous proteins. Curr. Opin. Biotechnol. 6, 517-522.

Yu, Y.A., T. Timiryasova, Q. Zhang, R. Beltz and A.A. Szalay 2003. Optical imaging, bacteria, viruses, and mammalian cells encoding light-emitting proteins reveal the locations of primary tumors and metastases in animals. An. Bioan. Chem. 377, 964-972.

Zhang, G., V. Gurtu and S.R. Kain 1996. An enhanced green fluorescent protein allows sensitive detection of gene transfer in mammalian cells. Biochem. Bioph. Res. Co. 227, 707-711.

Zhang, J., R.E. Campbell, A.Y. Ting and R.Y. Tsien 2002. Creating new fluorescent probes for cell biology. Nat. Rev. Mol. Cell Biol. 3, 906-918.

Zhao, Y., C. Thomas, C. Bremer and P. Roy 1994. Deletion and mutational analyses of bluetongue virus NS2 protein indicate that the amino but not the carboxy terminus of the protein is critical for RNA-protein interactions. J. Virol. 68, 2179-85.

Zhou, S. and D.N. Standring 1992. Hepatitis B virus capsid particles are assembled from core-protein dimer precursors. Proc. Natl. Acad. Sci. U.S.A. 89, 10046-10050.

Zientara, S., C. Sailleau, E. Plateau, S. Moulay, P.P. Mertens and C. Cruciere 1998. Molecular epidemiology of African horse sickness virus based on analyses and comparisons of genome segments 7 and 10. Arch. Virol. Suppl. 14, 221-34.

Zimmer, M. 2002. Green fluorescent protein (GFP), Applications, structure, and related photophysical behavior. Chem. Rev. 102, 759-781.

Zou, J., Y. Ye, K. Welshhans, M. Lurtz, A.L. Ellis, C. Louis, V. Rehder and J.J. Yang 2005. Expression and optical properties of green fluorescent protein expressed in different cellular environments. J. Biotechnol. 119, 368-378.